People's Democratic Republic of Algeria

Ministry of Higher Education and Scientific Research

University of Mohamed Seddik BenYahia, Jijel

Faculty of Sciences and Technology

Department of Process Engineering

THESIS

Presented to obtain the degree of

DOCTORATE –LMD-

Specialty: Process Engineering

By: BOULAICHE KHALED

Theme:

Recycling and Valorisation of Industrial Wastes In the Formulation of a Sanitary Ceramic Body

Supported on:

Board of Examiners:

Nabil Mahamdioua	Associate professor	Univ. M.S.B.Y. Jijel	President
Kamel Boudeghdegh	Professor	Univ. M.S.B.Y. Jijel	Supervisor
Abdelmalek Roula	Professor	Univ. M.S.B.Y. Jijel	Co-supervisor
Mohamed Hamidouche	Professor	Univ. F.A. Sétif 1	Examiner
Farouk Benali	Professor	Univ. F.A. Sétif 1	Examiner
Kamel Atamnia	Associate professor	Univ. M.S.B.Y. Jijel	Examiner

Academic Year: 2022/2023

Dedications

Thanks to "ALLAH" the most powerful, for giving me the will and guidance to follow the right path.

I dedicate this work:

To my parents who sacrificed everything for me; it is thanks to you that I am here and thanks to you that I will be away. You will always remain in my heart.

To my beloved family, my beloved brothers and sisters “Mahbouba, Souad, Daoud, Haroun, Said, Nafaa, Mouhcene and Merieme” who supported me during my studies.

Acknowledgement

First, I would like to thank Professor **Kamel Boudeghdegh** my supervisor; I also, thank the University of Mohammed Seddik Ben Yahia-Jijel, for its trust and its approval for the supervision of this research. I am very grateful again to my supervisor and for help in terms of guidance and follow-up, starting from the theoretical stage to the analysis of the results. I also thank Professor **Abdelmalek Roula,** for all his advice and guidance during the preparation of the scientific articles of this thesis. I don't forget to thank all members of the industrial laboratory of the sanitary ceramic company of El-Milia-JIJEL, which provided me with the necessary assistance to complete this work, especially my colleague during my university years **Hemici Fakhreddine;** indeed, he did everything in his power to provide the best working conditions in the factory's laboratory. I would like to thanks also my colleague researcher **Hichem Alioui** for all his help.

I sincerely thank all the factories and institutions that provided us with the raw materials and solid industrial wastes necessary to complete this work on the one hand. On the other, the institutions that contributed to the characterisation of the raw materials and samples of the produced materials, must not be forgotten. I mean each of the following:

- LEAM laboratory of Jijel University.
- Research Unit of Sétif University.
- Sanitary Ceramic Company of El-Milia-JIJEL.
- African Glass Company (Jijel, Algeria).
- El-Hadjar Iron-steel Factory (Annaba, Algeria).
- Cement Company of Ain el-Kebira (Sétif, Algeria).

I do not forget to thank the administrative staff, engineers and technicians for their valuable help and support at all levels.

TABLE OF CONTENTS

Tables list

Figures list

List of abbreviations

XFS: X-ray fluorescence spectrometry

TDA: Differential thermal analysis

TGA: Thermogravimetric analysis

XRD: X-ray diffraction

θ: Bragg diffraction angle

SEM: Scanning electron microscope

FTIR: Fourier transform infrared spectroscopy

H (%): Humidity content

L.O.I (%): loss of ignition

d: Rheological density

R (%): Residue on a sieve

Sh_d: Drying Shrinkage

WA: water absorption

D_A: apparent density

P_t (%): Total porosity

D_T: True density

Sh_f: Firing shrinkage

F_S: Flexural strength

BFS: Blast furnace slag

SLGW: Soda-lime glass waste

SCW: Sanitary ceramic waste

E1, VC: Sanitary ceramic body with 0 wt. % industrial waste

E2: Sanitary ceramic body with 5 wt. % blast furnace slag

E3: Sanitary ceramic body with 10 wt. % blast furnace slag

E4: Sanitary ceramic body with 15 wt. % blast furnace slag

E5: Sanitary ceramic body with 20 wt. % blast furnace slag

C2: Sanitary ceramic body with 5 wt. % soda-lime glass waste

C3: Sanitary ceramic body with 10 wt. % soda-lime glass waste

C4: Sanitary ceramic body with 15 wt. % soda-lime glass waste

C5: Sanitary ceramic body with 20 wt. % soda-lime glass waste

VC5: Sanitary ceramic body with 5 wt. % sanitary ceramic waste

VC10: Sanitary ceramic body with 10 wt. % sanitary ceramic waste

VC15: Sanitary ceramic body with 15 wt. % sanitary ceramic waste

VC20: Sanitary ceramic body with 20 wt. % sanitary ceramic waste

GENERAL INTRODUCTION

Background of the study

Ceramics may be defined as non-metallic and inorganic material produced by a firing process that gives them both rigidity and aesthetic properties. A high-temperature treatment is important to link all types of ceramic materials. Other factors, such as peak temperature, particles size distribution in addition to raw material properties, characterize the features of different ceramic products and their final applications. Generally, ceramics have some unique characteristics, which do not have metals or other solids; we can include a high melting point, good chemical inertness, high-temperature stability and electrical insulation ability [1].

Ceramics have a vast range of applications in modern technology and expect the demand for ceramics, is expected to increase strongly. They are grouped according to their mineralogical nature such as silicate, oxide, non-oxide, nitride and carbide. Besides, ceramics can also be categorized into traditional and advanced ceramics. Traditional ceramics are based on clay and silica, such as bricks, glass, tiles, table wares and sanitary wares. Advanced ceramics were developed to use in various fields such as biomedical (artificial bones and teeth), electrical and electronic devices. All these ceramic products are mostly manufactured by consuming a massive amount of raw materials. The oldest and most used raw material of traditional ceramic is a natural clay [2].

Sanitary ceramic ware are one of the most important applications of ceramic materials; they can be used as bathroom furniture in all kinds of buildings. They consist of two distinct parts: the ceramic body and the glazed surface. They are generally fired at about 1230°C to accelerate phase reactions, which are affected by the mineral composition of the raw materials, thus controlling the microstructure, technical and aesthetic properties of the final product [3]. .

The increase in production of ceramic materials over time, causes a depletion in natural resources. For this reason, recent studies are trying to find alternative materials to replace some of the natural raw materials to reduce their consumption. Recently, recycling and integrating industrial by-products into the ceramic industry is one of the proposed solutions to reduce environmental problems and make economical gains.

Problem statement

Ceramics are considered a high-quality material with excellent technical characteristics; World demand for its products is considerable. The production of sanitary ceramic bodies consumes large quantities of clay-kaolin, feldspar and quartz. The improvement of physical and mechanical properties by the incorporation of industrial wastes, is very important to save natural raw materials resources.

A huge volume of solid wastes is produced worldwide according to international statistics. For this reason, the integration of these wastes in various ceramic formulations, has been the subject of several studies. The most used are: red mud [4] , fly ash[5] , solid ceramic waste [6] , glass waste[7] and blast furnace slag [8].

The clay-kaolin mixture is the principal raw material in sanitary ceramic bodies providing the plasticity necessary for the forming process. Feldspar helps to improve vitrification. Meanwhile, quartz works as a filler to reduce shrinkage during firing.

Generally, Feldspar is the next most significant raw material which acts as a flux agent that provides high vitrification by decreasing the melting temperature. Calcium, potassium and sodium feldspar are the most common fluxes used in ceramic composition; feldspars are useful for industries due to their alkali and alumina content [9].

The rich contents in blast furnace slag (BFS) of CaO, SiO_2 and Al_2O_3, in addition to Na_2O in soda-lime glass waste (SLGW) and sanitary ceramic waste (SCW), has motivated us to investigate these three wastes as substitutes raw materials to feldspar from 5 up to 20 wt. % in manufacturing new sanitary ware body

The work of this thesis falls within the framework of proposing solutions for the development and improvement of the quality of sanitary ceramic bodies produced in the sanitary ceramics factory of El-Milia-Jijel. Among the questions raised in the industry of sanitary ceramics, to develop it further, we have:

- What is the optimum amount of industrial waste (BFS, SLGW and SCW) that can replace a raw material (feldspar) without affecting the technological properties of sanitary ceramic bodies?

- How to improve the physical-mechanical and structural properties, by using the adequate composition and how to control the glass-body interaction mechanism as it determines the quality of the final product?

- How do take into account possible changes in rheology, thermal cycle effects and chemical compatibility to enable an easy recovery of industrial waste in the sanitary ceramic industry?

Objectives of the study

This study aims to develop a new sanitary ceramic body by substituting feldspar with industrial wastes, such as: blast furnace slag (BFS), Soda-lime glass waste (SLGW) and sanitary ceramic waste (SCW) in the ceramic material composition. In order to achieve this goal, we must deal with the following problems :

- To control the rheological behaviour of the sanitary slip using Na-electrolytes. The combination of Na_2SiO_3 and Na_2CO_3 allows the understanding of the rheological properties when the addition of the industrial wastes.
- To define the optimum composition for obtaining good physical-mechanical and structural properties of fired ceramics.
- To evaluate the phase changes, thermal behavior and microstructure of ceramic bodies during the substitution of feldspar by these industrial wastes.

This investigation aims to reduce the depletion of natural raw materials; it also, leads to significant economic benefits by getting a less expensive ceramic body and reducing environmental pollution; we can added some technical benefits (improving the physical-mechanical properties and reducing the firing temperature) [10]. By the way, reducing the firing temperature allows us to make energy saving.

Scope of the study

This study consists of the following stages and areas of investigation:

- Industrial ceramic body composition: 52 wt. % of clay-Kaolin, 25 wt. % of quartz and 23 wt. % of feldspar (feldspar in replaced by various proportions of industrial wastes from 0 wt. % up to 20 wt. %).
- First, the raw materials were prepared by measuring the humidity to obtain an adequate slip mixture. Then, the clay is diluted in parallel with the milling of the sand in a jar mill. After that, the feldspar and sand are added with the appropriate amount of water. Deflocculating agents are added to the slip mixture to improve the rheological slip properties; the agents are mainly Na-electrolytes.
- The effect of partial substitution of feldspar by blast furnace slag, soda-lime glass waste and sanitary ceramic waste, on the rheological behaviour of sanitary slip, requires measuring and controlling its various properties (density, fluidity, viscosity, thixotropy, thickness and the amount of electrolytes).
- The thermal behaviour of green ceramic bodies, assessed by differential thermal analysis and thermal weight (TDA/TG) using (TGA-DSC, Universal V4.5A TA Instruments) equipment for temperatures up to 1300 °C, with a heating rate of 5°C / min, in an atmosphere of air.
- The sintering temperature of sanitary ceramic bodies is 1230°C.
- The physical properties of fired ceramics investigated are: water absorption, linear shrinkage, apparent porosity and bulk density.
- The mechanical property of fired samples and which interests us, is the flexural strength.
- Phase change, microstructure evolution and chemical bond variation of sanitary bodies are characterized using DRX, SEM and FTIR technics.

Following a general introduction, the thesis is structured as follows:

The first chapter includes an overview of the bibliographic research concerned with the study of sanitary ceramic bodies and their classifications as well as their manufacturing process. Then, this chapter gives a short synthesis of the transformations of sanitary ceramic bodies during the firing stage, a brief description of the chemical composition of ceramic bodies, the manufacturing steps, the rheological and the physical-mechanical properties of the sanitary bodies.

The second chapter is aimed at study of rheological properties of slip and various method of characterization of green and fired ceramics; in particular, we have the diffraction of X-rays (XRD), scanning electron microscope (SEM), Fourier transforms infrared spectroscopy (FTIR), differential thermal analysis (DTA), thermogravimetric analysis (TGA) and derivative thermogravimetry (DTG). Then, follows the evaluation of the physical-mechanical properties of fired ceramic bodies, which are: bulk density, porosity, water absorption, shrinkage and flexural strength. In this chapter, we have given information on all the raw materials and industrial wastes used in this work. Among these materials are: Hycast VC clay, RMB kaolin, Parkaolin, quartz, sodium and potassium feldspar. The industrial wastes used are: the blast furnace slag which comes from El-Hadjar Iron-steel Factory, Algeria. While the soda-lime glass waste powder is from the factory of the African Glass Company (Jijel, Algeria).

The third chapter presents the experimental results and discussion of the effect of partial substitution of feldspar by blast furnace slag on the rheological behaviour of slip using Na-electrolytes. Moreover, this chapter aims to determine the optimum composition for obtaining better physical-mechanical, thermal and structural properties of fired ceramics.

The fourth chapter looks at the potential use of soda-lime glass waste, in the preparation of sanitary ceramic bodies as a partial substitute for feldspar from 5 up to 20 wt. % . Then, we have carried out various characterization analyses on our samples: rheological behavior, physical-mechanical properties, DRX, IRTF, SEM and thermal analysis ATG/DTG.

The fifth chapter studies various effects of sanitary ceramic waste on rheological, physical-mechanical and structural properties of vitreous china bodies.

We hope that this technical approach results will be applied in our ceramic factories. Indeed, this study opens new horizons for the use of these industrial wastes in the formulation of sanitary ceramic bodies with many environmental, economical and technical benefits; thus, the modest contribution to the sustainable development of our country.

Finally, the general conclusion summarizes the main results obtained and presents possible topics for future research work.

1.LITERATURE REVIEW

1.1 Background to the literature review

The literature review for this thesis will focus on the published research results concerning the properties of the raw materials used in the manufacture of sanitary bodies, the slip casting method and the manufacturing steps. In addition, the literature review will include a basic discussion on the properties of sanitary bodies during their firing. Furthermore, the use of two industrial wastes (blast furnace slag, soda-lime glass waste and sanitary ceramic waste) in the composition of sanitary ceramic bodies requires also a discussion about the required properties and the selection criteria that allow their incorporation as alternative materials.

1.2 Introduction

The principle of ceramic manufacturing is based on the properties of the mixture of clay and raw materials with water, in appropriate and accurate proportions; ceramic bodies can be formed and fired to obtain final products without deformation. The ceramic body is partially white few-porous, it was first produced in china centuries ago [11].

Today, ceramic materials are produced in many countries, using modern technologies. The improvement of ceramic products is still in progress and many research works are discussed and published continuously [12].

Traditional ceramics consist mainly of plastic raw materials (clay–kaolin), and non-plastic materials: feldspar and quartz. Plastic minerals are the main components of ceramics, they have an important function in imparting plasticity and malleability to the material during firing [13].

sanitary ceramic bodies are well known types of traditional ceramics. Their production is based on the raw materials which are relatively available and inexpensive. They are not very dense and they resist very high temperatures, where most metals lose their strength. Finally, they have physical, mechanical, chemical and thermal properties, which make them irreplaceable in many industries [14]. The approved method for the production of sanitary bodies is the casting process where the slip is poured into a plaster mold, which will absorb water via capillarity; a solid ceramic body is formed before the molds are removed. Following the casting process completion, the bodies are dried and glazed by spraying, to

improve physical-chemical resistance. Then, the ceramic wares are fired in a tunnel kiln. To finish, the products are colored according to the desired decoration [15].

Generally, the principal phases in sanitary bodies are the glassy phase, mullite and residual quartz. Mullite is the main constituent. It has a low expansion coefficient with high strength; this allows improvement in the technical characteristics of ceramic products [16].

Our study aims to recycle three industrial wastes (blast furnace slag, soda-lime glass waste and sanitary ceramic waste) to find the optimal composition for a new sanitary ceramic body, which is a vitrified product of good quality and which contains the following raw materials: Hycast VC clay, RMB kaolin, Parkaolin, sodium and potassium feldspar and quartz. In addition, we want to assess the effect of industrial waste on the behavior and durability of ceramic bodies subjected to high temperatures. We chose this study to achieve ceramic materials that contain industrial waste to help reduce the depletion of raw materials and to reduce pollution problems. This work aims also to improve the quality of the final sanitary ceramic bodies.

1.3 The main classes of ceramics

Originally, the most ceramic materials produced in the industry, are: sanitary ware, floors, wall tiles, tableware and building materials. From the beginning of the 20th century onwards, through research work in the field of materials, it has been possible to develop innovations in processes, compositions and structures to develop new ceramics. with very specific physical properties (electrical, thermomechanical, optical). These new materials are grouped under the generic term of technical ceramics. Innovative high-potential companies have been created from technology transfers from research laboratories, for the development of new applications [2].

The production of ceramics products from clay raw materials, is different from other materials by the method of preparation, which involves the following four steps:

1. Milling

2. Homogenization of raw materials.

3. Shaping of raw materials.

4. Densification by heat treatment [17].

The following table shows the major classes of ceramics:

Table 1 : The major classes of ceramics[18]

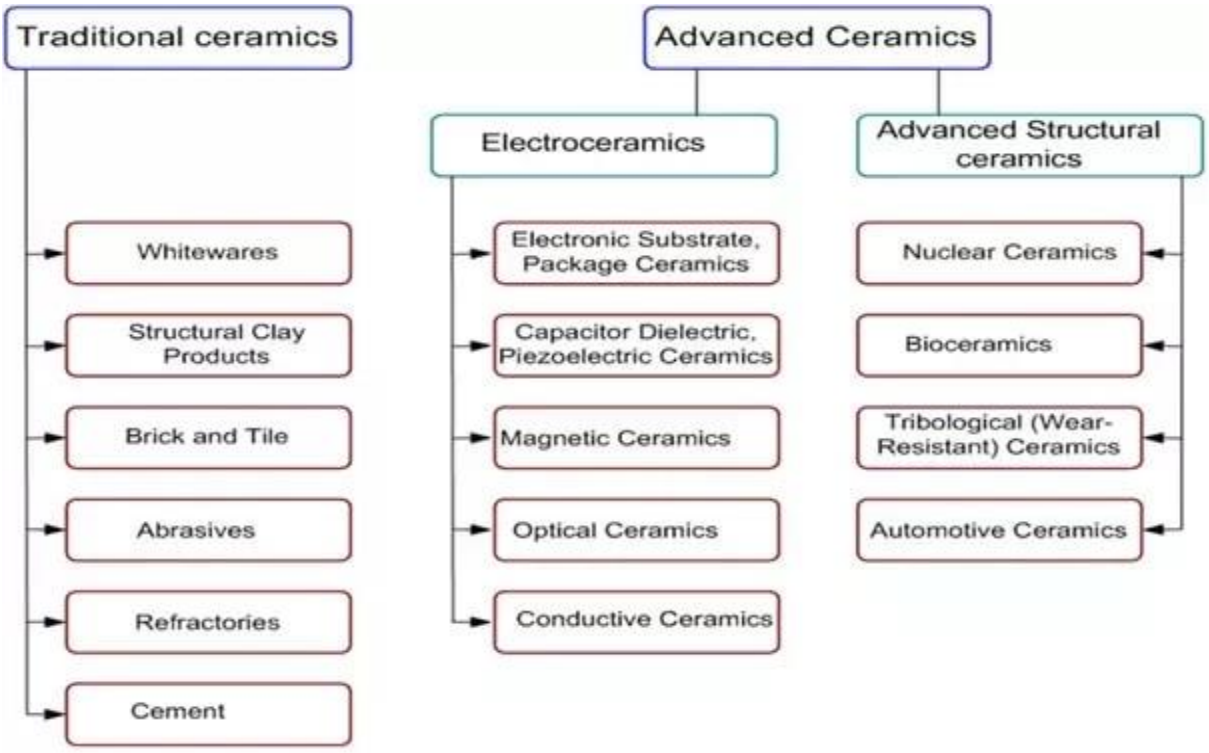

1.3.1 Traditional ceramics (Aliminosilicates)

Traditional ceramics are derived from natural raw materials (clay, feldspar, kaolin, quartz) and are generally produced by the casting slip method. "Traditional" ceramics are present in many fields of activity, such as building materials (bricks, tiles, etc.), sanitary ware, culinary products, cladding (tiles, earthenware, etc.) and refractories (kilns, etc.), they are made from natural silicate minerals [19].

Clay minerals are the main component in almost-all ceramic materials. Their specific properties, due to their colloidal nature in the presence of water, allow the shaping of ceramic products and ensure the cohesion of the raw materials.

Before the firing of the ceramics, it is necessary to eliminate the water that was used for forming, particularly when the quantity is large (in the case of slip). The drying cycle causes a significant or minor shrinkage according to the composition of the mixture. The firing is the final and decisive phase in the manufacturing process. Firing temperatures vary greatly depending on the product. From 800 to 1000°C for fired-clay and common pottery,

from 1100 to 1350°C for sanitary ware, wall tile and porcelain, 1500 to 2000°C and more for refractories and technical ceramics. Firing times are also very variable, depending on the type of product and kiln [2].

Figure 1: Example of traditional ceramics: (a)-Porcelain, (b)- wall tile, (c)- pottery, (d)- sanitary ware.

Another overview of the various ceramics can be seen from the three-phase diagram of clay-kaolin, quartz and feldspar (Figure. 2).

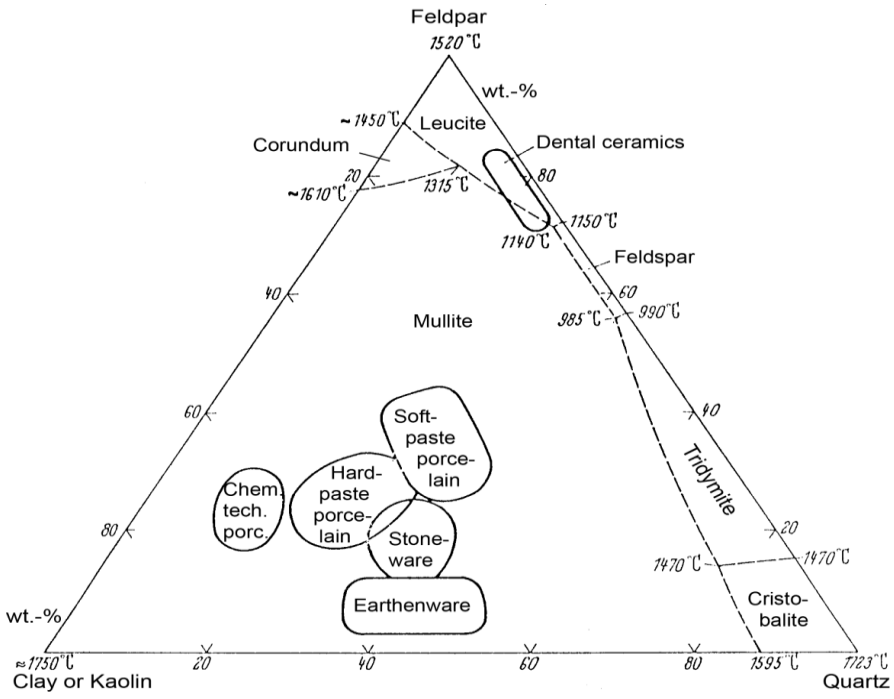

Figure 2: Diagram with different ceramic compositions from the system clay or kaolin-feldspar-quartz in dependence of the temperature [20].

1.3.2 Technical ceramics

Technical ceramics are present in new fields and are in full expansion in areas such as electronics, aerospace, automotive and biomedical. Their compounds are essentially non-silicated and the raw materials used are synthetic (oxides, carbides, nitrides, etc.)

Products are most often obtained by sintering (thermo mechanical treatment which, in the first step, causes the cohesion of powder granules with an "agglomerate" prepared by cold compression, this blank being then heated in special furnaces) or electro fusion, the oxides are them poured directly into a mold [19] .

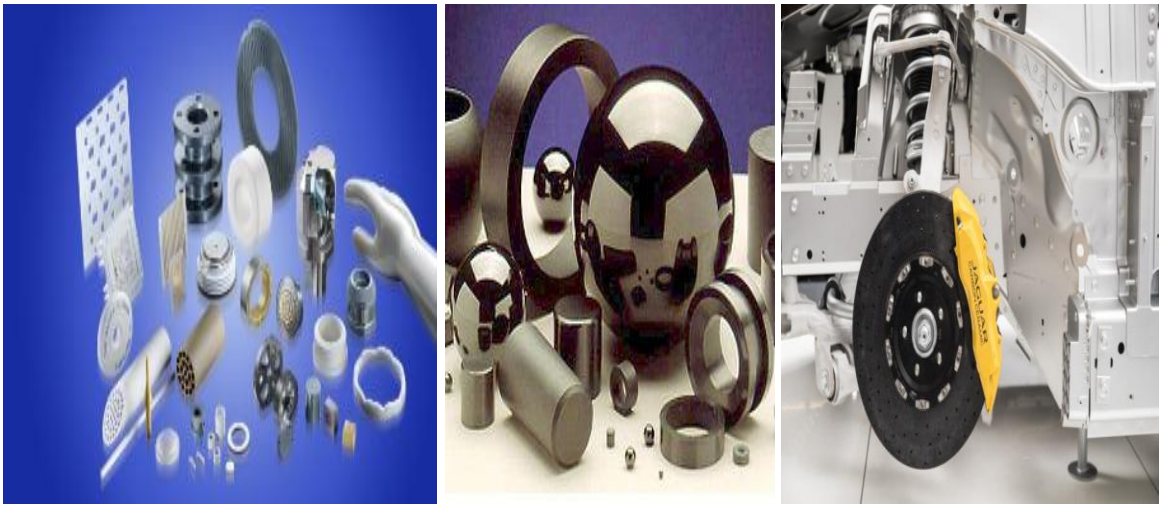

Figure 3: Some examples of technical ceramics..

1.4 Sanitary ceramic bodies

Ceramic sanitary ware consists of an inner body, often covered by a glaze; they are usually fired in a tunnel kiln at high temperatures. This results in a high level of hardness, providing durability, even in public sanitation facilities. The hygienic smooth glaze makes the product resistant to abrasion and scratching and also, easy to clean.

Clay, feldspar, kaolin, chamote and quartz are the main raw materials for various sanitary ware bodies' composition. After vitrification, the process of sintering sanitary ware bodies is performed at temperatures up to 1230 °C. The firing process is important because it controls all properties such as microstructural, physical and mechanical are related to the densification degree and kinetics of sintering [21].

1.5 Classification of sanitary ceramic bodies

In general, sanitary ware can be divided into two classes:

1.5.1 Vitreous china

Vitreous china (sanitary porcelain) is the most common type used in sanitary-ware industry. It has a high amount of glassy phase which increases the body strength; this is the main cause for its use in the manufacture of toilet bowls. Vitreous china has less than 0.5% water absorption and a shrinkage with an average of 11.2%. As an industry standard, this high shrinkage means that vitreous china has a greater tendency to warp and distort. In other words, maintaining the shape particularly long or flat panels, is much harder to achieve [22, 23].

The raw mass contains plastic, melting and degreasing materials. The plastic materials represent 45 to 60 % of the composition. It consists of a combination of clay and kaolin. The clays confer plasticity and cohesion to the green body; it may also participate in the formation of the glassy phase during the thermal treatment. Kaolin improves the casting behaviour and enhances the over-fired whiteness of the body. The role of the melting feldspars (sodium and potassium), is to reduce the melting temperature. The vitreous phase results from the solid-phase reaction of melting feldspar with amorphous silica, at around 1050°C. A vitrification aid such as talc, is often used to improve vitrification kinetics and lower the firing temperature [23, 24].

1.5.2 Fine fire clay.

Fine fireclay contains chamotte (calcined clay) which reduces the glassy phase in the body. The low amount of liquid phase causes an increase in the porosity of the body; that makes fine fireclay absorb between 6% and 11% of water. The shrinkage of Fine Fireclay is much lower compared to Vitreous China (usually between 4% and 6%). Also, fine fireclay can maintain a flat and straight surface more easily [23, 25].

Generally, fine fire clay consist of a mixture of fired clay/kaolin (chamotte), white clay, kaolin and quartz. Thermal expansion is controlled by changing the amount of quartz used. Fine fire clay material is one of the best solution for manufacturing trendy sanitary-wares. Chamotte reduces deformation of large ceramic bodies such as bathtubs, large sinks (generally greater than 100 cm) and kitchen sinks, etc [22].

1.6 Raw materials for sanitary ceramic bodies

1.6.1 Plastic raw materials

1.6.1.1 Clay

Clays are the most important raw materials for the manufacture of ceramic products, which have a fine-grained type of natural soil material containing clay minerals that develop plasticity when wet, due to a molecular layer of water around the clay particles. They have a secondary geological origin; they were formed by the degradation of volcanic rocks, caused by erosion and chemical alteration, under the action of atmospheric agents [26].

Clays are more or less hydrated alumino-silicates. The majority of clay minerals belong to the group of phyllite silico-aluminates. They are arranged in planes, consisting of tetrahedral and octahedral structural units connected by their peaks; this type of structure is very specific and has particular physicochemical characteristics.This explains the capacity of clays to allow many exchanges of cations and anions in the lattice.

The structure of clays is formed from elementary structural elements: silica tetrahedra (SiO_4) and aluminium octahedra ($Al(OH)_6$). Water layers are often interposed between the sheets, which is the reason for the plastic properties of the clays. This characteristic is particularly exploited in the moulding of traditional ceramics from slip [27].

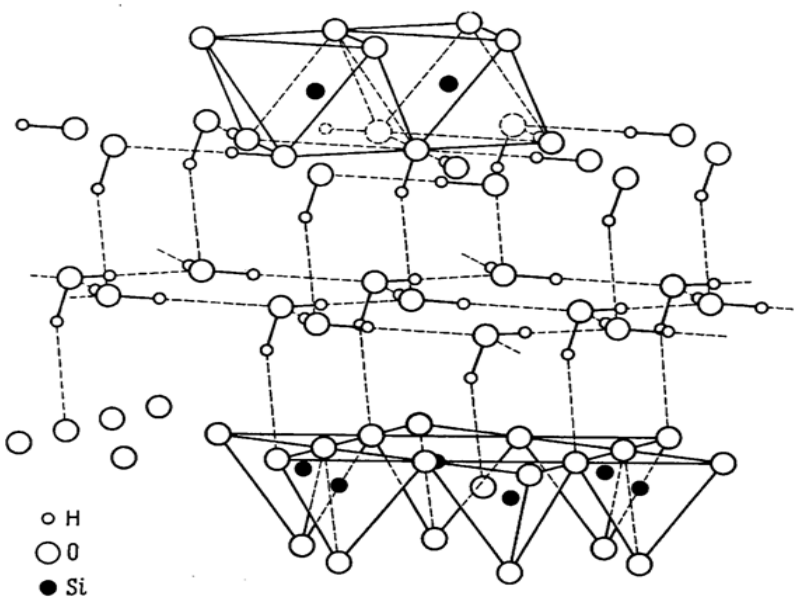

Figure 4: Orientated layer of water in halloysite. Bottom: Tetrahedra layer; top: Octahedra layer from the further unit [28].

1.6.1.2 Kaolin

Kaolins are basically rocks composed, principally, of the kaolin group of minerals, namely: kaolinite, halloysite, dickite and nacrite. The main constituent of kaolin is kaolinite having as structural formulae $Al_2O_3.2SiO_2.2H_2O$ or $Si_2Al_2O_5(OH)_4$.

Kaolin is primarily used in domestic ceramics, as it is the main source for the production of most refractory materials. The typical chemical species of interest for refractories, is aluminous kaolinite, which is the basic element of most clays used in the ceramic industry [29, 30]. This rock is in the form of hexagonal tablets (Figure. 5).

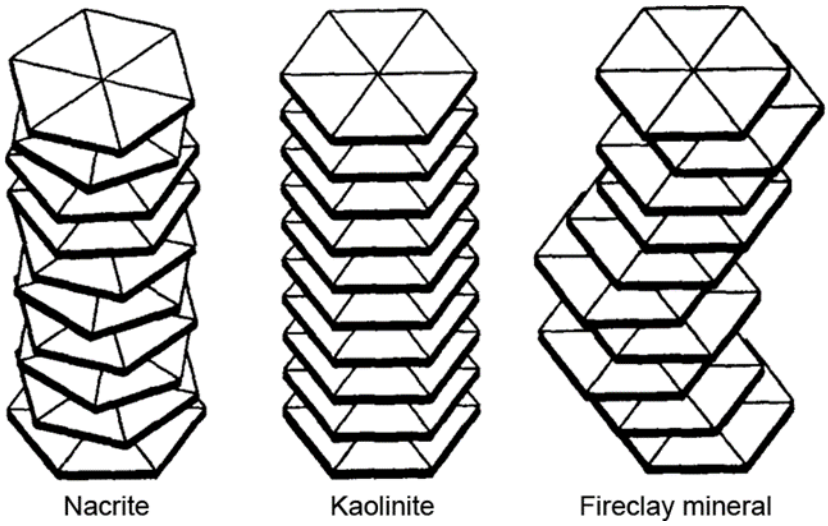

Figure 5: Order and disorder in minerals of kaolinite group [28].

Several studies have been made on the behaviour of kaolin during the firing stage. The first reaction in this series of transformations, is the endothermic reaction in the temperature range 450-600 °C; it is due to the liberation of all the constitutive water contained in the kaolinite with the formation of dehydroxylated kaolinite. defined as meta-kaolinite ($Al_2O_3.2SiO_2$).

$$\underset{\text{(kaolinite)}}{Al_2O_3.2SiO_2.2H_2O} \xrightarrow{450\text{-}600\ °C} \underset{\text{(méta-kaolinite)}}{Al_2O_3.2SiO_2} + 2H_2O_{(g)} \quad \text{.....(1)}$$

The start of the structural reorganization of meta-kaolinite is at a temperature of about 980 °C, with an exothermic reaction resulting in a spinel structure.

$$\underset{\text{(meta-kaolinite)}}{Al_2O_3.2SiO_2} \xrightarrow{980\ °C} \underset{\text{(primary mullite)}}{3Al_2O_3.2SiO_2} + \underset{\text{(spinel)}}{\gamma\text{-}Al_2O_3} + \underset{\text{(amorphous silica)}}{SiO_2} \quad \text{.....(2)}$$

The transformation above at 1100 °C, is due to the formation of cristobalite according to the following reaction:

$$\underset{\text{(mullite)}}{(3Al_2O_3.2SiO_2)} + \underset{\text{(amorphous)}}{4SiO_2} \xrightarrow{1100\ °C} \underset{\text{(mullite)}}{(3Al_2O_3.2SiO_2)} + \underset{\text{(cristobalite)}}{4SiO2} \quad \text{..... (3)}$$

Above 1500°C cristobalite is transformed to amorphous glass by the following reaction [24]:

$$\underset{\text{(mullite)}}{(3Al_2O_3\ .2SiO_2)} + 4SiO_2 \xrightarrow{1500°C} \underset{\text{(mullite)}}{(3Al_2O_3\ .2SiO_2)} + \underset{\text{(amorphous glass)}}{4SiO_2} \quad \text{..... (4)}$$

1.6.2 Non-plastic raw materials

1.6.2.1 Melting materials

1.6.2.1.1 Feldspars:

These are minerals consisting of sodium, potassium or calcium silico-aluminates. Their vitrifying action varies according to the nature of the melting element. The purest feldspars bake white and melt at various temperatures, generally above 1200°C, into a viscous glass [31].

- ❖Potassium feldspar (orthoclase): $6SiO_2Al_2O_3\ K_2O$
- ❖Sodium feldspar (Albite): $6SiO_2Al_2O_3\ Na_2O$
- ❖Calcium feldspar (anorthite): $2SiO_2Al_2O_3\ CaO$

Feldspars are groups of two, four or six silica molecules connected to an alumina molecule and an alkali metal oxide (potassium, sodium, calcium or lithium).

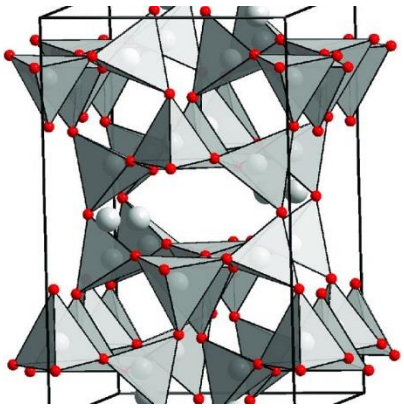

Figure 6: tetrahedral arrangement of feldspar [32].

Feldspar is the most important material in the manufacture of ceramics, after clay. As it does not have a specific melting point, it melts gradually as the temperature changes. This property facilitates the melting of quartz and clays. Feldspars are used as fluxes to form a glassy phase at low temperatures. They increase the strength, toughness and solidity of the ceramic core and also, cement the crystalline phase and the other ingredients, while softening, melting and liquefying the other constituents [24, 33].

A selection of feldspars found in nature is summarized in Table 2.

Table 2: Properties of some feldspars [28].

Mineral	Chemical formula	Crystal system	Lattice constants		Density (20 °C) [g/cm³]	Refractive index	Annotations
			a b c [Å]	α β γ		n α n β nγ	
Microcline	$K[AlSi_3O_8]$	triclinic	8,57	90° 41'	2,57	1,514	Stable low-temperature
			12,98	115° 59'		1,518	modification, ordered
			7,22	87° 30'		1,521	Stable high-temperature
Sanidine	$K[AlSi_3O_8]$	monoclinic	8,56 13,03 7,18	– 115° 59' –	2,57	1,521 1,527 1,527	modification, disordered
Albite	$Na[AlSi_3O_8]$	triclinic	8,14	94° 19'	2,62	1,528	Stable low-temperature
			12,79	116° 34'		1,532	modification,
			7,16	87° 39'		1,538	ordered
Analbite	$Na[AlSi_3O_8]$	triclinic	8,23	94° 03'	2,62	1,527	Instable
			13,00	116° 20'		1,532	modification,
			7,25	88° 09'		1,534	unordered
Monalbite	$Na[AlSi_3O_8]$	monoclinic	7,25	–		1,523	stable high-
			12,98	116° 07'		1,528	temperature
			6,41	–		1,529	modification,
							unordered
Anorthite	$Ca[Al_2Si_2O_8]$	triclinic	8,18	93° 10'	2,77	1,576	ordered
			12,88	115° 51'		1,583	
			14,17	91° 13'		1,589	
Celsian	$Ba[Al_2Si_2O_8]$	monoclinic	8,65	–	3,8	1,587	
			13,13	115° 02'		1,593	
			14,60	–		1,600	

1.6.2.1.2 Chalk

These rocks consist of calcium carbonate or calcite; they are found in a large proportion in the main exploitation of sediments in the Paris and Aquitaine basin. Their formula is $CaCO_3$[31].

1.6.2.1.3 Mica

Micas are a group of minerals whose outstanding physical characteristics; individual mica crystals can easily be split into extremely thin elastic plates. This characteristic is described as perfect basal cleavage. Mica is common in igneous and metamorphic rock and is occasionally found as small flakes in sedimentary rock.

Formula in oxides (muscovite): 6 SiO_2, 3Al_2O_3, K_2O, 2H_2O.

1.6.2.1.4 Talc

It enhances clays crystallizations, which confer to the shard a good resistance to thermal shock with a low expansion [31].

Formula of talc in oxides : 4 SiO_2, 3MgO H_2O.

1.6.2.2 Degreasing materials

The role of these materials is to reduce shrinkage caused by the plasticity of the clay. The addition of these agents to clays, generally, has the effect of improving some properties of the raw body, facilitating the drying of the products by facilitating the diffusion of water, during the drying process.

1.6.2.2.1 Quartz

Silica is the most abundant compound on the earth's surface, in its free state; it is, mainly, found in the crystallized form as α-quartz (in quartzite), but it is also found in the composition of a large number of natural and artificial substances. Thus, it is an essential component of kaolin, mica and feldspar in their natural state. It is also, a basic constituent of natural materials transformed by firing to give refractory materials.

Quartz originates from a three-dimensional linkage of SiO_4 tetrahedra. The figures shown in figure. 7 describe again the distance from the base level.

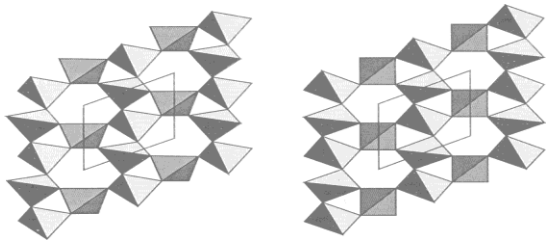

Figure 7: Two crystal structures of SiO_4 tetrahedra drawn with the same unit cells, viewed down a common [001] direction [34] .

SiO_2 can be found in different crystallographic structures **(**Figure. 8**)**. Low temperature transformation of quartz (β-quartz) into α-quartz takes place at a temperature of 573° C; there is just a marginal shift of silicon and oxygen ions. At the high temperature of 870°C we have the transformation of quartz to tridymite. In this case, new bonds are formed. Therefore, this process does not happen very quickly, while the transformation from α-quartz into β-quartz is quick and unavoidable. Reconversion of tridymite into quartz can be prevented, if it is cooled very quickly, leaving no time for the structure to reconvert. Further transformations are related to α-cristobalite at 1,470°C, and SiO_2 melting at 1,713°C. Such transformations cause tremendous problems for the sintering of ceramic products, because they are partly combined with major volume changes. Quartz inversion at 573°C, leads to a volume expansion of 0.8 %. This may, indeed, cause cracks in the porcelain during the cooling stages, after sintering. This problem is accentuated during the quartz transformation into cristobalite or tridymite, with a volume expansion of more than 15 % (figure. 9); after sintering, this causes stresses in the structure and destroys the components during cooling [20].

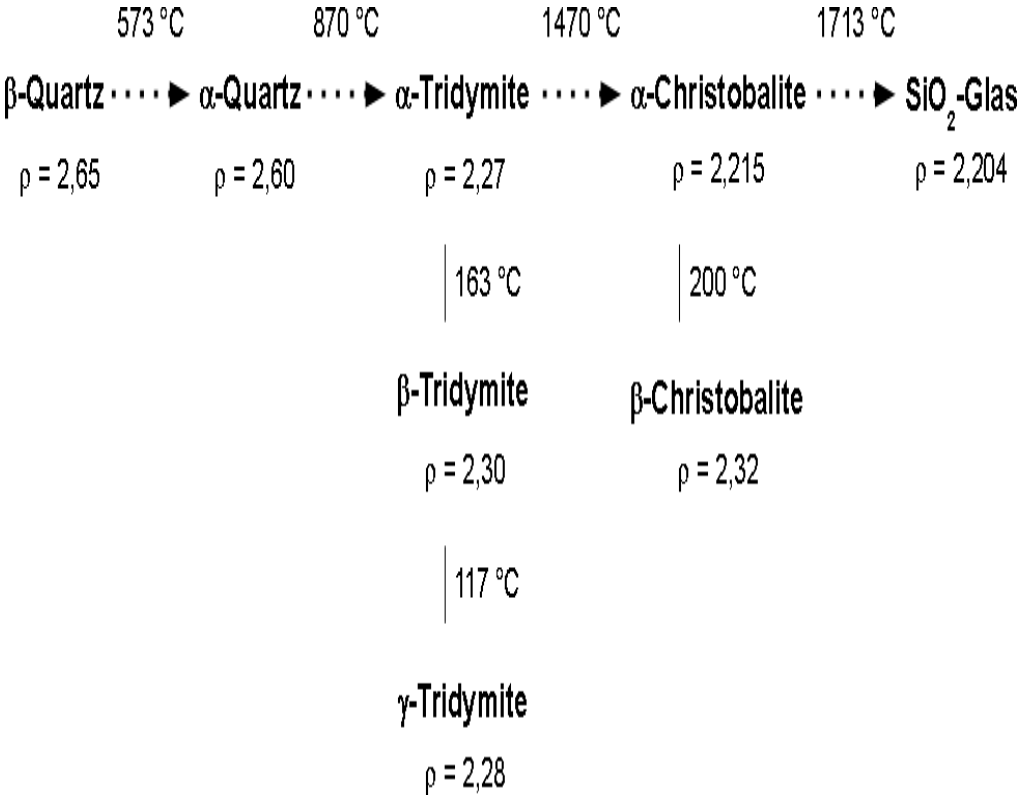

Figure 8: Phase transformation of SiO_2 with temperature [28].

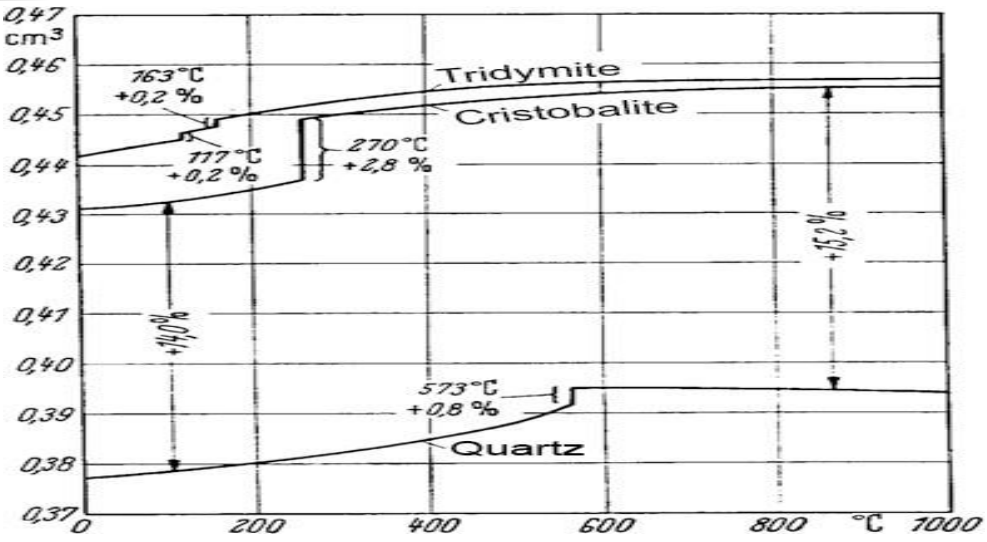

Figure 9: Dependence of the specific volume on the temperature for quartz, cristobalite and tridymite [28].

1.6.2.2.2 Chamotte

Chamotte, also known as fire-clay and Grog, is a raw material for making ceramics. It has a high percentage of silica and alumina. It can be produced by firing selected fire clays or recycled production residues, at high temperature before grinding and screening to specific particle sizes. It is added to clay, in a defined percentage to make a limitation of shrinkage, improvement of drying and stability during the firing stage [35].

1.7 The manufacturing steps of sanitary ceramics

The necessity of obtaining a product with a homogeneous structure, means using raw materials with a small particle size. Thus, grinding and mixing operations are essential in the manufacturing process of ceramics. Figure 10 illustrates the manufacturing steps of sanitary ceramics.

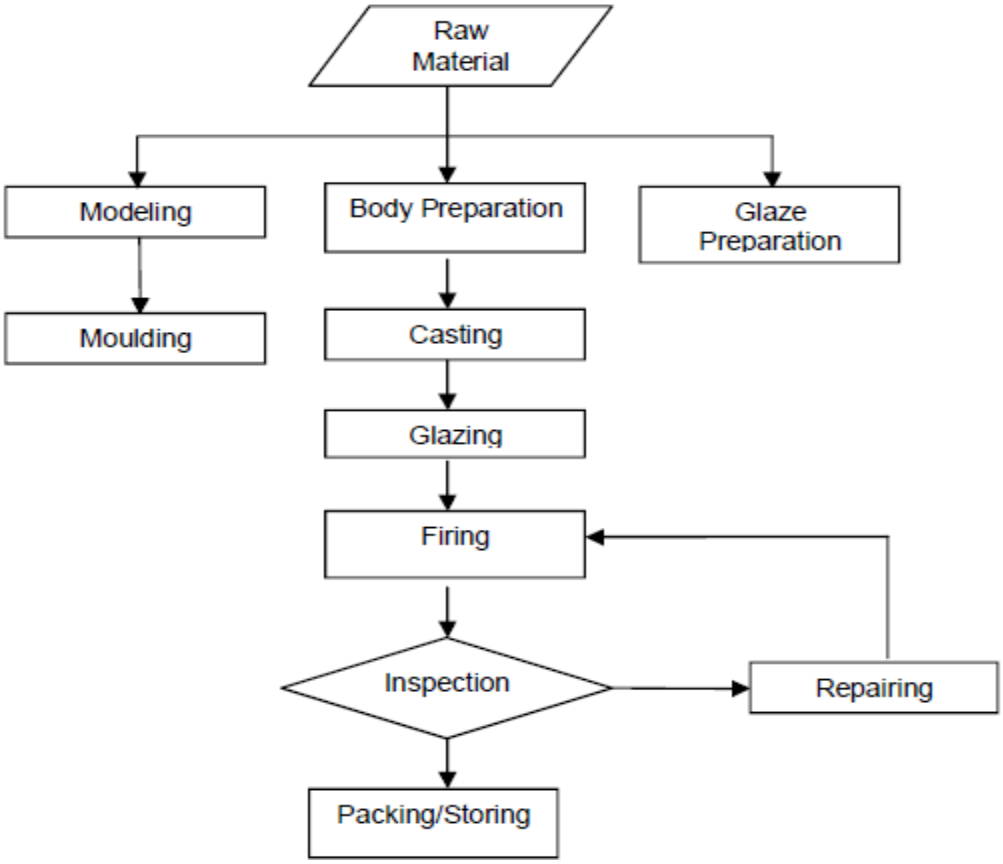

Figure 10:Manufacturing steps of sanitary ceramics [36].

Generally. The steps of sanitary ceramic production can be summarized as follows:

1.7.1 Slip Preparation

The sanitary ceramics production is generally based on the preparation of the slip from a mixture of clay-kaolin plastic (kaolin 15-20 wt. % and clay 30-35 wt. %) and others non-plastics 25 wt. % quartz and 25 wt. % feldspar, with a suitable amount of water.

For the ceramic raw materials to react homogeneously and quickly throughout the manufacturing process, they must have a very fine and regular particle size. There are several grinding systems; the most common in the ceramic industry is the so-called "alsing" or ball mill.

The raw material is introduced, with a grinding charge represented by (alumina balls of different diameters), into a cylinder rotating on its horizontal axis. The friction caused by the movement of the balls mass on the raw material, ensures its fragmentation, which depends on the speed and time of grinding.

Figure 11: Milling of the mixture of the raw materials in the jars.

The rheology of slip is affected by the composition and properties of raw materials. Besides, several types of electrolytes such as sodium silicate and sodium carbonate are added to improve various rheological properties. Afterwards, the slip is poured into a plaster mold, which will absorb water via capillarity; a solid ceramic body is formed before the molds are removed [37, 38].

Figure 12: slip casting in plaster molds.

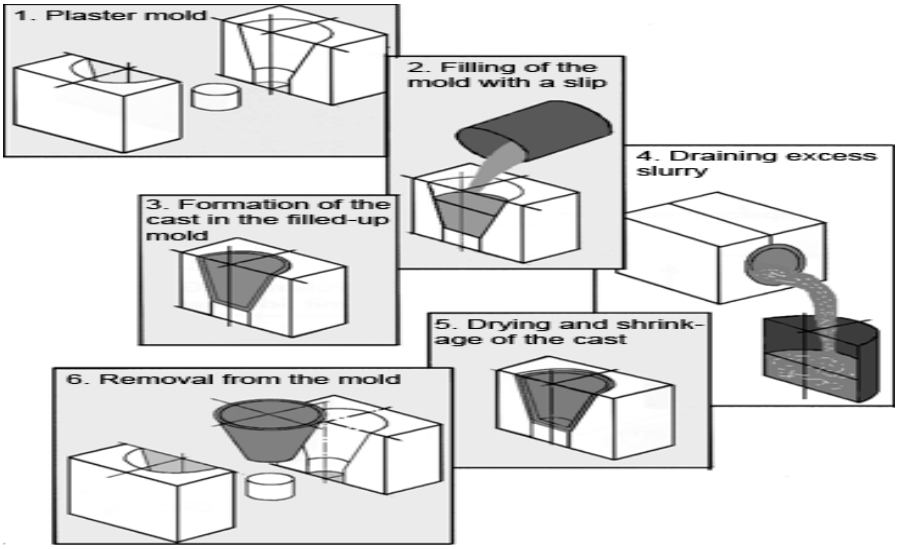

Figure 13: The slip casting process (schematic)[28].

1.7.2 Drying of green bodies

After the green ceramic bodies are formed, the drying process is started, the evaporation of water leads to the convergence of the particles, causing shrinkage. The choice of drying technique is important, as it is energy intensive (to provide the latent heat of evaporation). Today, industrial drying with hot air is most common method. Generally, drying is done at temperatures between 90° and 130°C, with the possibility of recovering the hot air from the kiln.

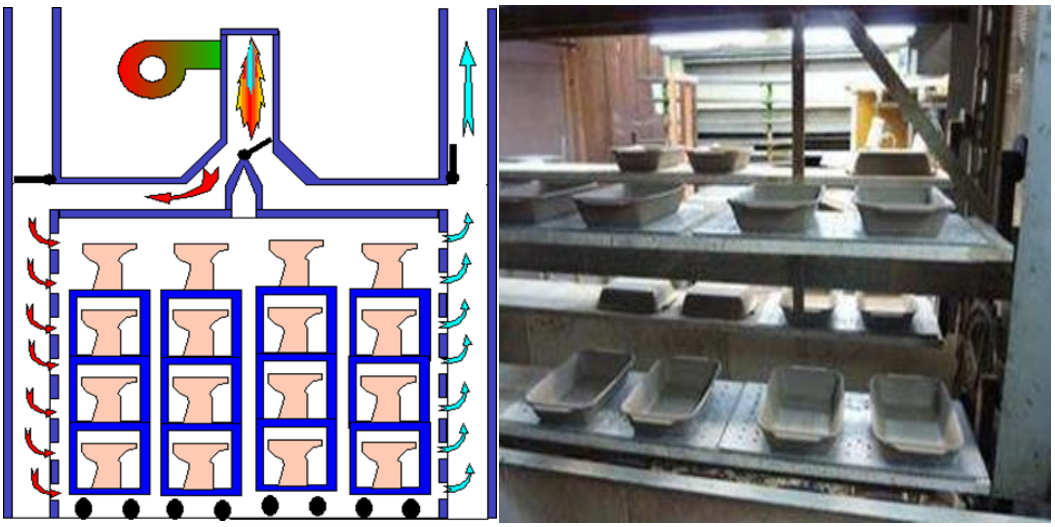

Figure 14: Industrial drying of sanitary bodies.

1.7.3 Glazing

Sanitary ceramic bodies surfaces are relatively mat and rough. Therefore, they need to be glazed is glazed to seal the surface. After glazing, the bodies are often decorated and color prints are applied. During glazing, the ceramic bodies are dipped in a glass powder suspension; the glaze can be applied either by immersion or by spraying. For small amounts of bodies, glazing is performed manually while for large amounts, automatically (Figure.15) [24].

Figure 15: Glazing methods.

1.7.4 Sintering

Sintering is the last phase of the production cycle of sanitary ceramics; the most critical operation during which the materials are heated to high temperatures (up to 1250°C), so that a series of complex chemical and physical transformations can occur. As a result of these changes, ceramic sanitary ware achieve their final characteristics: - hardness and mechanical strength - abrasion resistance - fusion of the glazes - non-absorbency of the body (at least for that of vitreous china).

Sintering can be considered as an operation, which consists in transforming a shaped material into a ceramic product (dense or porous) with a certain mechanical strength. It is a process of consolidation without total fusion, as shown in figure 16. The consolidation due to the development of links (or necks) between the grains, is often accompanied by a densification (elimination of the pores) and a coarsening of the grains (decrease of the number of grains).

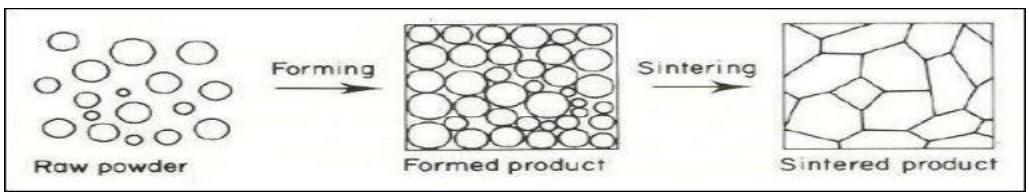

Figure 16: Diagram illustrating densifying sintering [19].

1.7.5 Decoration

Various techniques can be used to apply the colors to sanitary ceramic products. Direct techniques, include manually or by direct or indirect printing on the surfaces of sanitary ware.

Figure 17: Decoration techniques.

1.8 Physical-chemical changes during the sintering process

The raw materials used in ceramic bodies, are usually complex mixtures of clay minerals with other mineral materials such as quartz, feldspars, carbonates, gypsum, iron oxides and sometimes-organic materials.

- **30°C - 150 °C**

When clay-based ceramics products are fired in a kiln, the residual humidity is removed at this temperatures range. After this step, the body should not contain more than 1% humidity.

- **150°C - 550°C**

This temperature leads to the loss of chemical water, and the transformation of the crystal structure of kaolin, thus the phase transformation into a new phase with high reaction capacity, which is the metakaolin $Al_2O_3 .2SiO_2$.

In ceramic bodies which have a composition (50% mass of kaolinite clay, 25% mass of feldspar and 25% mass of quartz), Metakaolin is formed by dehydroxilation of kaolin clay in the temperature range 450-550 °C [39].

$$Al_2O_3.2SiO_2.2H_2O \text{ (kaolinite)} \longrightarrow Al_2O_3 .2SiO_2 \text{ (méta-kaolinite)} + 2H_2O \text{ (g)}$$

- **550ºC - 700ºC**

Then at 573°C, α quartz transforms to β quartz. The decomposition of biotic carbonates and micas in the clay, also begins at this stage.

- **700ºC - 1050ºC**

Calcium carbonate and magnesium in ceramic bodies begins to decompose.

- **950ºC – 1100ºC**

At this temperature, the vitreous phase formation and the shrinkage of bodies start.

- **1100ºC – 1250ºC**

At this high temperature, the silica melts and forms glass and a strong shrinkage occurs. At the same temperature, the spinel phase transforms to form mullite. The cristobalite and the amorphous silica form the residual quartz. A sufficient soak time is given to even out the temperature in all areas of the sanitary ware body [40, 41].

1.9 Industrial solid wastes

Sanitary ceramics are the most common in daily life; they are used everywhere. The population growth in the world requires an increase in the production of these products. All this may cause a depletion of raw materials over time. For these reasons, more research is needed among the scientific community, to find new resources or alternative materials that meet the standards and needs [42].

In general, the increase of solid wastes produced by various industries requires ecological management and forward vision. Solid wastes are produced by chemical, metallurgical, cement, ceramic, glass, food processing, paint, pharmaceutical, textile and petroleum industries. Solid waste can be classified into two broad categories: organic and inorganic. Mostly, organic waste comes from food processing plants, paper mills and textile industries. Moreover, inorganic wastes include wastes resulting from metals, ceramics, glasses and some chemicals manufacturing [43]. The volume of inorganic waste (from construction and demolition activities and from mining and quarrying) across Europe, exceeds 1500 million tons [44].Inorganic waste does not decompose, usually taking more than 500 years to decompose [45].

The growth in industrial activities has increased the amount of solid waste generated in Algeria, particularly in the capital and major cities. From the national register of industrial and hazardous waste, the total industrial waste generation, including both non-hazardous and inert industrial waste, is 2,547,000 tons annually[46]. The source of these wastes can be assumed to be as follows:

- 50 % - Steel, metallurgical, mechanical and electrical industry.
- 5 % - Construction materials industry.
- 2 % - Chemical and plastics industry.
- 29 % - Food and tobacco industry.
- 14 % - Textiles, confection, leather, shoes and paper industry [46].

The National Waste Agency (AND) reports that each inhabitant produces 0.9 kg/day of solid waste for urban areas and 0.6 kg/day for rural areas. The production of solid wastes in the capital is close to 1.2 kg/day [47].

Figure 18: Landfill of Ouled Fayet (Algiers)[48].

Considering the most densely populated wilaya's, their current and future waste generation can be approximated as summarized in following table:

Table 3 :Waste generation in 6 wilaya's with the most dense population [49].

	2016		2028	
	population (mln)	waste production (ton/year)	population (mln)	waste production (ton/year)
Algiers	3,600	1.314.000	5,542	2.256.821
Oran	1,752	639.480	2,697	1.098.320
Blida	1,208	440.920	1,860	757.289
Constantine	1,130	412.450	1,740	708.391
Boumerdès	0,966	352.590	1,487	605.580
Annaba	0,734	267.910	1,130	460.141
Total	**9,390**	**3.427.350**	**14,455**	**5.886.543**

Industrial waste is dealt with through laws and orders; technical backfill centers are established locally in all wilaya's. Their role is to receive, sort and landfill these wastes. The operation of such a center is as follows: the wastes are transferred to a separation line after the process of weight, storing and verification. PET, metals and other recyclables are sorted, mainly by hand. Finally, the organic wastes are carefully buried [49].

Until now, the recycling and valorisation of building materials wastes and glass wastes in Algeria, is not engaged by any factory. This is a source of concern and a motivation to study the mechanisms of recovery of these wastes [49].

In this thesis, we have investigated the recycling and valorization of 3 industrial wastes as partial substitutes for feldspar in the composition of sanitary ceramic bodies. These wastes are the blast furnace slags (from the El-Hadjar factory, Annaba, Algeria). Soda-lime glass wastes (from the African glass factory, Jijel, Algeria) and sanitary ceramic wastes (from the sanitary ceramic factory, Jijel, Algeria).

1.10 Blast furnace slag, soda-lime glass waste and sanitary ceramic waste in the ceramic industry.

The chemical and mineral compositions of certain inorganic industrial wastes are similar to those of some raw materials; this is what guides us in selecting which waste as a partial substitute material in the composition of various types of ceramics. Blast furnace slags, Soda-lime glass wastes and sanitary ceramic wastes have a chemical composition rich in various elementswhich enhance the performance of the products, when they are incorporated in ceramic slip composition. In this way, many types of ceramics have been prepared from these wastes.

1.10.1 Blast furnace slag (BFS)

Blast furnace slag is a by-product of the iron production. The annual worldwide production is around 390. 000 million tons [50]. In the north-east of Algeria in particular, the El-Hadjar Iron Factorie produces over 700 million Kg/year of BFS [51]. Each ton of steel can produce about 300 to 900 kg of blast furnace slag. In blast furnaces, iron ore is transformed into coke between 1350°C and 1550°C to form raw iron while the combination of silica and alumina with lime and magnesium, form molten slag (Figure. 19). Afterwards, the raw iron settles in the lower part of the furnace, due to its high density of about 7, while the molten slag floats in the higher part, because of its low density compared to the raw iron which is 3. Finally, the molten slag is separated from the cast iron and cooled [52].

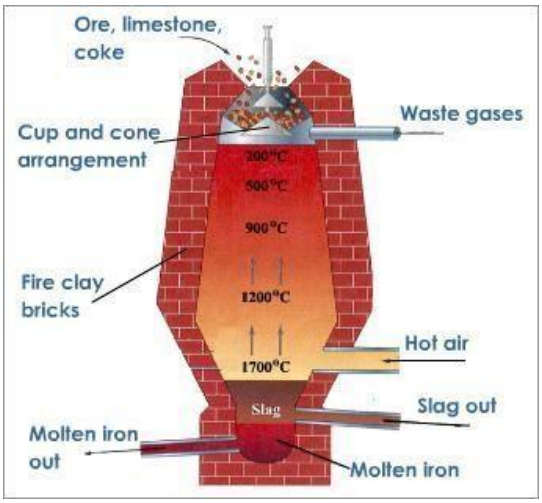

Figure 19: Generation of iron and slag in blast furnace.

According to the cooling process, the slag can be divided into two parts: crystalline and vitrified (granular) (Fig 26). Slag slowly crystallizes, in open air, into a hard rock after

solidification begins, then crumbles crushes and sifts. It can then be used as aggregate (used in sub-road piles for example). However, a slag is said to be vitrified, if it is cooled or quenched suddenly (water sprayed abundantly at a high pressure of 0.6 MPa); more than 80% of amorphous structure is formed. Therefore it has an internal energy higher than that of the crystalline state, which makes it more reactive chemically and having latent hydraulic properties [53].

Figure 20: Blast furnace slag, crystalized and vitrified [54].

The main constituents of blast furnace slag include CaO (30-50 %), SiO_2 (28-38 %), Al_2O_3 (8-24 %) and MgO (1-18 %). Usually, the increase of CaO content in the slag leads to an increase in basicity and compressive strength of the slag. MgO and Al_2O_3 contents show the same effect up to 10-12 % and 14 % respectively [55, 56].

The rich content in CaO, SiO_2 and Al_2O_3 of blast furnace slag and its low cost as industrial waste, motivated researchers to conduct studies on its incorporation and valorization in the formulation of various ceramics. In this respect, many scientists have demonstrated that the use of BFS as a substitute material enhances the microstructure and physical properties and therefore, the success of the product.

1.10.1.1 Blast furnace slag in glass-ceramic

In 2004, A.A. Francis found that blast furnace slag (BFS), with its varied chemical and crystalline composition, could transform into a glass-ceramic material. Barium aluminium silicate, diopside pyroxene and gehlenite, were identified as the main crystalline phases. The level of crystallisation was estimated according to the evaluation of density changes at different temperatures; a maximum density was reached at 900 C [57].

In 2009, Liu et al incorporated blast furnace slag with 5 wt.% potassium feldspar in the composition of the glass-ceramic, this enhanced the sintering properties and contributed to the formation of gehlenite ($2CaO. Al_2O_3. SiO_2$) as the main phase. This combination also leads to a high flexural strength of 85 MPa, a high hardness of 5.2 GPa and a water absorption smaller than 0.14% [52].

In 2011, glass-ceramics were also produced using molten BFS up to 90 wt. % with about 10 wt. % silica sand by Zhao et al. The sensible heat of the molten BFS reduces significantly energy consumption. The crystallisation process happens at 960°C, where the main crystalline phases were akermanite and diopside. The strength of glass-ceramic obtained with the mixture (84 wt. % BFS-8.48 wt. % SiO_2) was also improved, up to 120 MPa using 7.6% CaF_2 addition [58].

In 2021, $CaO-MgO-Al_2O_3-SiO_2$ glass-ceramic has been produced from BFS, which was used as starting material. The findings indicate an early crystallisation at 980°C with high corrosion resistance and have acid and alkaline resistance of 96.64% and 99.41%, respectively. Moreover, this incorporation of BFS as a raw material leads to preparing ceramic-glass using one-step method, which is extremely important for saving energy and waste valorisation [59].

1.10.1.2 Blast furnace slag in traditional porcelain

Dana et al proved that the partial substitution of feldspar by BFS, in a triaxial porcelain formulation (45 wt.% Clay-Kaolin, 30 wt.% feldspar and 25 wt.% quartz) enhances strength up to 60 Mpa by 5 wt.% BFS addition. that is due to the stronger pre-stress from the difference in the coefficient of thermal expansion between the glassy phase, quartz and the formed anorthite. The density was also improved by the early glazing [60].

New low-cost porcelain, with no traditional fluxes and containing 30, 50 and 70 wt. % BFS, was produced at 1200 °C. A high crystallinity material was formed by the presence of pyroxene and anorthite solid solutions. Flexural strength and hardness increase with the BFS incorporation amount. Ceramic with 70 wt. %, achieved the most positive results, which could be attributed to its fine crystalline structure and the additional crystallisation upon the cooling process[8].

Mixed BFS-kaolin was used to prepare new ceramic by the traditional firing process. Combination of BFS with 10wt. % kaolin gives gehlenite ($Ca_2Al_2SiO_7$) as the main phase with a gradual appearance of anorthite with increasing kaolin contents. The melting of BFS is at a low temperature of 800–900 °C; this affects the sintering process such as the formation of the early glassy phase, which enhances the densification of the ceramic. The mixture BFS- 10 wt.% kaolin was found to be the optimal ceramic composition with high physical-mechanical and structural properties [61].

In 2014, Siddiqui et al produced traditional porcelain with a ceramics composition: (45 wt. % kaolin, 25 wt. %fly ash and 30 wt. %feldspar), then feldspar was substituted by BFS up to 20 wt. % which enhanced various physical properties. The ceramic body containing a combination of BFS and feldspar has the maximum strength (90 MPa) caused by the existence of mullite particles and a reduced number of fractures resulting from the high difference in the coefficient of thermal expansion between the formed anorthite, quartz and glassy matrix during the cooling process [62].

1.10.1.3 Blast furnace slag in ceramic tiles and wall tiles

The ceramic tiles were produced from a mixture of granulated BFS and ordinary clay. The optimal physical-mechanical properties were obtained when the lime/silica ratio is in the interval of 0.1–0.3. Tiles containing 50 wt. % granulated BFS recorded a high mechanical strength by the formation of a great number of fine grains embedded in the vitreous matrix. The use of kaolin with BFS helps to enhance the formation of the liquid phase, which is reduced when using BFS alone [63]. 2002

Unglazed ceramic tiles based on granulated BFS and clay mixture have been prepared with 0 to 100 wt. % BFS. The crystalline phases of the standard unglazed tile was mullite with the formation of anorthite, gehlenite and wollastonite during the addition of BFS. Ceramic with 60 to 100 wt. % BFS, can be used in tile formulations as they meet the requirements of standard tile properties, such as water absorption, thermal shock (Harcourt), the freeze–thawand efflorescence[64].2007

In 2005, Dana et al substituted feldspar-quartz by including BFS–fly ash wastes in the same composition of traditional porcelain tiles (45 wt. % Clay-Kaolin, 30 wt.% feldspar and 25 wt.% quartz); this substitution enhances anorthite phase formation and improves the mechanical strength by the effect of stronger pre-stress between glassy phase, mullite and

the formed anorthite. The addition of two combined wastes in porcelain composition, provokes the early vitrification process at 1175°C by the effect of mixed quartz-mullite in fly ash with alkaline earth oxides in BFS. This early vitrification reduces the thermal energy without affecting the physical-mechanical properties [65].

In 2015, Ozturk et al showed that ceramic wall tiles can be produced using 33 wt. % BFS instead of a kaolin-limestone mixture, which reduces water absorption and increases bending strength by 25%. BFS is considered a source of anorthite phase, formed by its high content in CaO. The anorthite crystallisation enhances the strength and chemical stability of the ceramic body and reduces the thermal expansion coefficient [66].

1.10.1.4 Blast furnace slag in porcelain stoneware, refractory ceramic and sanitary ware bodies.

In 2016, Pal et al synthetized a porcelain stoneware using the composition mass (45% kaolin, 40% feldspar and 15% quartz) with a progressive substitution of feldspar by BFS up to 30%. The peaks of kaolin dehydroxylation and mullite crystallisation were not affected by BFS addition. The thermal expansion rate of porcelain containing BFS was lower (0.35–0.37 %) than that of standard porcelain (0.437 %) attributed to the formation of anorthite crystals. Moreover, a high flexural strength (81 MPa) was recorded from samples containing 30 wt. % BFS; this results from the difference in thermal expansion coefficient between mullite, glassy phase and the formed anorthite [39].

In 2021, conventional ceramic refractory was prepared by replacing fine clay with BFS up to 20 wt.%. The incorporation of 10 wt.% BFS, was found to be the optimal composition that enhances various physical-mechanical properties, including a bulk density of 2.61 g/cm^3, an apparent porosity of 10.64%, a water absorption of 4.08% and a mechanical strength of 94.5 MPa. CaO-rich BFS provides a denser ceramic matrix by reducing the porosity through the crystallization of anorthite with the silica-rich liquid phase, thus improving mechanical resistance by about 74% [67].

Sanitary ceramic bodies were synthetized by the substitution of sodium feldspar with 15 wt. % of BFS and 4 wt. % % spodumene. The flexural strength increased approximately by 67% and the thermal expansion coefficient values were reduced approximately by 17%. This is significant for the stability of the final product. BFS with spodumene decrease both

raw material and energy costs by reducing the firing temperature by about 60°C and improves physical-mechanical properties [21].

1.10.2 Soda-lime glass waste (SLGW)

Waste glass is generally considered as a highly recyclable material in the manufacture of the same product. As a very high proportion, without affecting the technical characteristics and the quality. It has been evaluated by the Glass Packaging Institute (2015), that about one ton of natural raw material can be saved by the use of ton of recycled glass, in the manufacture of new glass products [68].

Soda lime glass is the most common and most used in daily life; thus, it is available at a low cost. It is manufactured by melting limestone ($CaCO_3$), silica sand (SiO_2), sodium carbonate (Na_2CO_3). Soda-lime glass is technically classified as: flat glass for windows, glass for containers or container glass. These two types of glass are different in their applications and their manufacturing methods (float glass for windows, blowing and pressing glass for containers) [68].

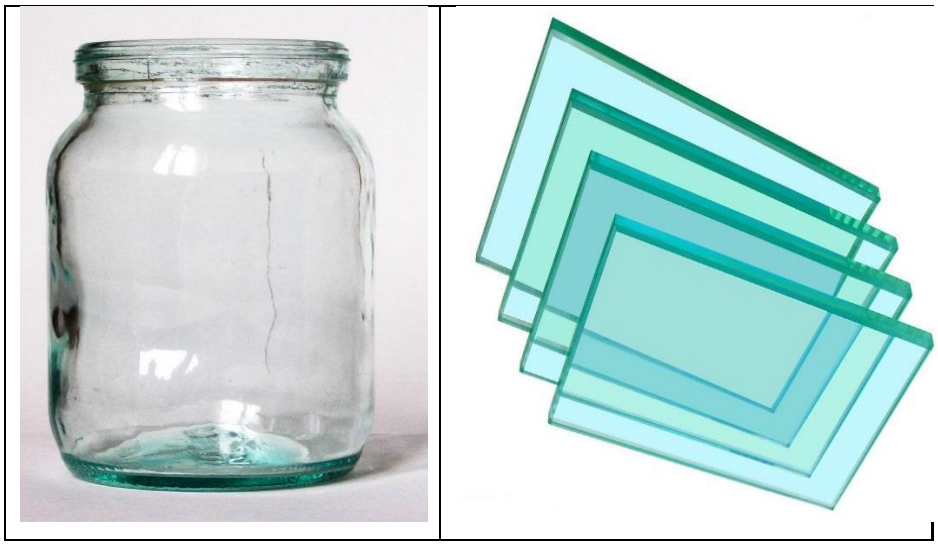

Figure 21: Soda lime glass, container glass and flat glass.

The increase in the production over time, is accompanied by an increase in waste production. According to statistics, the volume of glass waste generated in the European Union in 2014, is nearly 18.5 million tons [68]. The continuous increase in the generation of waste glass worldwide, requires its use in various fields of recycling. In addition to its use in construction, recent studies have shown promising results for using waste glass in the manufacture of various types of ceramics.

Soda-lime glass waste is one of the most common glass wastes, generally, coming from containers and flat glass. However, although they have similar chemical compositions, the different sizes, colors and shapes of packaging containers, make the recycling of waste glass containers more difficult than recycling flat glass waste.

Figure 22: Soda lime glass waste.

The composition of soda lime glass waste is very rich in SiO_2, alkali-alkaline earth oxides (CaO and Na_2O). In the ceramic industry, the amount of alkali–alkaline earth oxides is very significant in improving the glassy phase and reduce firing temperature. For these reasons, many researchers have investigated the recycling and incorporation of soda-lime glass waste in various ceramics.

1.10.2.1 Soda-lime glass waste in glass-ceramic

Glass-ceramic was prepared from coal ash and SLGW in the range 20 to 60 wt. %. The XRD analyses of the glass with 100 wt. % ash, revealed cristobalite as the main phase with small quantities of mullite, $Ca(Al, Fe)_{12}O_{19}$ and hematite. Glass-ceramic with 20 wt. % SLGW reduced cristobalite phase and replaced it by the main phase Al_2SiO_5, forming the solid solution of albite ($NaAlSi_3O_8$)-anorthite ($CaAl_2Si_2O_8$) with a small amorphous phase at 25°. With 40 wt. % SLGW addition, the solid solution albite-anorthite is the main element with a small formation of pyroxene. The solid solution albite-anorthite is well developed with augite $Ca(Mg,Fe)Si_2O_8$ as the secondary crystalline phase (augite peak intensity is~20% of albite-anorthite peak) in glass containing 60 wt. % SLGW. The formation of solid solution albite-anorthite increases with soda-lime glass waste addition [69].

Wollastonite glass-ceramics were produced by mixing SLGW powder from the waste of window glass with a synthetic crystallisation promoter. The promoter has a chemical

composition of 30 wt. % kaolin, 50 wt. % $CaCO_3$, 10 wt.% $BaCO_3$ and 10 wt.% ZnO. SLGW was combined with 12, 15, 20 and 25 wt. % crystallization promoter, to prepare four glass-ceramics. The optimal composition is 85 wt. % SLGW with 15 wt. % crystallization promoter at 850°C; this improved the compressive strength 247 MPa, bending strength 119 MPa, hardness 5.32 GPa and reduced water absorption to 0.27%, This process is very effective in reducing energy consumption and is also environmentally friendly; So, it can be valued in the building materials industry [70].

Moreover, SLGW was used to prepare sintered glass-ceramic, in the range 50 to 65 wt. % with clay and fly ash. Low water absorption was recorded at 1050°C in glass-ceramic with 65 wt. % SLGW, we noted a bending strength of 38.2 ± 5.4 MPa. The main crystalline phases are wollastonite and anorthite, with traces of albite which increased during the SLGW addition [71].

High CaO glass-ceramic was prepared using 79 wt. % SLGW and 21 wt. % CaO with a ratio of SiO_2: CaO set at 51:44; measurement were made at various temperatures. The density values increased with temperature; the highest bulk density reached (2.82 g/cm^3) at 1100°C. Wollastonite ($CaSiO_3$) was the major phase in the fired glasses at 1100°C, with a small amount of nepheline ($NaAlSiO_4$) phases appearing at 900°C. The high mechanical chemical strength of the nepheline phase maked it suitable for use in microwave ovens and dental applications. The energy band values acquired band were increased from 3.87 to 4.83 eV with the increasing sintering temperature. The existence of Si-O-Ca vibrational bands in the FTIR spectra, confirms the formation of the wollastonite phase [72].

Fluoride glass-ceramics were produced using 25 wt. % SLGW, and heated at different sintering temperatures. The samples sintered at 1000 °C showed the best properties: the highest density was 2.81g/cm^3 and shrinkage was about 5.3%. XRD analysis indicates fluorapatite, mullite and anorthite were the main phases at 1000°C. SEM showed an increase of porosity values at higher temperatures, due to the growth of crystals resulting from the transformation glass phase. FTIR spectra were consistent with XRD, SEM and physical properties [73].

Turquoise jewelry glass-ceramic was prepared by mixing 90 wt. % SLGW- 10 wt. % kaolin with progressive addition of coloring oxides by 1 wt. %. Synthetic turquoise based on recycled waste glass has ideal properties compared to natural turquoise. It can be made

into all desired shapes for jewelry items. The production of this turquoise was low cost because of the sole heat treatment at 1000°C without the consumption of high-quality raw materials. The final results show that one-step sintering is the most beneficial method for producing jewelry imitation glass ceramics from waste materials [74].

1.10.2.2 Soda-lime glass waste in tiles

The porcelain stoneware tile body was manufactured by incorporating soda-lime glass waste as a substitute for feldspar flux by 6 wt. %. Mullite and quartz were the main phases with the glassy phase. Mullite and glassy phase formation increased, while quartz was reduced by the addition of SLGW; this change in microstructural evolution is attributed to the presence of mixed alkali-alkaline earth oxides (Na2O and CaO) in SLGW, which leads to the early glassy phase formation. There was a slight improvement in the physical properties and a decrease in the deformation of pyroplastics at all temperatures [75].

Soda-lime glass waste was added to a mixture composed of orthoclase feldspar, quartz, grog and three types of kaolin to produce floor tiles. The glazed floor tile containing 23 wt. % SLGW, which is the optimal composition resulting in high mechanical strength at 1100°C. The sample containing 33,3 wt.% SLGW with a fast-fired time of 1 h at 1100°C, has the best physical-mechanical properties for unglazed floor tiles. SLGW speeds up the sintering process by the early glassy phase formation, which makes it a very economical additive by reducing the firing time and raw material consumption [76].

SLGW could replace traditional fluxes, such as sodium feldspar in the composition of stoneware tile bodies. Its presence does not significantly affect the technological properties during the milling, pressing and drying process. However, it has important effects on the properties of the final product. During the firing cycle, SLGW speeded the densification procedure, with positive effects (reduced open porosity) combined with some negative effects (increased shrinkage values and closed porosity...). Although these differences are minor and acceptable with the addition of 5 wt. % waste, they were evident when 10 wt. % waste added. SLGW improved the sintering kinetics by balancing the low viscosity glass phase with the mullite and quartz crystalline phases [77].

Substitution of various amounts of feldspar with glass waste in a stoneware tile mixture changes the alkali contents in the composition. Calcium and magnesium amounts increase by SLGW addition with alumina decreasing, thus affecting the viscosity of the formed

glassy phase. 20 wt. % SLGW– 80 wt. % clay is the optimal formulation for stoneware tile in terms of water absorption and abrasion resistance at 1150°C. The composition: 60 wt. % clay– 20 wt. % feldspar- 10 wt. % quartz– 10 wt. % SLGW, gives the best flexural strength and Weibull's modulus, with a clear reduction in total porosity. From XRD analysis mullite and quartz are the main crystalline, with a gradual formation of the anorthite phase by increasing the SLGW. The 25 wt. % feldspar– 5 wt. % SLGW was the only product which could be considered convenient as a porcelain tile due to its optimal physical-mechanical and structural properties [78].

As the firing temperature increased, the properties of floor tiles containing SLGW changed: water absorption reduced to 2.54% and bulk density increased to 2.02g/cm^3 when 25 wt. % SLGW added. The flexural strength of the floor tiles increased and reached a maximum; the highest value recorded in tiles containing 25 wt. % glass waste, is up to 21.64 MPa. This composition could be applied as wall or floor tiles using soda-lime glass waste content 25 wt. % at 1200 °C [10].

1.10.2.3 Soda-lime glass waste in traditional porcelain

Traditional porcelain made of from clay-kaolin, flux and quartz, is one of the most common ceramic types. Soda-lime glass waste was introduced in the porcelain composition as raw material. Water absorption decreased below 1%, while the porosity dropped below 4% for samples fired at 1200°C, which was according to the standard requirement. Bulk density increased with temperature and glass phase formation increased by the SLGW addition, while shrinkage reduced at 1200°C. Low wear loss was recorded for ceramics subjected to 1200°C. Flexural strength values were not consistent with physical-structural properties, although it was within the requirements of the porcelain industry. The optimal sintering temperature for soft porcelain, is 1200°C, better properties are obtained. These results are supported by the literature [79].

Feldspar was substituted by Soda-lime glass waste to prepare triaxial porcelain 50 wt. % kaolin 25 wt. % quartz and 25 wt. % SLGW. The prepared porcelain had excellent properties, SLGW reduced the firing temperature to1240°C compared to the traditional porcelain 1340°C, thus reducing production costs. SLGW worked as a strong flux and reduced water absorption to 0.39 % at 1240 °C and 0.15 % at 1260°C, while its value was 2.55 for traditional porcelain (containing feldspar), at the same temperatures. XRD analysis

showed that mullite and quartz were the main phases, while the presence of calcium oxide CaO within the soda-lime glass waste, caused a casualization of the anorthite phase in the matrix. The mechanical properties including fracture toughness and flexural strength were responsive to the requirements of porcelain industry [80].

The effect of SLGW incorporations, on the sintering properties of fly ash -based porcelain was investigated. The addition of 10-25 wt. % SLGW to the porcelain, lowered the activation energy necessary to initiate the sintering process. Therefore, the level of densification could be higher by the lower activation energy and glassy phase formation. SLGW accelerated the condensation process, increased shrinkage and reduced open porosity. Porcelain production may be possible at 1200C instead of 1350C. Moreover, it is possible to substitute quartz and potassium feldspar with soda-lime glass waste and fly ash as raw materials for porcelain production [81].

1.10.2.4 Soda-lime glass waste in sanitary ceramic bodies

The effect of firing time, the particle size of soda-lime glass waste and quartz on sanitary ceramic reactions and their macroscopic properties, has been investigated. The mullite/glass formation, the activation energy evolution and macroscopic properties (linear shrinking linear thermal expansion and water absorption), were affected by SLGW addition and its particle size. The mullite phase formation was accelerated when Na-feldspar was substituted by SLGW and also by the decreasing of quartz d_{50}, which increases the reactivity of slip and reduces the vitrification grade, while mullite increased with a decrease of SLGW d50. SLGW reduced the firing temperature of the sanitary-ware body (30–90 K); in the same interval values (1500–1530 K); this reduces fuel consumption and CO_2 emissions. Sanitary bodies based on soda-lime glass waste recycling have multiple advantages, including accelerating the reactions of the mullite and glassy phase, as well as meeting the technological characteristics and the requirements of the sanitary ceramic industry [82].

Reducing the firing temperature for the sanitary ceramic bodies (from 1250 to 1170 °C) was the subject of a study by “Sanitser” Life European project. Quartz and feldspar were substituted by recycled blend materials (soda-lime glass waste 9.5 wt. % + pitcher +granite) with a small amount of flux (2.38 wt. %) in the production of new vitreous china body (sanitser ceramic). The total amount of introduced recycled blend materials was 43.62wt. %. Tests on the sanitser composition, indicated that it has the same final physical-

chemical properties as the industrial vitreous china (VC) body. Sanitser's dilatometric coefficient had values consistent with traditional sanitary ware bodies. The main phase found after firing, was the glassy phase (58% to 63%), quartz (14-18%) and mullite (11-18%). Small quantities of feldspar (plagioclase) and cristobalite also were present. The raw materials (feldspar and quartz) were substituted with recycled (materials containing low-free silica. This facility obtains a ceramic body less hazardous to employees' health. Finally, regarding technology, the possibility of firing the VC body at a lower temperature of about 80°C, could leads to energy saving [83].

The kinetics of mullite formation in vitreous ceramics containing soda-lime glass waste and its effect on microstructure development was studied. The substitution of 30-50 wt. % feldspar with SLGW accelerates the kinetics of the mullite growth reaction and provides macroscopic characteristics of the ceramic produced, that satisfy the latest technological requirements (significant flexural strength and very low water absorption values). The incorporation of SLGW lowered the firing temperature by 70-100 °C in the same traditional process, which leads to less fuel consumption and reduced CO_2 emissions during the firing cycle. This work has many good results and perspectives including, the conservation of mineral materials in terms of feldspars, a reduction in production costs, recommendation for the rational management of used glass waste by its recycling in other ceramic materials [84].

1.10.3 Sanitary ceramic waste (SCW)

Sanitary ceramic waste (SCW) comes from defective pieces, which have deformation in their technical characteristics such as shrinkage, cracks or glaze imperfections. Every month about 20-30 tons of SCW are disposed of, from sanitary ware factories [85]. Sanitary ceramic waste represents 8% of the seven million pieces manufactured each year in Spain, due to a variety of deformations. Sanitary ceramic waste (SCW) has environmental benefits because it can be easily separated and recycled. Generally, SCW does not contain impurities such as cement, gypsum or bonded mineral reinforcements [86].

In general, sanitary ceramic waste has a chemical composition rich in SiO_2 and Al_2O_3 with some alkaline oxides, which include: Na_2O, K_2O and CaO, in addition to Fe_2O_3 and some traces of various oxides used in the preparation of the glaze. This ideal composition makes SCW worth recycling.

Figure 23: Sanitary ceramic waste.

1.10.3.1 Sanitary ceramic waste in glass- ceramic production

The low-cost ceramic glass was prepared from sanitary ceramic waste and basalt glass crystal. Sanitary ceramic waste was incorporated into the glass-ceramic composition in amounts ranging from 10 to 50 wt. % of the batch components. XRD analysis shows that the samples containing 0 to 20 wt. % sanitary ceramic waste, have anorthite ($CaAl_2Si_2O_8$), olivine (Fe, Mg)$2SiO_4$, magnetite (Fe_3O_4) and augite Ca (Fe, Mg)Si_2O_6 as the major crystalline phases. In glasses with 30 to 50 wt. % SCW, the augite was more developed with the appearance of quartz resulting from high SiO_2 content in SCW. The final glasses are characterized by very low water absorption, a low-cost production cycle, also, the mechanical properties were significantly superior to those of conventional ceramics including, hardness values in the range 9624 and 10074 MPa and flexural strength values between 92 and 135 MPa. The physical-mechanical properties showed that the best-tested glass was the glass with a mixture of 40 wt. % ceramic waste and 60 wt. % basaltic rock. These glass ceramics could be used for various purposes including floor, wall tiles and other products[87].

1.10.3.2 Sanitary ceramic waste in tiles production

Porcelain stoneware tiles were prepared using ceramic waste as an alternative raw material to feldspar in the range 0-32 wt. %. Partial substitution of feldspar by SCW, improved various physical-mechanical properties. XRD analysis showed that Quartz and mullite as major phases with some traces of corundum and albite. Quartz is a result of the siliceous nature of the ceramic waste, in addition to the undissolved quartz present in the compositions of the raw materials. The mullite phase results from the agglomeration of pure

clay residues infiltrated with feldspar. Secondary mullite is formed from the feldspar-rich melt in the firing process. Bulk density was increased (2.35-2.42 g/cm^3) which can be attributed to high mullite formation with SCW addition as well as reduction of the glassy phase; the latter has a lower density than other crystalline phases. The addition of ceramic waste up to 16 wt.%, decreases the water absorption by about 1%, which is attributed to the lower viscosity of SiO_2–rich melts of the SCW. The modulus of rupture achieved: 50-70 MPa may be related to the high crystalline phase's content in the matrix. Small colour darkening (ΔE around 0.25-1 for 4-16wt. % SCW addition; ΔE around1-2% for 16-32 wt. % SCW addition) was recorded; it may be the result of the presence of colouring oxides as TiO_2 and Fe_2O_3 in ceramic waste. Sanitary ceramic waste can be introduced into the porcelain stoneware industry as an economic, technological and environmentally correct solution. In conclusion, the addition of sanitary ceramic waste to stoneware tiles, reduces the sintering range and results in better mechanical properties [6].

Fired sanitary ceramic waste was introduced in floor tile compositions, by partially substituting potassium feldspar and albite, with up to 15 mass-%. The standard mass composition was: 50 wt.% ball clay, 25 wt.% albite, 20 wt.% potassium feldspar and 5 wt.% talc. The experimental findings showed that a suitable introduction of sanitary ceramic waste resulted in floor tiles with better physical-mechanical properties. 1200°C was the optimal firing temperature, the water absorption of tiles containing SCW-albite was decreased by SCW addition. The same behaviour was observed for tiles containing SCW-potassium feldspar. While the best water absorption value was recorded in the tile mass 20 wt.% albite, 15 wt.% potassium feldspar and 10 wt.% SCW; this can be explained by the reduction of ($RO+R_2O$) oxides by increasing waste and decreasing albite, thus leading to a low glassy phase and the presence of the highly viscous SiO_2-rich melt from the waste. Bulk density values increased with the increasing firing temperature and tiles containing SCW reached a bulk density in the range of values suitable for the manufacture of sanitary ware bodies. Flexural strength was in the range of (40 – 50 MPa), which is controlled the crystalline nature of the newly formed phases in the samples. SCW addition increased the coefficient of thermal expansion. More addition of SCW, reduced the dissolution of quartz and resulted in the development of the glassy phase, which has a lower coefficient of thermal expansion, favouring the presence of stable crystalline quartz having a high thermal expansion coefficient. The SCW addition to floor tile productions does not induce

significant changes in the technological properties. The optimal amount for albite substitution in 5 – 10 wt. % and 10 – 15 wt. % potassium feldspar respectively [88].

Kaolin was substituted by sanitary ceramic waste (max. 15 wt. %) in the formulation of ceramic wall tiles products. All compositions were sintered at 1145°C. The apparent density and flexural strength increased with the increasing amount of sanitary ceramic waste, while the firing shrinkage was reduced. Lower shrinkage values and larger open porosity values (30.77-31.46%) resulted from $CaCO_3$ decomposition to CaO. The interaction of calcium oxide with the amorphous phase of the kaolin, led to the fractionation of the mixture and the formation of a low-viscosity liquid phase, which allowed the formation of high porosity and the crystalline phases of anorthite and gehlenite in the ceramic. Flexural strength increased (202.5–205.5 kg/cm^2) with the increase of the content of the ceramic waste. Flexural strength has a direct relationship with the amount of mullite present in SCW, strength increases with mullite content. There was the no-significant effect on the mass loss of tiles; a slight increase appeared in the samples containing SCW due to the dehydration of crystal water and calcite decomposition. Quartz and anorthite were the main phases, with the appearance of mullite and cristobalite, brought by SCW addition. First, gehlenite was crystallised from calcium oxide and meta kaolinite. Next, anorthite was produced from gehlenite, meta kaolinite and fine-grained quartz. The addition of sanitary ceramic waste reduced the moisture expansion from the formed crystalline phases, including anorthite, gehlenite and mullite [89].

Glazed porcelain tiles were produced using sanitary ceramic waste as an alternative material to feldspar and pegmatite. The technological properties of glazed tiles were affected by the amount of ceramic waste added and the type of material replaced. Flexural strength increased with the increase of SCW amount as a replacement for pegmatite. The tile bodies were affected by the mullite content in ceramic waste, while thermal shrinkage remained almost constant. The density increased above 900 °C; this directly related to the increase in the glassy phase amount. In addition, the crystallization of primary mullite crystals from the spinel phase, produced greater densification. There was an increase in water absorption and thermal shrinkage values for the samples containing ceramic waste as an alternative to sodium feldspar, while flexural strength was reduced; therefore, replacement of feldspar with ceramic waste is only appropriate with the addition of less than 5 wt. %. The crystalline phases in glazed tile bodies, include a glassy phase, mullite,

quartz, albite and a small amount of cristobalite. Quartz in fired tiles is a residual phase and mullite showed up during the firing process, while the cristobalite crystals, originates from SCW. The sintering process is mainly controlled by the viscosity of the liquid phase. The incorporation of alkali and alkaline earth oxides into SiO_2 glass, leads to a reduction in the glass phase viscosity due to a greater number of non-bridging oxygen sites. Thermal expansion is a significant factor in determining the dimensional stability of tile bodies. The difference between the coefficients of thermal expansion of the quartz and the matrix, results in stress during the cooling process. This stress lead to cracks around the quartz particles and lead to increased microstructural damage. The most important finding of this study about the substitution of pegmatite and feldspar by sanitary ceramic waste is the reduction in the coefficients of thermal expansion, indicating that final products with dimensional stability and suitable deformation properties can be obtained [90].

1.10.3.3 Sanitary ceramic waste in its bodies production

Sanitary ceramic waste was utilised to substitute granite in ceramic slip compositions, Recycled sanitary ceramic formulations of 5, 10, 25, 50 and 100 wt.% SCW, were considered. The rheological behaviour of slips containing SCW show that the drying time and residue percentage, are similar to the standard slip. In addition, the rheology results showed that the addition of SCW enhanced the rheological performance with a lower thixotropy index. The dry shrinkage stayed the same for all samples, while the total shrinkage increased for the formulations containing SCW, due to a greater firing shrinkage. This confirms SCW action as a flux material, which develop the liquid phase during sintering and fill open pores, leading to decreased porosity. The granite is also used as a fluxing agent in the industry, the milled particles of SCW may be responsible for the liquid phase formation. The results of pyroplastic deformation meet sanitary industry requirements for samples containing 5 and 10 wt. % SCW, while the ceramics containing 25 wt. % SCW and above reduce the deformation. However, water absorption results did not show a clear correlation to SCW contents. All samples had a water absorption below 0.5%, which is recommended by the industry. Flexural strength was slightly reduced during SCW addition, the sample containing 5 wt. % SCW had a flexural strength equal to that of the standard ceramic (4.5 MPa); the ceramic industry adopts 2 MPa as the minimum flexural strength for raw bodies. For this reason, regardless of the reduction in strength, all bodies containing SCW satisfy the minimum requirement for flexural strength. Replacing granite

with ceramic waste by 100 % is considered a successful solution in the manufacture of ceramic bodies because it respects the industry requirements. However. The use of ceramic waste as a substitute for granite within 5 % the obtention of a good ceramic body with excellent properties. This process would reduce damage to the environment as well as reduce production costs [91].

Feldspathic flux was replaced by sanitary ceramic sludge waste (SCSW) in the rate 5, 10, 25, 50, 75, and 100 wt. % in the production of sanitary ceramic bodies. Rheological behavior was affected by pH and SCSW content. All proportions gave a rheological behaviour similar to the standard slip. The total substitution of granite by sanitary sludge waste showed promising results in all tests. Porosity was reduced by SCSW addition via the effect of liquid phase formation, which filled the open pores. Water absorption was reduced after SCSW addition; this was related to the high fluxing of SCSW, so that granite formed in high liquid phase amount. The evolution of water absorption values was very consistent with the results of linear shrinkage because increased pore filling leads to increased ceramics shrinkage. The flexural strength was decreased initially with replacement granite in mixtures, after which it regained its strength, but was not stray far from the ceramic industry requirements. The potential application of SCSW has been proved by the development of large hollow ceramic blocks, with higher wall thicknesses than without waste [92].

Sanitary ceramic bodies were produced using their glazed waste, as an alternative raw material for feldspar by amounts of 5 and 10 wt. % under three different sintering temperatures (1150 °C, 1175 °C, and 1200 °C). The incorporation of 5 wt. % SCW in the composition reduced the water absorption, while 10 wt. % SCW increased it. Generally, feldspar's role is to improve the liquid phase formation, which fills pores and enhances densification. 10 wt. % SCW reduced the fluxing reaction, as a result of the composition rich in Na_2O, K_2O, CaO and Fe_2O_3 which act on the sintering properties including crystallization, densification and eutectic point. A high density was recorded for ceramic containing 5 wt. % SCW at 1150°C, with a lower porosity of 2.8 %. All samples had a linear shrinkage of less than 12 %, which is very consistent with the sanitary ceramic requirement. Mass loss was reduced at all temperatures for ceramic containing 5 wt. % SCW. Impact and compressive strength were increased using 5 wt. % SCW, which enhanced mullite formation which is the main phase in the sanitary ceramic, that improve

the strength of the material. Post-sintering sanitary ceramic waste of 0-5 wt. %, could be used in the composition of commercial products. It is preferable to keep the firing temperature at about 1150 °C or below [85].

1.11 Conclusion

The enhancement of the properties of sanitary ceramic bodies has been the subject of many studies. Generally, sanitary ceramic bodies are constituted of a vitreous matrix including different crystalline phases, which are mullite, quartz and the vitreous phase. The mullite confers to the ceramic body, the necessary mechanical resistance aluminosilicate oxides existing in clay-kaolin mixture. Quartz regulates the softness of the clay, the expansion of the quartz volume, which can partially compensate for the shrinking effect of the glassy body when a large amount of vitreous phase appears during the firing process. The glassy phase is the most important constituent in the vitreous china bodies. Feldspar is the main source of glassy phase because of the rich alkali oxides content. This glassy phase helps to improve the physical-mechanical properties and contributes to reducing the firing temperature.

The incorporation of solid industrial wastes containing alkali oxides in ceramic formulations, has been the subject of recent research by the scientific community. This thesis investigates the incorporation of three industrial wastes in the composition of industrial sanitary ceramic bodies, as substitute materials to feldspar. These wastes include blast furnace slag from the El Hadjar Iron and Steel Factory (Annaba, Algeria), soda-lime glass waste from the factory of the African Glass Company (Jijel, Algeria) and sanitary ceramic waste from te factory of sanitary ceramic (Jijel, Algeria).

2.METHODOLOGY AND CHARACTERISATION OF RAW MATERIALS

2.1 Introduction

This chapter is focused on the presentation of different techniques to characterize the raw materials, the behavior of ceramic slips and sanitary ceramic bodies before and after firing. To carry out an in-depth study, we have taken into account the microscopic and macroscopic analyses, i.e the follow-up of the evolution of the rheological, the physical-chemical, thermal, mechanical and structural properties.

2.2 Characterisation techniques

2.2.1 X-ray fluorescence spectrometry (XFS)

X-ray fluorescence spectrometry is used to determine the elemental composition of the sample in a quantitative and qualitative way. The principle of the analysis is the excitation of a sample with standard radiation (X-ray tube stress) by ionising it, then analysing the clean radiation re-emitted by each sample.

We used this analytical technique to identify the chemical composition i.e the major elements (> 0.5 wt. %) in the raw materials used in our study. The instrument used is KLA Tencor D500 and Rigaku ZSX Primus IV. It is capable to analyse the chemical composition containing heavy elements (Al,Fe, Cu...) as well as lighter elements (Si, Mg ...), it also, allows to analyse the chemical composition of oxides[24].

2.2.2 Particle size analysis

The purpose of granulometry, is to measure the particle size distribution and the separation of different classes of elements by weight. For industrial wastes (blast furnace slag, Soda-lime glass waste and sanitary ceramic waste) a laser granulometer was used: the powder dust is conveyed by water or air and passes through a laser beam, which diffracts on the particles. The particle diameter measurement is between 0.02 and 2000 microns. The obtained suspension is introduced into a granulometer (HORIBA, model Analyzer LA-960).

The dispersion mechanism is achieved by the acceleration of the particles in a compressed air stream flow of compressed air, plus the collision of the particles with each other and with the walls. The control of the air pressure is done by increments of 0.02 bar in the range of 0 to 4 bar.

Figure 24: Granulometer (HORIBA, model Analyzer LA- 960).

2.2.3 Thermal analyses

Thermal analysis is used to observe changes in a parameter as a function of temperature. The techniques used include differential thermal analysis (DTA), thermogravimetric analysis (TGA).

2.2.3.1 Differential thermal analysis (DTA)

Differential thermal analysis is based on the measurement of the temperature difference between the sample and a reference body, as a function of time or temperature of the sample. Thus, it allows to identify endothermic transformations, exothermic transformations and invariant phenomena (occurring at fixed temperatures)[93].

2.2.3.2 Thermogravimetric analysis (TGA)

This characterisation technique makes it possible to follow the variations in the mass of a sample during a heat treatment. It is suitable for the study of reactions involving the volatilisation of certain constituents, or the combination with a gas phase. It is also simple to apply; the information given is very often complementary to that of the DTA. For this reason, the development of coupled DTA/TGA set-ups have increased in recent years [94].

In our work, the differential thermal and gravimetric analysis measurements were made using a DSC/ATD/ATG device (SDT Q 600 - TA instrument) with alumina-α as reference material. We placed about 40 mg of green powder mixture in an alumina crucible. The capsules are subjected to a nitrogen flow at a rate of 10 ml/min, to avoid any degradation process facilitated by the presence of oxygen. Heating is carried out from 0 to 1300 °C at a rate of 5 °C/min. The calibration of the equipment, is checked daily by the temperature (± 0.5 °C), and the enthalpy of fusion (± 0.5 J/g) under nitrogen flow.

Figure 25: TA Instruments SDT-Q600 Simultaneous TGA / TDA.

2.2.4 X-ray diffraction (XRD)

XRD is an analytical technique that allows for studying the different phases of crystalline materials and their crystallographic structures. This method consists of sending a beam of X-rays of wavelength λ, onto the sample than, the diffracted signal is analysed. For each incident (diffraction) wave of the beam, corresponds an intensity of the diffracted signal which appears as an X-ray diffraction peak. When an X-ray of wavelength λ is incident at an angle θ on all the reticular planes of the crystalline body of the clay, separated by a distance d, a diffraction phenomenon appears, given by the relation called Bragg's law:

$$\lambda = 2d\sin\theta \quad \text{..... (1)}$$

Where:

λ: wavelength of the beam used

d: reticular distance (distance between diffraction planes)

θ: angle of the incident ray

X-ray diffraction studies were conducted using an Empyrean Alpha-1 X-ray diffractometer at 65kV tension, using Cu Kα1 radiation (λ=1.5406 Å) in the Bragg-Brentano configuration. All experiments were carried out using powder samples. Wide-angle X-ray spectra were recorded with a PIXcel 1D detector to treat the results and plot their spectra. The identification of the phases, was carried out using PDF-ICDD (Powder Diffraction File-International Centre for Diffraction Data).

Figure 26: Empyrean Alpha 1 X-ray Diffractometer.

2.2.5 Scanning electron microscopy (SEM)

Electron microscopy is an essential method for investigating the evolution of a material's microstructure. This technique is based on the strong interaction between electrons and matter. In scanning electron microscopy, the secondary electrons are emitted and reflected to reconstruct the image of the object. The working voltages (between 10 and 30kV) are generally lower than in a transmission electron microscope (100kV and more) which allows for greater resolution, almost to the atomic scale for high-resolution microscopes.

The morphology of the ceramic bodies was identified by scanning electron microscopy (SEM) using a reference microscope (JEOL- JSM- 7600 F). The maximum resolution is 1nm at 15 kV. The acceleration voltage can vary from 100V to 30 kV. An electron beam is projected onto the sample to be analysed. The interaction between the electrons and the sample generates low-energy secondary electrons, which are accelerated towards a secondary electron detector to amplify the signal.

Figure 27: Scanning Electron Microscope (JEOL JSM-7600F).

2.2.6 Fourier transform infrared spectroscopy (FTIR)

Fourier transform infrared spectroscopy is based on the absorption of polychromatic infrared radiation by the material being analysed. It allows, using the detection of the characteristic vibrations of chemical bonds, to carry out the analysis of the chemical functions present in the material. The interaction between electromagnetic waves and matter allows a wide variety of studies depending on the wavelength. If matter is subjected to infrared radiation, energy is absorbed whenever there is a resonance between the frequency of the incident wave and that of the possible vibratory movements of the atoms (oscillator) constituting the substance. The latter, initially in the quantum state E, can change to an excited state, if the resonance condition is respected, the relation will be:

$$\Delta E = E_2 - E_1 = h\,\nu \quad \text{..... (2)}$$

Where:

E1: Initial quantum state.

E2: Excited quantum state.

h ν : Energy absorption quantity.

The intensity of the absorption, is determined by the probable transition from the basic to the excited level. These transitions are only allowed if they are associated with vibrational modes that are accompanied by a change in the dipole moment [2].

A pellet of 16 mm diameter and 2cm^2 of surface area (mass 20 mg) is hydraulically pressed under a pressure of 4.10^8 Pa. In this way, 150 mg of pure, dry KBr (purity: 99.9%, Spectral quality) is intimately crushed. This mixture will be fixed to a cell and must be placed in the trajectory of the beam. The data was registered by a spectrophotometer of Shimadzu, in the interval 4000-500 cm^{-1}.

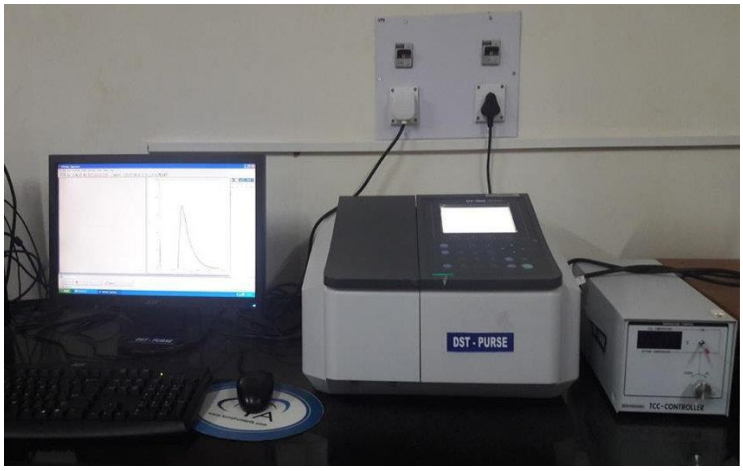

Figure 28: Spectrophotometer (Shimadzu UV1800).

2.2.7 Measurement of the humidity content of raw materials

Each 100 g of raw material $\mathbf{M_0}$ (initial wet mass) is weighed into a capsule. The capsule is placed in a Memmert-type oven at 110 °C for 15 minutes to dry the sample. We weigh regularly to obtain a constant mass, $\mathbf{M_1}$ the mass of the dry matter (evaporation of free water).

The humidity content is calculated according to the following formula:

$$\mathbf{H(\%) = 100 \left(\frac{M_0 - M_1}{M_0}\right)} \quad \text{..... (3)}$$

Where:

H is the humidity content (%).

$\mathbf{M_0}$ is the mass of the wet sample (g).

$\mathbf{M_1}$ is the mass of the dry sample (g).

2.2.8 Measurement of the loss of ignition in raw materials

The loss of ignition allows the measurement of volatile gases such as (CO_2, H_2O) during the calcination of raw materials. The protocol followed in our thesis is:

All raw materials are dried in the oven at 100 °C, and an initial mass $\mathbf{m_1}$ is introduced into the oven. The temperature is gradually increased to 1000 °C, and maintained for 1 hour. The sample is then allowed to cool down, then it is weighed again after firing; its mass is noted $\mathbf{m_2}$. The loss of ignition L.O.I. is given by the following formula:

$$\mathbf{L.O.I\ (\%) = 100\ \left(\frac{m_1 - m_2}{m_1}\right)} \quad \mathbf{(4)}$$

Where:

L.O.I is the loss on ignition.

$\mathbf{m_1}$ is the mass after drying.

$\mathbf{m_2}$ is the mass after calcination at 1000 °C.

2.2.9 Rheological properties of slip

2.2.9.1 Deflocculent electolytes

Sodium salts are generally used to adjust the pH of the aqueous medium of the slip. The optimal fluidity of the slip is between pH 9 and pH 10; it starts to manifest itself at pH 7. The most common electrolytes used in sanitary ceramic ware, are sodium silicate (Na_2SiO_4) and sodium carbonate (Na_2CO_3). These two deflocculants have been used for a very long time to adjust the slip. Some people prefer synthetic polyelectrolytes on their own, to adjust casting parameters, to suit their needs; these products really do offer many possibilities.

2.2.9.1.1 Sodium carbonate (Na_2CO_3)

Sodium carbonate is a white powder with a molecular weight of 105.99 g. It is not very soluble in water; to introduce it into a slip composition, it must therefore be dissolved in hot water (50-60°C). This salt has a very slow deflocculating action, but it does act on the thixotropy by giving a certain rigidity to the suspension at rest. The carbonate will therefore be used in small quantities (0.04 to 0.10% of the dry mass to be deflocculated) to regulate the slip thixotropy. It should be introduced in its entirety, at the beginning of the preparation by adding it dissolved to the diluting water, before adding the materials [95].

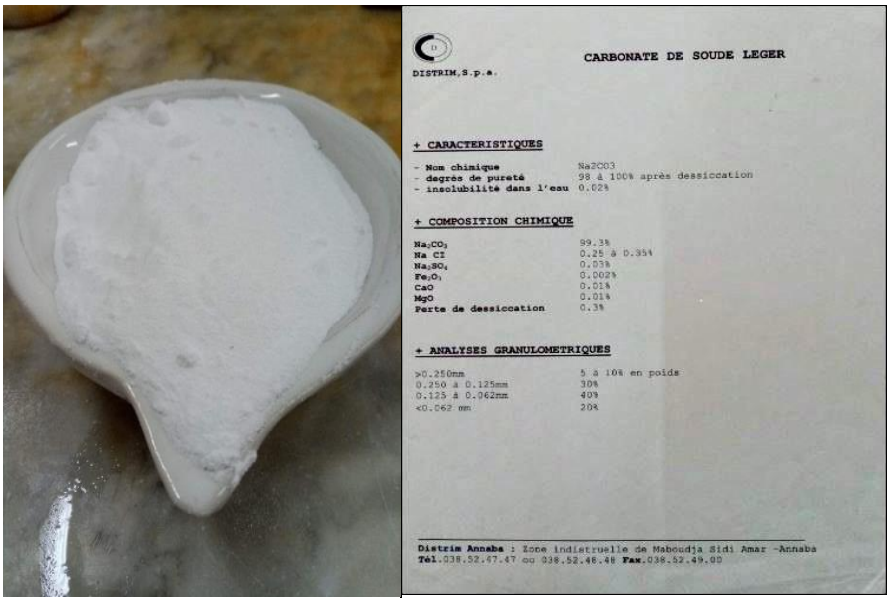

DISTRIM,S.p.a.

CARBONATE DE SOUDE LEGER

+ CARACTERISTIQUES

- Nom chimique	Na2CO3
- degrés de pureté	98 à 100% après dessiccation
- insolubilité dans l'eau	0.02%

+ COMPOSITION CHIMIQUE

Na_2CO_3	99.3%
Na Cl	0.25 à 0.35%
Na_2SO_4	0.05%
Fe_2O_3	0.002%
CaO	0.01%
MgO	0.01%
Perte de dessiccation	0.3%

+ ANALYSES GRANULOMETRIQUES

>0.250mm	5 à 10% en poids
0.250 à 0.125mm	30%
0.125 à 0.062mm	40%
<0.062 mm	20%

Distrim Annaba : Zone industrielle de Maboudja Sidi Amar -Annaba
Tél.038.52.47.47 ou 038.52.48.48 Fax.038.52.49.00

Figure 29: Sodium carbonate used in slip preparation and its technical card.

2.2.9.1.2 Sodium silicate (Na_2SiO_4)

Sodium silicate is a liquid, translucent and colourless substance. Its density is often expressed in degrees Baumé. The most common grade is 37-38 °Baumé, which corresponds to a density of 1.34 to 1.35 to water. The action of the silicate is very fast, it fluidizes the slip and its effect persists for a long time, so that thixotropy does not appear much with this electrolyte used alone. The quantities used are less than 1% of the dry mass, usually around 0.20 to 0.60%. When the dose necessary to deflocculate a paste is known approximately, 50 to 75% of the silicate, is introduced into the dilution water with all the carbonate [95].

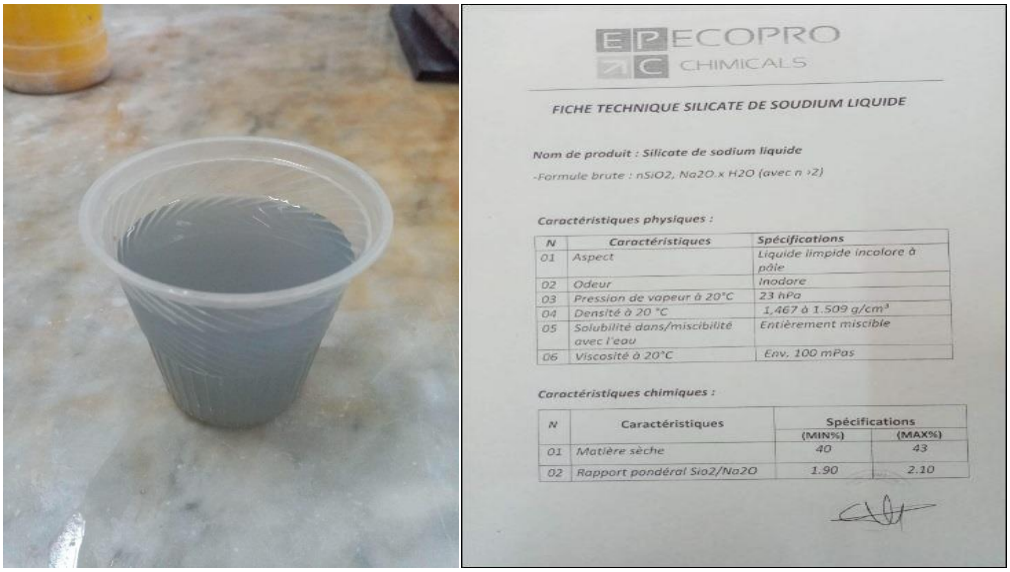

EP ECOPRO CHIMICALS

FICHE TECHNIQUE SILICATE DE SOUDIUM LIQUIDE

Nom de produit : Silicate de sodium liquide

-Formule brute : nSiO2, Na2O.x H2O (avec n >2)

Caractéristiques physiques :

N	Caractéristiques	Spécifications
01	Aspect	Liquide limpide incolore à pâle
02	Odeur	Inodore
03	Pression de vapeur à 20°C	23 hPa
04	Densité à 20 °C	1,467 à 1.509 g/cm³
05	Solubilité dans/miscibilité avec l'eau	Entièrement miscible
06	Viscosité à 20°C	Env. 100 mPas

Caractéristiques chimiques :

N	Caractéristiques	Spécifications (MIN%)	Spécifications (MAX%)
01	Matière sèche	40	43
02	Rapport pondéral Sio2/Na2O	1.90	2.10

Figure 30: Sodium silicate used in slip preparation and its technical card.

2.2.9.2 Density control

The density of the resulting slip, was determined by hydrostatic weighing. The slips were weighed into a 100ml pycnometer ($\mathbf{m_f}$); then, the empty pycnometer (m_e) was weighed using an automatic balance. We determine the density by the formula [96]:

$$\mathbf{d\ (g/ml)\ = 100\ (\frac{m_f - m_e}{V})} \quad \text{..... (5)}$$

Where:

$\mathbf{m_f}$ is the mass of the beaker full of slip (g).

$\mathbf{m_e}$ is the mass of the empty pycnometer (g).

V is the volume of the pycnometer (100ml).

2.2.9.3 Viscosity and thixotropy control

The universal torsion viscometer Gallenkamp is one of the most used instruments in the ceramic field, for rapid measurements of slip viscosity and thixotropy. Manually operated and with the lifting system of the sample cup, it comprises a wire with vertical torsion, a disk mounted on a graduated scale, and a cylinder suspended under the scale. During the test, the disk is rotated by 360°; and then released, the braking effect of the sample on the outer part of the cylinder is used to measure viscosity. The thixotropy value is determined by making a second measurement after 1, 5 or 15 minutes (in which the sample remains in a static condition), then calculating the difference with respect to the first measurement.

Figure 31: Torsion viscometer (Gallenkamp type).

2.2.9.4 Fluidity control

Fluidity is the time required for a certain volume of slip to flow through an orifice with a given diameter. The purpose of this procedure is to determine the flow speed of the slip. The fluidity of the slips was determined by using a measuring device called a LEHMAN Ford cup with a 2.6 mm diameter orifice. The ford cup is filled with the slip, closing the opening, to fill the 100 ml flask then measuring the flow time with a chronometer.

Figure 32 : Viscometer (Ford cup).

2.2.9.5 Residue on a sieve, pH and thicknesses control

The determination of the percentage of residue on a sieve of the slips, after the density calculation, is very important and should be carried out. We weigh 100g of the slip of each mixture ($\mathbf{m_w}$), and then pass it through the 63µm sieve (wet sieving). The residue is dried in the oven (T=110°C); we weigh the mass of residue $\mathbf{m_r}$. The percentage of the residue on a sieve is calculated by the formula:

$$\mathbf{R\ (\%) = \left(\frac{m_h - m_r}{m_h}\right)} \quad \mathbf{(6)}$$

Where :

R is the percentage of the residue on a sieve (%).

$\mathbf{m_w}$ is the mass of wet slip (g).

$\mathbf{m_r}$ is the mass of the dry residue (g).

The pH of the slips was determined after each agitation of the suspensions to eliminate the phenomenon of thixotropy, by using a portable digital pH meter (PH-S2).

The thicknesses during casting, were measured according to time steps of 10, 30, and 60 minutes.

2.2.10 Drying Shrinkage

The rectangular samples (120×20×20mm) were dried at room temperature (in the ambient air) for 48 hours, then at 105°C for 24 hours in an oven. The dried specimens were then weighed and measured to determine the variation in their dimensions (shrinkage).

Figure 33: Example of green and fired ceramic bars for shrinkage and flexural testing.

The determination of the shrinkage value is done by estimating the variation of the line lengths (10cm) recorded on the specimens after drying at 105°C. The following formula is used to calculate the drying shrinkage:

$$\mathbf{Sh_d\ (\%) = \left(\frac{L_0 - L_1}{L_0}\right) \times 100\% \quad (6)}$$

Where:

$\mathbf{L_0}$ is the initial length (cm).

$\mathbf{L_1}$ is the length after drying (cm).

$\mathbf{Sh_d}$ is the drying shrinkage (%).

2.2.11 Physical-mechanical characterisation after sintering

2.2.11.1 Firing of sanitary ceramic bodies

The ceramic bodies are fired in the tunnel kiln of the sanitary ceramics production unit of El Milia (Jijel, Algeria) at 1230 °C during 21 hours, as showen in the firing curve in figure 34.

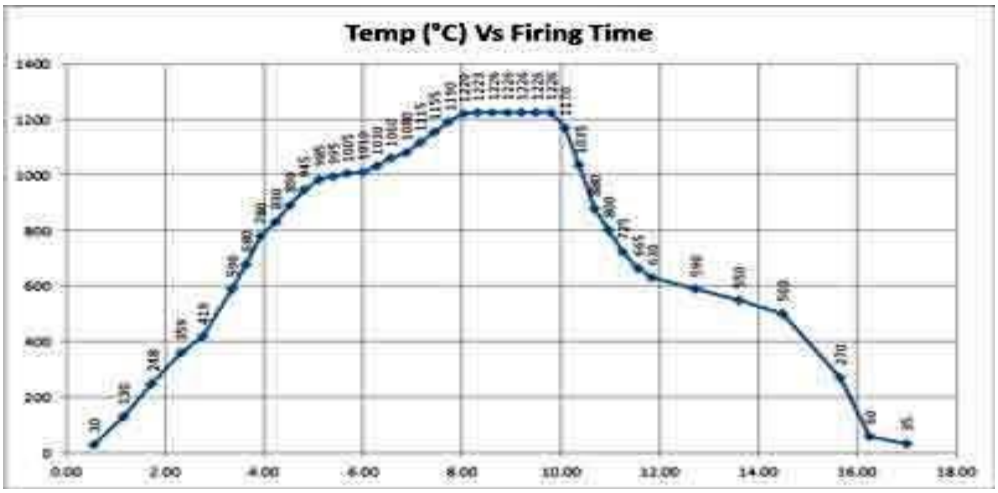

Figure 34: The firing curve for sanitary ceramics.

Water absorption, bulk density and total porosity were measured according to ASTM C373-88 [97]. While, the drying and firing shrinkage of ceramic bodies were determined according to ASTM C326 [98]. The flexural strength was measured according to ASTM C1161[99].

2.2.11.2 Water absorption

The amount of water absorption (WA) of fired sanitary ceramic bodies at 1230 °C, is determined according to ASTM C373-88. 2006, by measuring the difference in weight between the dried samples (m_d), size 70 × 20 × 10 mm. These were immersed for 2 hours in boiling water, the wet samples were cooled for 12 hours and the surface was dried with a wet towel (m_w). The water absorption is determined by Eq.7

$$WA\ (\%) = \frac{(M_w - M_d)}{M_d} * 100 \quad \text{..... (7)}$$

Where:

$\mathbf{M_w}$ is the mass of wet sample (g).

$\mathbf{M_d}$ is the mass of the dry sample (g).

2.2.11.3 Apparent density

To determine the apparent density of the test samples (70 x 20 x 10 mm), we follow this procedure: We fill a graduated cylinder with water to a specified point. Then, we put the samples in the water bath at 60-80 ° C; they are removed after two hours, wiped with a tissue and finally, we put the samples in the graduated cylinder. We record the volume change. The apparent density is determined according to the following relationship

$$D_A\ (g/cm^3) = \frac{(M_{wm} - M_w)}{V} \quad \text{..... (8)}$$

Where:

M_{wm}: Mass of the cylinder filled with water and the material (g).

M_w: Mass of the cylinder filled with water (g).

V: Volume change (cm^3).

2.2.11.4 Total porosity

To determine the total porosity of test samples (70 x 20 x 10 mm), we use the following relationship:

$$P_t\ (\%) = 1 - \frac{D_A}{D_T} * 100 \quad \text{..... (9)}$$

Where:

D_T: True density (g/cm^3). This mass is determined by a densimeter according to the following method:

*Grind 50 to 70g of ceramic powder and sieve it through the 80µm sieve.

*Dry the powder until a constant mass is obtained and leave it to cool down in a desiccator.

*Weigh the water densimeter to the lower mark.

*Fill with the powder the densimeter and weigh it

*To calculate the true density we used the following formula:

$$D_T\ (g/cm^3) = \frac{(M_{wp} - M_w)}{V} \quad \text{..... (10)}$$

Where:

M_{wp}: Mass of the densimeter filled with water and powder (g).

M_w: Mass of the densimetre filled with water (g).

V: Volume change (cm^3).

2.2.11.5 Firing shrinkage

The sintering process shrinks the samples, due to physical and chemical changes, at high temperatures. The firing shrinkage value is calculated by measuring the variation of the line lengths recorded on the specimens after firing at 1230°C. Firing shrinkage is determined according to the following formula [2]:

$$Sh_f\ (\%) = \frac{(L_1 - L_2)}{L_1} * 100 \quad \text{..... (11)}$$

Where:

L_1 is the dry length (cm).

L_2 is the length after firing (cm).

Sh_f is the firing shrinkage (%).

2.2.11.6 Flexural strength

We have investigated the mechanical properties (bending strength) by applying three-point bending to 120 × 20 × 20 mm ceramic bars. A NASSETTI type device measures the applied force. The flexural strength is given by the formula:

$$F_S\ (kgf/cm^2) = \frac{3Fw}{2t\,h^2} \quad \text{.....(12)}$$

F is the force that causes the bar to break (Kg.f).

w is the width of the bar (12 cm).

t is the thickness of the bar (2 cm).

h is the height of the bar (2 cm).

2.3 Raw materials and industrial wastes characterisation

2.3.1 Raw materials characterisation

2.3.1.1 Clay (Hycast VC)

Ball clay is a fine-grained plastic, mainly kaolinous sedimentary clay, which plays a significant role in the composition of the ceramic bodies slip. They consist of varying proportions of kaolin, mica, and quartz, with small amounts of organic matter and other minerals. They have commercial values since they increase the workability and strength of various ceramic bodies.

The clay used in this work is named Hycast VC; Imerys Minerals Ltd. UK supplies this material.

Figure 35: Clay raw material.

2.3.1.1.1 Quantitative XFS analysis of Hycast VC clay

The chemical composition of Hycast VC Clay is presented in Table 3:

Table 4: Chemical composition of Hycast VC clay

Oxides (%)	SiO_2	Al_2O_3	TiO_2	Fe_2O_3	K_2O	Na_2O	CaO	MgO	Loss on ignition at 1000°C
Hycast VC Clay	52	31	1	1	2.1	0.2	0.2	0.4	12

The results of this table show that the major oxides in the chemical composition of Hycast VC Clay are SiO_2, Al_2O_3 and K_2O, this clay has a high humidity rate (13%). This confirms that it is a natural rock material based on hydrated silicate or aluminum silicate with a laminar structure.

2.3.1.1.2 XRD analysis of Hycast VC clay

The XRD analysis of Hycast VC clay is carried out using an X-ray diffractometer over a range of 0 to 75° (Figure. 36).

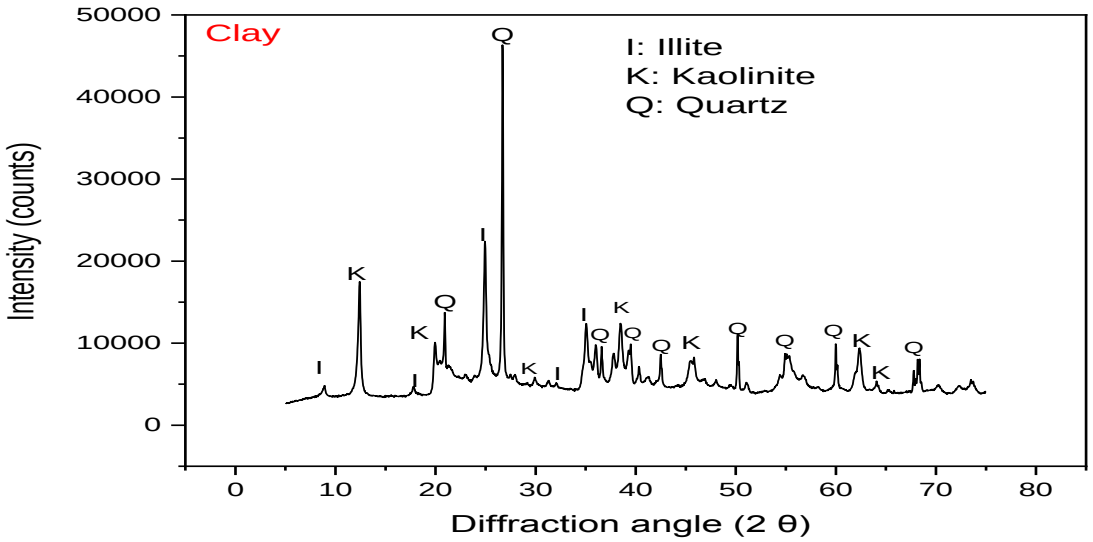

Figure 36: XRD patterns of Hycast VC Clay.

The XRD pattern of the Hycast VC Clay shows the presence of illite and kaolinite as the main phases, with quartz appearing as minor phase. The formation of illite as the main phase, is due to the small amounts of iron, potassium and titanium present in the clay[100].

2.3.1.2 Remblend Kaolin (RMB)

This type of kaolin used in this study was supplied by Imerys Minerals Ltd. It originates from a large open pit mine near St Austell, Cornwall, UK, Remblend kaolin is a white, friable, heat-resistant clay composed mainly of Kaolinite and aluminosilicates.

Figure 37: RMB Kaolin raw material.

2.3.1.2.1 Quantitative XFS analysis of RMB Kaolin

The chemical composition of RMB Kaolin is presented in Table 5:

Table 5: Chemical composition of RMB Kaolin

Oxides (%)	SiO_2	Al_2O_3	TiO_2	Fe_2O_3	K_2O	Na_2O	CaO	MgO	Loss on ignition at 1000°C
RMB Kaolin	48	37	0.05	0.8	1.5	0.1	0.07	0.3	12.1

The chemical composition of RMB kaolin shows high SiO_2 and Al_2O_3 contents; while Fe_2O_3 content is not negligible. The loss on ignition and the humidity rate are relatively low, close to the theoretical value of pure kaolinite.

2.3.1.2.2 XRD analysis of RMB Kaolin

The XRD analysis of RMB kaolin is carried out using an X-ray diffractometer over a range of 0 to 75° (see Figure 38).

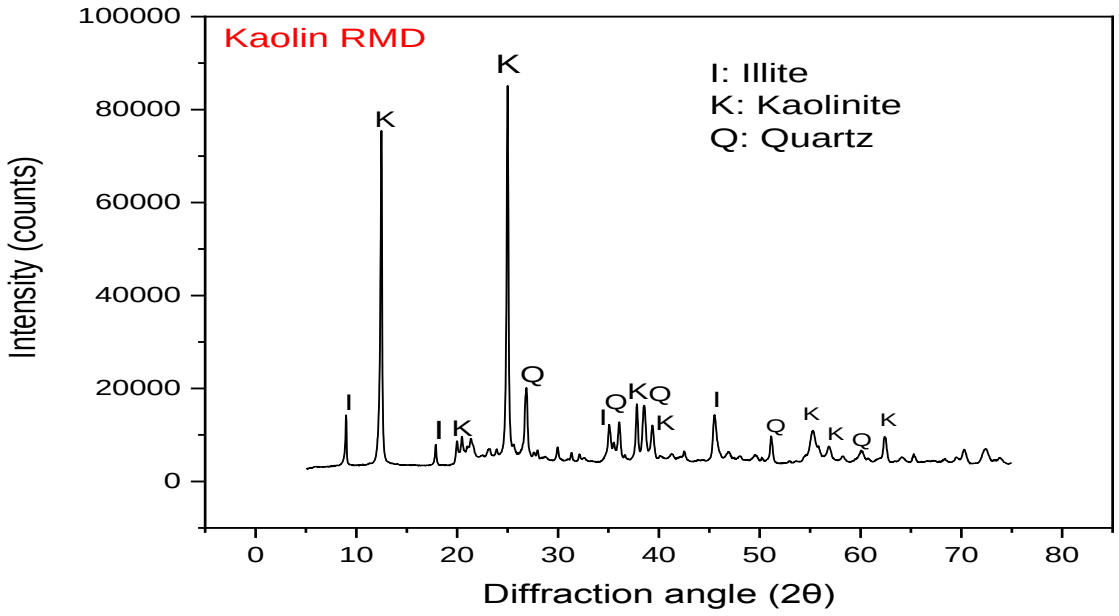

Figure 38: XRD patterns of RMB Kaolin.

The XRD spectrum in figure 38 shows a predominance of kaolinite with small quantities of crystalline impurities (non-clay minerals); besides, also the presence of illite, increases the plasticity of the mixture.

2.3.1.2.3 FTIR analysis of RMB kaolin

The infrared spectrum of RMB kaolin, is shown in figure 41. This spectrum is divided into 2 main zones.

-The first zone corresponds to the high frequency bands between 3700-3400 cm^{-1}.

-The second zone corresponds to the lower frequencies in the 1500-400 cm^{-1} range .

In the first zone, we have the valence vibrations of the OH groups. The absorption bands are centred on frequencies in the range 3693 - 3697 cm^{-1} (external OH); in the range 3618-3622 cm^{-1} (internal OH), there is a broad absorption band of low intensity centred around the range 1630-1656 cm^{-1} which is attributed to water molecules (H_2O).

-The absorption band in the range 1005-1020 cm^{-1}, corresponds to the elongation of the Si-O bond and the antisymmetric stretching of the Si-O-Si bond.

-The deformation vibrations of the Al-OH bond, are located at 913 and 915 cm^{-1}.

-The two bands of low and almost equal intensity, located between 800 cm^{-1} and 750 cm^{-1} indicate the presence of kaolinite [24].

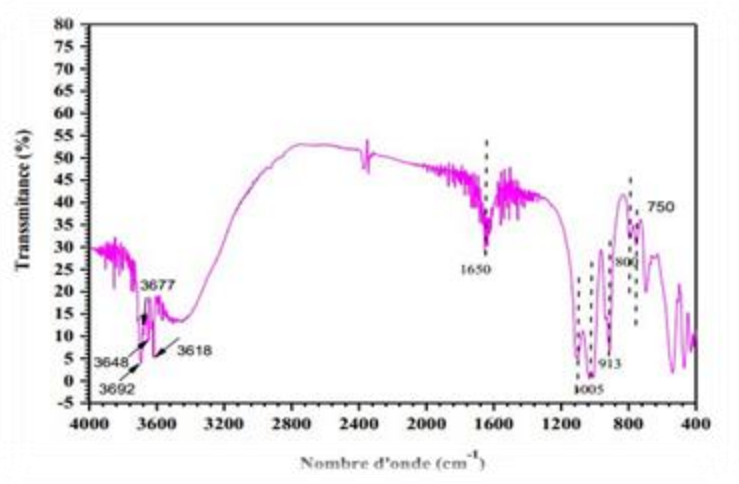

Figure 39: IR spectrum of RMB kaolin [24].

2.3.1.3 Parkaolin

Parkaolin is used in the sanitary ware industry. IMERYS Minerals Ltd. UK also supplies Parkaolin, which is composed mainly of aluminosilicates and Kaolinite. Parkaolin offers a good combination of plasticity, fluidity and casting speed suitable for the production of large series of sanitary parts.

Figure 40: ParKaolin raw material.

2.3.1.3.1 Quantitative XFS analysis of ParKaolin

The chemical composition of parkaolin is presented in Table 5:

Table 6: Chemical composition of parkaolin

Oxides (%)	SiO_2	Al_2O_3	TiO_2	Fe_2O_3	K_2O	Na_2O	CaO	MgO	Loss on ignition at 1000°C
Parkaolin	48	37	0.06	0.19	1.9	0.1	0.07	0.3	11.8

Parkaolin has a similar composition to RMB kaolin, except a slight difference in the content of iron and potassium oxides. In addition, it has a lower ignition loss than RMB and a higher amount of humidity.

2.3.1.3.2 XRD analysis of ParKaolin

The XRD analysis of RMB kaolin is carried out using an X-ray diffractometer over a range from 0 to 75° (see Figure 41).

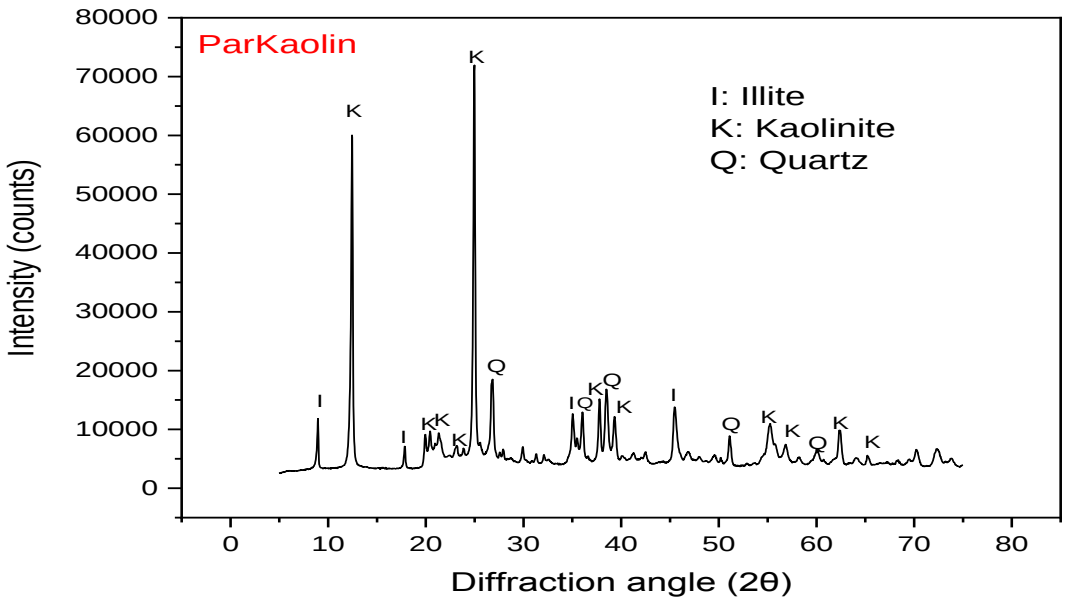

Figure 41: XRD patterns of ParKaolin.

Parkaolin contains a significant amount of kaolinite and small quantities of illite and quartz. The high content in kaolinite and illite, increases the plasticity of the mixture, while the presence of a large amount of quartz can reduce the plasticity[2].

2.3.1.4 Sodium feldspar

In this work, feldspar is the main component for the formation of the vitreous phase of sanitary ceramic bodies. It is introduced into the ceramic body to avoid defects and ensure the cleanliness of the final product. The sodium feldspar used in our work, is imported from the Çine-Aydin- Turkey.

Figure 42: Sodium feldspar raw material.

2.3.1.4.1 Quantitative XFS analysis of sodium feldspar

The chemical composition of sodium feldspar is presented in Table 7:

Table 7: Chemical composition of sodium feldspar

Oxides (%)	SiO_2	Al_2O_3	TiO_2	Fe_2O_3	K_2O	Na_2O	CaO	MgO	Loss on ignition at 1000°C
Sodium feldspar	70.44	17.92	0.26	0.08	0.4	9.6	0.5	0.2	0.5

The results in this table, show that the major oxides in the chemical composition of soda feldspar are SiO_2, Al_2O_3 and Na_2O. It should be noted that the humidity content of soda feldspar, is of the order of 0.10% with a lower loss on ignition of 0.5% compared to that of kaolin.

2.3.1.4.2 XRD analysis of sodium feldspar

The XRD analysis of sodium feldspar is carried out using an X-ray diffractometer over a range of 0 to 75° (see Figure 43).

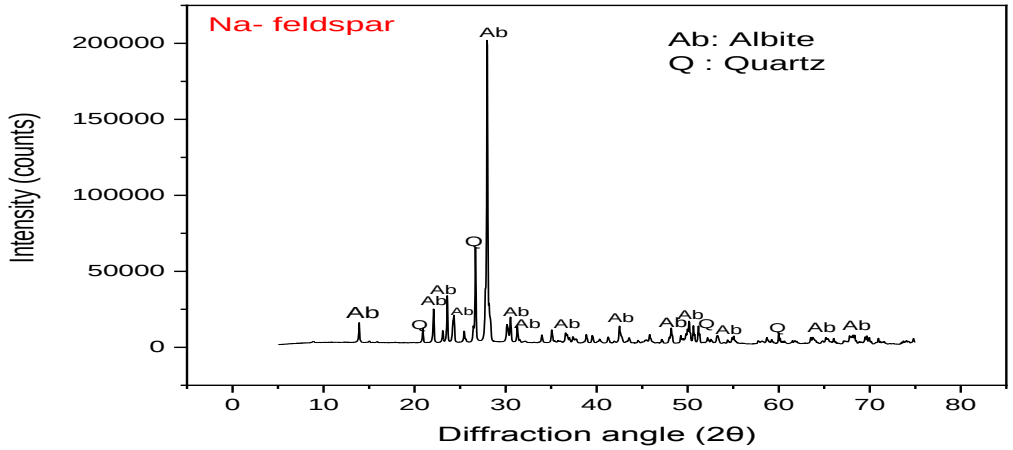

Figure 43: XRD patterns of sodium feldspar.

The most intense ray (2θ= 28.10) characterises the Albite $NaAlSi_3O_8$, which is presented as the principal phase. The others less intense peaks represent quartz. The sodium feldspar tends to lower the fusion temperature[101]. The presence of quartz in sufficient quantity, limits the plasticity of the mixture[2].

2.3.1.5 Potassium feldspar

In general, sodium feldspar is used for soft porcelain, whereas potassium feldspar is used for hard porcelain [102, 103]. Feldspar forms the glassy matrix of ceramics; it has a melting temperature = 1050 to 1300°C. Potassium feldspar (orthoclase) has the chemical formula $KAlSi_3O_8$.

Figure 44: Potassium feldspar raw material.

2.3.1.5.1 Quantitative XFS analysis of potassium feldspar

The chemical composition of potassium feldspar is presented in Table 8:

Table 8: Chemical composition of potassium feldspar

Oxides (%)	SiO_2	Al_2O_3	TiO_2	Fe_2O_3	K_2O	Na_2O	CaO	MgO	Loss on ignition at 1000°C
Sodium feldspar	69.5	17.3	0	0.1	9	3.1	0.4	0.2	0.4

When the K_2O concentration is high, we obtain the so-called new-generation ceramics (rich in leucite), they have better mechanical properties [104, 105]. Table 7 shows the chemical composition of potassium feldspar at different percentages of metal oxides. In this table, we notice a high percentage of K_2O and the humidity content in the order of 0.35% with a low loss on ignition of 0.4%.

2.3.1.5.2 XRD analysis of potassium feldspar

The XRD analysis of potassium feldspar, is carried out using an X-ray diffractometer over a range of 0 to 75° (see Figure 45).

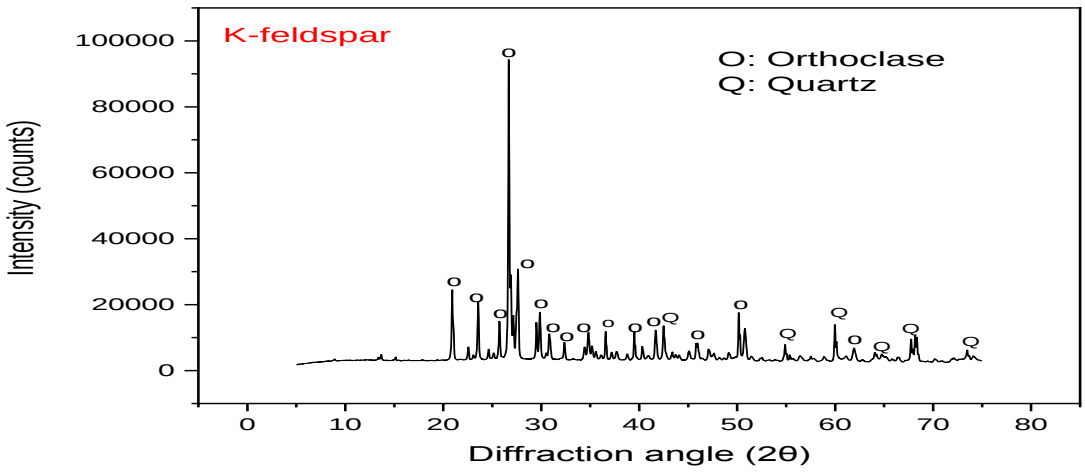

Figure 45: XRD patterns of potassium feldspar.

The most intense peaks (2θ = 27.22 and 28.34°), characterize the orthoclase $KAlSi_3O_3$. Other small peaks characterize quartz. The main role of potassium feldspar, is to increase the viscosity of molten glass[101].

2.3.1.6 Sand of Bir El-Ater

Silica is usually introduced in the compositions of as milled quartz, and also as alumino-silicates in various clay-kaolin materials. The quartz is melted at various temperatures by the addition of a melting agent, or a mixture of melting agents. The quartz used in this study is of local origin, from the Bir El-Attar area in Tebessa, eastern Algeria. The quartz used is of natural siliceous origin, especially in its finest fractions. It is wet-milled in alumina jars, until a residue is obtained on a 63µm sieve between 4 and 6%.

Figure 46: Sand of Bir El-Ater raw material.

2.3.1.6.1 Quantitative XFS analysis of the sand of Bir El-Ater

Table 9: Chemical composition of the sand of Bir El-Ater

Oxides (%)	SiO_2	Al_2O_3	TiO_2	Fe_2O_3	K_2O	Na_2O	CaO	MgO	Loss on ignition at 1000°C
Sand of Bir El-Ater	96.35	0.52	0.05	0.24	0.17	0.08	1.19	0.08	1.2

The results of this table show that silica is the main oxide in the chemical composition of Bir El Ater sand. It should be noted that the humidity level of this sand, is null with a low loss on ignition of 1.5%.

2.3.1.6.2 XRD analysis of the sand of Bir El-Ater

The XRD analysis of the sand of Bir El-Ater is carried out using an X-ray diffractometer over a range of 0 to 75° (Figure. 47).

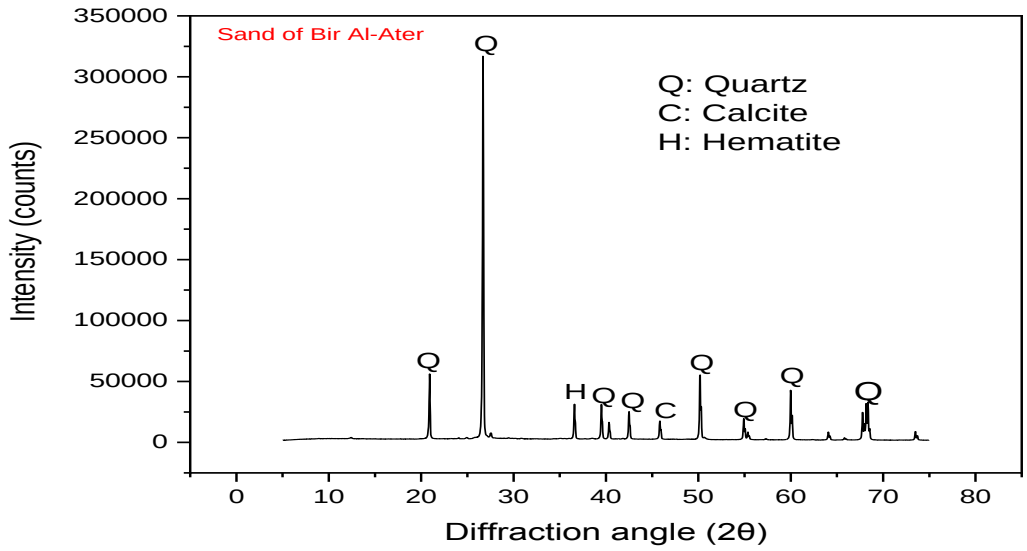

Figure 47: XRD patterns of sand of Bir Al-Ater.

The major non-swelling phase found in these materials, is quartz. The most intense peak (2θ=27°), is characterised by quartz SiO_2, with the appearance of other peaks such as: calcite and hematite. The presence of quartz in large quantities, reduces the plasticity of the mixture; the presence of calcite acts as a flux in the ceramic material during firing[2].

2.3.2 Solid wastes characterisation

2.3.2.1 Blast furnace slag (BFS)

In the first part of this study, Algerian blast furnace slag (BFS) from the El Hadjar steel factory (Annaba-Algeria) was used. The BFS was repeatedly ground until the particles got a size below 150 µm.

Figure 48: Milled blast furnace slag.

2.3.2.1.1 Quantitative XFS analysis of the Algerian blast furnace slag

Table 10: Chemical composition of the sand of Algerian blast furnace slag

Oxides (%)	SiO_2	Al_2O_3	TiO_2	Fe_2O_3	K_2O	Na_2O	CaO	MgO	SO_3	MnO	SrO	BaO	Loss on ignition at 1000°C
Algerian blast furnace slag	33	6.18	0.29	1.43	0.68	0.19	44.1	3.7	1.3	2	0.28	1.01	1.2

The above table shows that the Algerian blast furnace slag is rich in SiO_2, CaO, Al_2O_3 and MgO in smaller quantities. BFS is characterised by having a null humidity, as it is originally the result of volatilisation after passing through a high temperature. It also has a low loss on ignition. This composition makes it suitable for use as an alternative raw material in ceramic production.

2.3.2.1.2 SEM analysis of the Algerian blast furnace slag

The SEM analysis of the Algerian blast furnace slag is presented in the following figure.

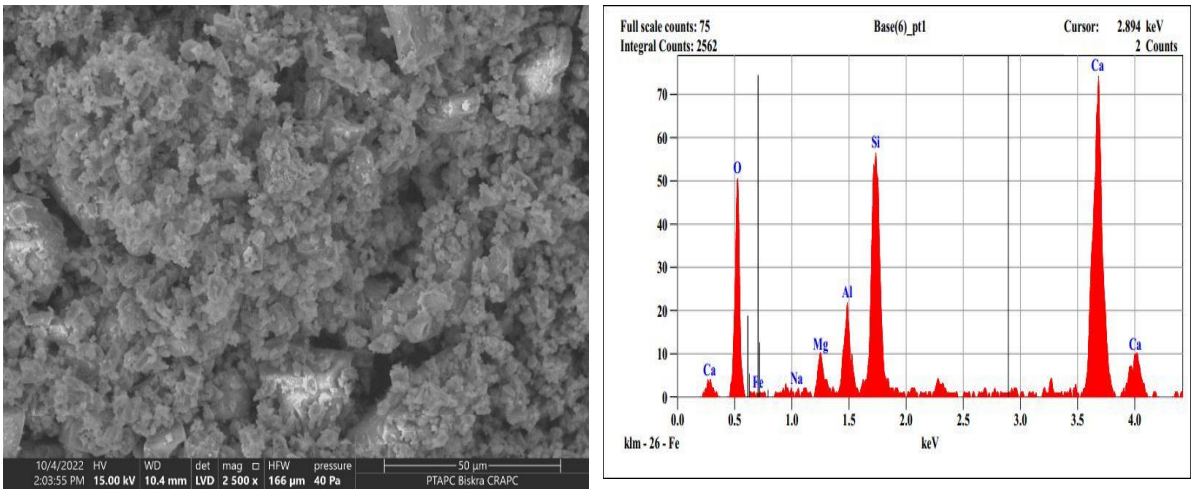

Figure 49: SEM micrographs of milled blast furnace slag with EDX microanalysis.

SEM micrographs of the milled blast furnace slag sample, show different grain shapes and irregular particle texture with clear porosity, as shown in Figure 49. In addition, the EDX spectrum indicates the presence of silicon (Si), oxygen (O) and calcium (Ca) which appeared with a high peak at 3.7 keV as the main constituent in the sample; we also have a small amount of aluminium (Al) and magnesium (Mg). These results are in agreement with the chemical composition analysis (XFS) of the starting materials mentioned in Table 9.

2.3.2.2 Soda-lime glass waste (SLGW)

Soda-lime glass waste is one of the most known industrial solid waste in the world. In the second part of this thesis, the effect of SLGW on various technical properties of sanitary ceramic bodies is studied. SLGW pieces has been brought from the factory of the African Glass Company (Jijel, Algeria). They were milled to obtain a particle size of about 100µm.

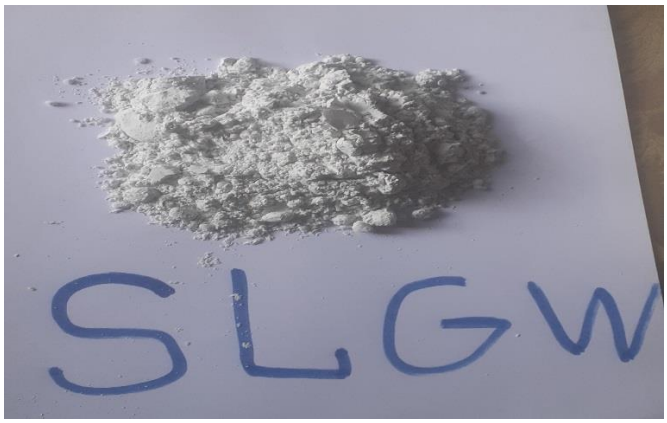

Figure 50: Milled soda-lime glass waste.

2.3.2.2.1 Quantitative XFS analysis of milled soda-lime glass waste

Table 11: Chemical composition of soda lime glass waste

Oxides (%)	SiO_2	Al_2O_3	TiO_2	Fe_2O_3	K_2O	Na_2O	CaO	MgO	Loss on ignition at 1000°C
soda-lime glass waste	70.25	1.71	0	0.33	0.28	13.43	13.43	0.52	0.1

Table 11 shows the chemical composition of soda-lime glass waste, which contains mainly silica oxide, sodium and calcium. This composition rich in alkali-oxides makes it an important proposed alternative to feldspar in the composition of sanitary ceramic bodies.

2.3.2.2.2 SEM analysis of the Soda-lime glass waste

The SEM analysis of the soda-lime glass waste is presented in the figure 51.

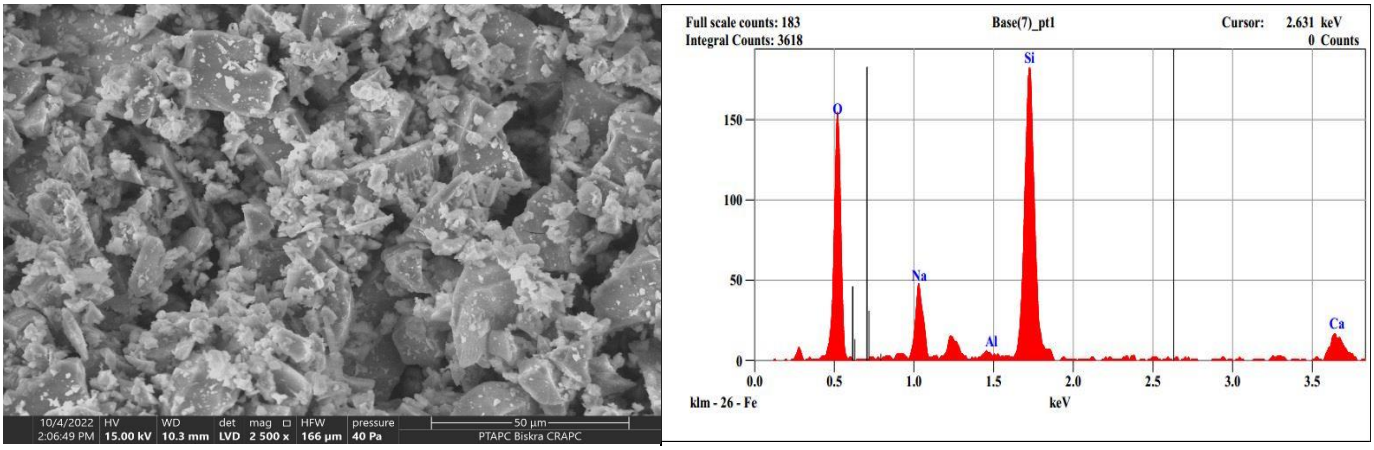

Figure 51: SEM micrographs of milled soda-lime glass waste with EDX microanalysis.

Figure 51 shows the SEM-EDX analysis of SLGW. From the figure, it is shown that the particles have an irregular geometry with sizes around 50 µm; the quartz particles and the vitreous phase can be seen with a significant porosity appearing in dark colour. The EDX analysis also shows the same chemical compositions as the XFS analysis included in table 10, where it shows large proportions of oxygen, silicon, calcium, sodium and a lower amount of aluminum. They which are the predominant elements in Industrial soda-lime glass.

2.3.2.3 Sanitary ceramic waste (SCW)

Sanitary ceramic waste is produced in huge quantities worldwide. Sanitary ceramic waste can be used as chamotte in the composition of (fine) fireclay bodies for sanitary wares. SCW pieces have been brought from the factory of the sanitary ceramic (El Milia - Jijel, Algeria) and then ground up to obtain a particle size smaller than 100µm.

Figure 52: Milled sanitary ceramic waste.

2.3.2.3.1 Quantitative XFS analysis of the sanitary ceramic waste

Table 11: Chemical composition of sanitary ceramic waste

Oxides (%)	SiO_2	Al_2O_3	TiO_2	Fe_2O_3	K_2O	Na_2O	CaO	MgO	ZnO	ZrO_2	Loss on ignition at 1000°C
soda-lime glass waste	69.2	22	0.43	1.42	3.17	1.64	1.14	0.27	0.18	0.4	0.8

Sanitary ceramic waste has a chemical composition rich in SiO_2 and Al_2O_3 oxides with less content of alkali oxides (Na_2O and K_2O), in addition to CaO and Fe_2O_3 oxides. It should be noted that the humidity rate of SCW, is null with a low loss on ignition of 0.8%.

2.3.2.3.2 SEM analysis of sanitary ceramic waste

The SEM analysis of the sanitary ceramic waste is presented in figure 53.

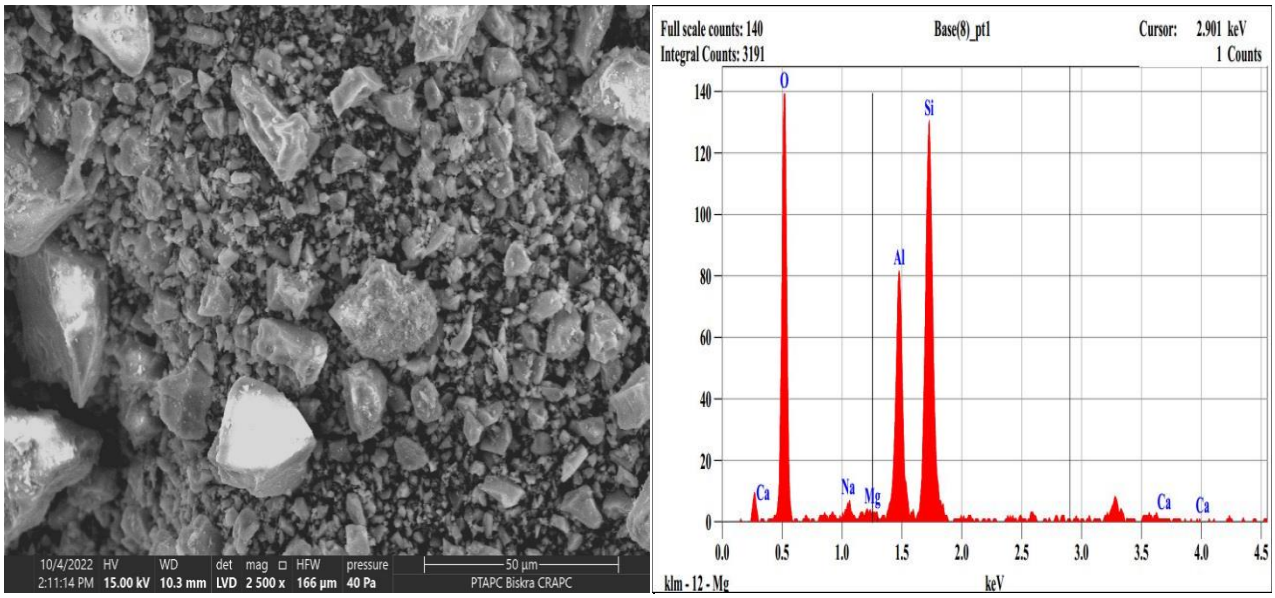

Figure 53: SEM micrographs of sanitary ceramic waste with EDX microanalysis.

SEM micrographs of the milled sanitary ceramic waste sample, the bulk appears as a vitrified matrix with different particles of different shapes and sizes; these are are mostly quartz, mullite particles and melted feldspar-penetrated clay. Besides, we have a significant presence of porosity that appears in dark. The EDX spectrum of the sample indicates the presence of oxygen (O), and silicon (Si) which appeared at a significant peak at 1.7 keV with a small amount of aluminium (Al), calcium (Ca), sodium (Na) and magnesium (Mg).

2.4 Conclusion

In this chapter, we presented different characterisation techniques and preparation methods of our sanitary ceramic bodies, including rheological, chemical, structural, microstructural, thermal and mechanical characterisation. This methodology allow us to control the quality of the raw material used, via the study of its properties. All this in order to manufacture a good quality final product.

3.EFFECT OF BLAST FURNACE SLAG ON THE QUALITY OF SANITARY CERAMIC BODIES

3.1 Introduction

In sanitary-ware bodies' production, the most important factor is the selection of raw materials which are rich in aluminosilicate oxides. The chemical composition, particle size distribution and humidity content of the raw materials must be investigated to obtain the right dosage.

Blast furnace slag is one of the most important industrial wastes; it is rich in aluminosilicates (SiO_2, Al_2O_3) and calcium oxide (CaO). Recently, there has been a growing interest in the idea of incorporation of blast furnace slag in various traditional ceramics formulations, as an alternative to some raw materials. The high calcium oxide content may cause the blast furnace slag to affect the rheological properties of slip casting. Therefore, different types of electrolytes are usually used to allow it to be homogeneous in composition without affecting the technical properties.

In this chapter, we first present the method of preparation of sanitary ceramic bodies, starting from the preparation of the slip until the heat treatment. Then, we will show the rheological and physical-mechanical results obtained by different experimental techniques. In addition, the thermal, structural and micro structural characterisation techniques will be used to identify the effect of the blast furnace slag on the quality of the products.

3.2 Production of sanitary ceramic bodies containing solid industrial wastes

The process of producing sanitary ceramic bodies can be divided into three steps. In the first step, a mixture of oxides is prepared resulting in a ceramic liquid (slip). In the second step, the slip is poured into gypsum moulds to obtain shapes suitable for various applications. Finally, the third step, sintering, produces a dense ceramic body with the desired properties.

The following figure shows the steps for the preparation of sanitary ceramic bodies:

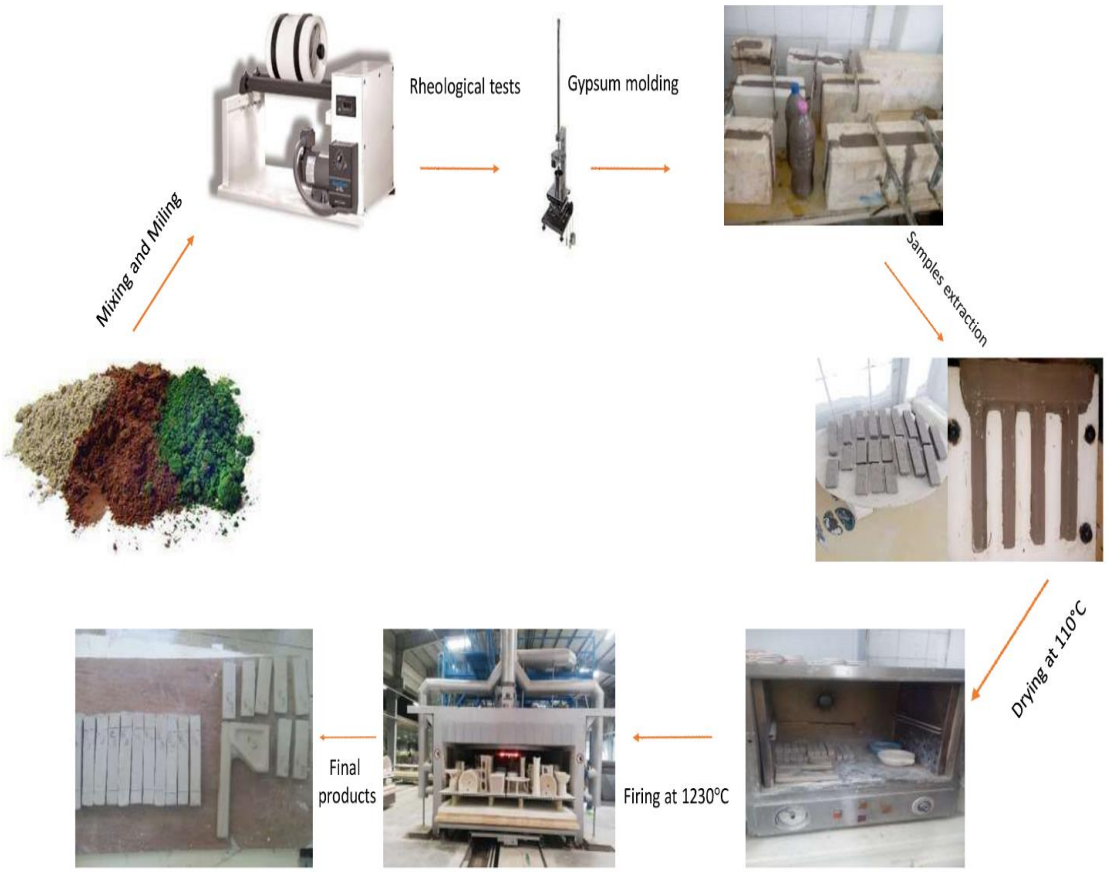

Figure 54: Manufacturing steps of sanitary VC bodies.

3.2.1 Preparation of the slip

The selection of the raw materials is mainly based on purity and grain size characteristics. The materials are weighed, taking into account the loss on ignition and the humidity content. The chemical composition of the raw materials and blast furnace slag is presented in table12.

The proposed formulations of the slips are summarised in table 13, while the composition of each batch is presented in table 14. The reference formulation represents the composition of the slip of the sanitary ceramic factory of El-Milia - Jijel. Algeria.

Table 12: Chemical compositions of the raw materials.

Oxides	Clay Hycast VC	PAR KAOLIN	Kaolin RMB	Sodium feldspar	Potassium feldspar	Quartz	BFS
SiO_2	52	48	48	70.44	69.5	96.35	33
Al_2O_3	31	37	37	17.92	17.3	0.52	6.18
TiO_2	1	0.06	0.05	0.26	0	0.05	0.294
CaO	0,2	0.07	0.07	0.5	0.5	1.19	44.1
MgO	0.4	0.3	0.3	0.2	0.2	0.08	3.7
K_2O	2.1	1.9	1.5	0.4	9	0.17	0.681
Na_2O	0.2	0.1	0.1	9.6	3.1	0.08	0.196
Fe_2O_3	1	0.19	0.8	0.08	0.1	0.24	1.43
SO_3	0	0	0	0	0	0	1.38
MnO	0	0	0	0	0	0	2
SrO	0	0	0	0	0	0	0.28
BaO	0	0	0	0	0	0	1.01
L. O. I	12	11.8	12.1	0.5	0.4	1.2	0.83

Table 13: Formulations (in wt. %) of ceramic compositions E1, E2, E3, E4 and E5.

Raw materials	E1	E2	E3	E4	E5
Clay (Hycast VC)	28	28	28	28	28
PARKAOLIN	12	12	12	12	12
kaolin RMB	12	12	12	12	12
Sodium feldspar	12	9.5	7	4.5	2
Potasium feldspar	11	8.5	6	3.5	1
Quartz	25	25	25	25	25
BF Slag	0	5	10	15	20

Table 14: Chemical analysis of slip modified by BFS.

Oxides	E1	E2	E3	E4	E5
SiO_2	68.21	66.45	64.63	62.94	62.18
Al_2O_3	21.1	22.53	22.04	21.43	20.86
TiO2	0.26	0.38	0.39	0.4	0.41
CaO	0.55	2.81	5.12	7.44	9.75
MgO	0.27	0.46	0.64	0.83	1.02
K_2O	2.24	2.04	1.84	1.65	1.45
Na_2O	1.77	1.45	1.13	0.82	0.5
Fe_2O_3	0.61	0.68	0.75	0.82	0.89
SO_3	0	0.07	0.14	0.21	0.29
MnO	0	0.1	0.21	0.31	0.42
SrO	0	0.01	0.02	0.04	0.05
BaO	0	0.01	0.1	0.16	0.21

After the selection of raw materials and the calculation of formulations, we prepare the slip as follows:

First, we grind the quartz having added a small quantity of sodium silicate and 30 wt. % water, in conjunction with the diluting of the clay with 30 wt. % water by adding sodium electrolytes Na_2SiO_3 and Na_2CO_3 (high purity: 99.9%, ACS grade). The crushed sand and the diluted clay are milled in a ceramic jar (containing an Al_2O_3 ball mill). We use a mixture of balls of three different diameters (5, 10 and 20 mm). These balls are distributed according to the following proportions, expressed as a mass percentage: 25% of small particles, 50% medium and 25% large. Grinding reduces the particle size as well as the space between the particles. The jar is rotated for 4 hours at 120 rpm. Then, we add feldspar, kaolin, and another amount of water. The milling must be continued until we obtain a residue on a 63 µm (less than 2%) sieve. To improve the milling efficiency, small amounts of deflocculating agents: Na_2SiO_3 and Na_2CO_3 are added to the slip mixture. Water and electrolytes are added to slip according to the rheological behaviour by repeated controlling slip properties for specific periods (we add water in case of high density, electrolytes in case of high fluidity (viscosity). We extend the grinding time of the mixture if the residue above the 63 µm sieve is higher than 2%). The jar milling system is presented in figure 55.

Figure 55: Schematic of a jar milling system using alumina balls.

Two rotating rotors turn the raw materials and balls. The grinding is carried out by cutting the powder grains between the balls. The advantage of this method it is speed, in other words, it is time saving.

3.2.2 Slip casting in plaster moulds

After milling, the slip is poured into plaster moulds, which will absorb water via capillarity; a solid ceramic body is formed before the molds are removed. The obtained slip was poured into rectangular moulds, at room temperature. For each mixture 8 test pieces (70×20×10mm), were prepared to measure water absorption; while rectangular samples (120×20×20mm) were prepared to measure both linear shrinkage and flexural strength. Figure 56 shows the casting of the slip into a plaster mould and the final piece.

Figure 56: Casting slip into the plaster mould and re-emptying the slip.

3.2.3 Drying

The samples were then dried at room temperature for 48 hours, then, at 105°C for 8 hours.

Figure 57: samples drying at 105°C.

3.2.4 Firing

The green bodies were fired in a tunnel kiln, for 21 h, at a maximum temperature of 1230°C, under industrial conditions.

Figure 58: Firing at 1230°C in an industrial tunnel kiln.

3.3 Effect of blast furnace slag on the rheological parameters of the slip

The incorporation of blast furnace slag within the composition of the sanitary ceramic bodies caused an increase in the viscosity of the slip and slowed its rheological behaviour. For this reason, the addition of electrolytes was necessary. Accordingly, specific amounts of sodium silicate and sodium carbonate were mixed. Figure 59 shows the effect of the electrolyte ratio on the fluidity of different slips. According to the results, the optimum liquidity isobtained at the ratio Na_2CO_3 / Na_2SiO_3 = 1.5. While Figure 60 shows the effect of the combined amount of the ideal electrolyte mixture on the fluidity of different slips. It

can be seen that fluidity decreases with the added amount of the electrolyte mixture up to 0.375 wt. %. The higher amount of sodium cations Na+ in the mixture reduces the thickness of the diffusion layer and contributes to this rheological behaviour [37].

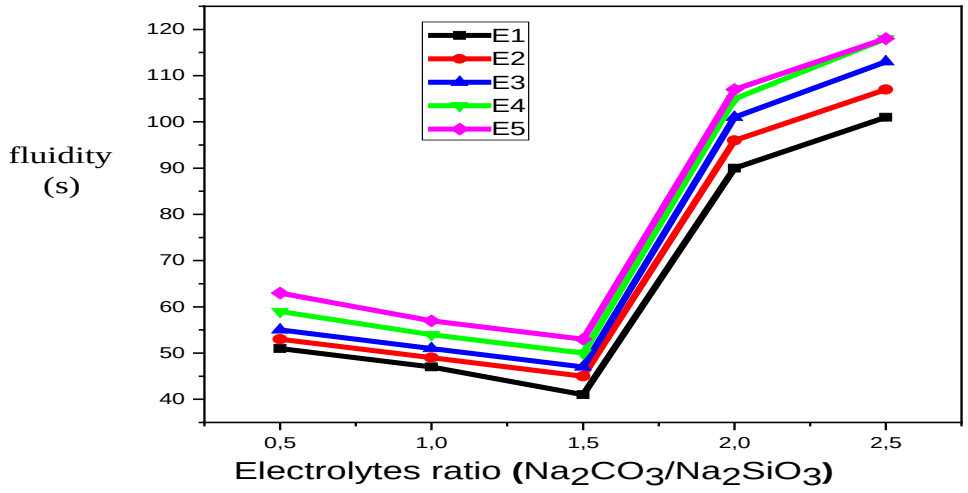

Figure 59: Variation of the fluidity for different mixtures depending on the ratio between electrolytes (Na2CO3 / Na2SiO3).

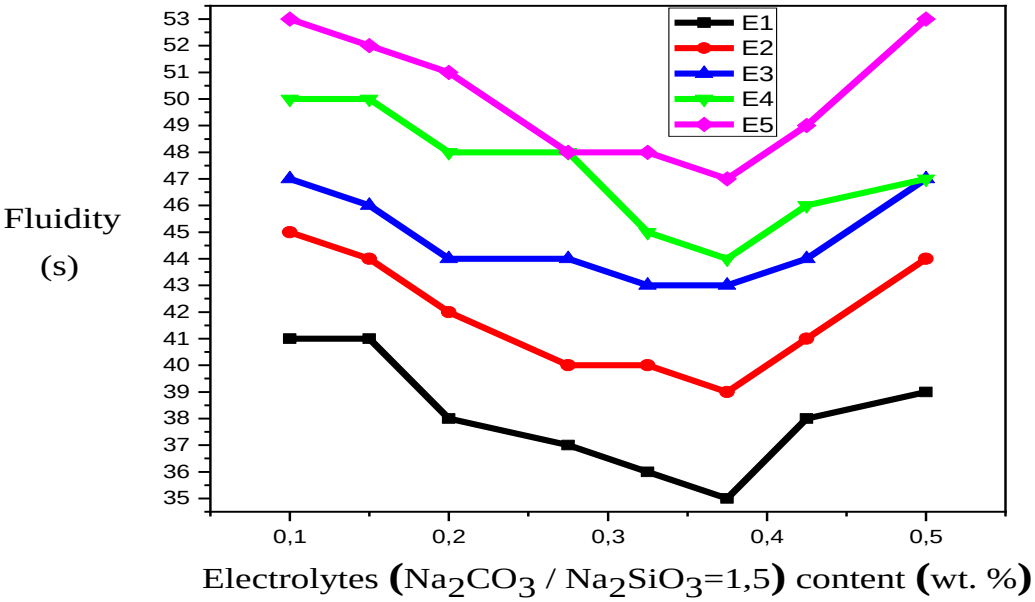

Figure 60: Variation of the fluidity for different mixtures depending on the content of electrolytes (Na2CO3 / Na2SiO3 = 1.5).

Some other rheological properties of slip are summarized in Table 15. It may be noted that the pH and density goes up with the reduced residue on sieve, resulting from the BFS additions. The viscosity of the slip significantly influences the surface charge of the ceramic particles, which leads to a modification of the slip pH [106]. In such manner, according to the findings in the table, it is also clear that the use of sodium silicate alone is not sufficient to improve the rheological properties. For that, polyelectrolytes should be used with the addition of sodium carbonate, as they are more effective. Several authors in previous studies have obtained the same observations [107].

Table 15: Evolution of the density, residue on sieve and pH of slip as a function of added BFS concentration.

	E1	***E2***	***E3***	***E4***	***E5***
Density (g/cm^3)	***1.771***	***1.802***	***1.807***	***1.817***	***1.822***
Residue on sieve (63 µm) (%)	***1.6***	***1.2***	***0.9***	***0.9***	***0.7***
pH	***8.3***	***9.5***	***10.2***	***10.4***	***10.5***

3.4 TDA/TGA analysis of green ceramics

TDA and TGA analyses of E1, E2, E3, E4 and E5 ceramics are shown in figures 61 and 62.

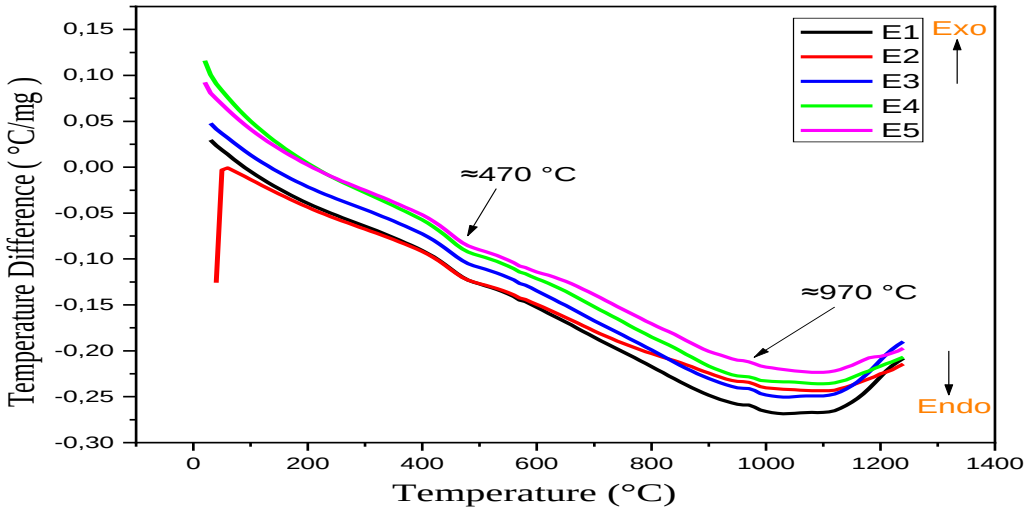

Figure 61: TDA analysis of the mixtures E1.E2.E3.E4 and E5.

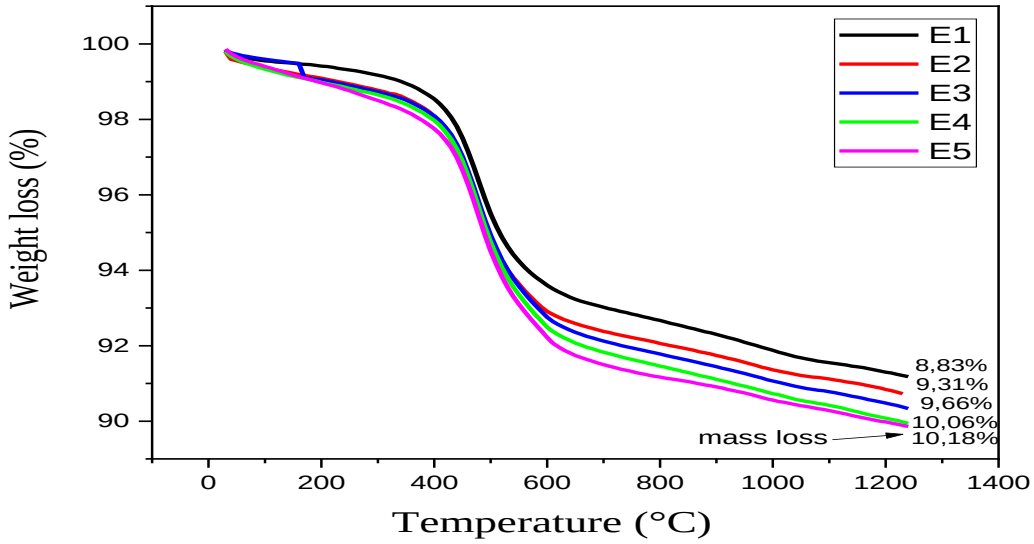

Figure 62: TGA analysis of the mixtures E1.E2.E3.E4 and E5.

From TDA curves, significant endothermic peaks appear at ~470 °C; they are attributed to the dehydroxylation of hydroxyl groups in kaolin leading to the formation of metakaolin ($A1_2O_3.2SiO_2$)[39, 108] and the dehydroxylation of montmorillonite [2].

$$Al_2O_3.2SiO_2.2H_2O \longrightarrow Al_2O_3.2SiO_2 + 2H_2O_{(g)}$$

(Kaolin) (metakaolin)

Exothermic peaks appeared at ~970 °C for (0, 5, 10, 15 and 20 wt. % BFS), which are mainly assigned to the transformation of metakaolin into mullite crystals [109].

$$Al_2O_3.2SiO_2 \longrightarrow 3Al_2O_3.2SiO_2$$

(metakaolin) (primary mullite)

Along with these microstructural transformations, there is a loss of mass, as seen in the TGA curves in figure 63. The values of the total mass loss in the 0, 5, 10, 15 and 20 wt.% BFS ceramics are: 8.83, 9.31, 9.66, 10.06 and 10.18%, respectively. These losses are generally attributed to the removal of water from plastic materials such as kaolin and clay.

$$2OH + O^{-2} \longrightarrow H_2O \text{ (as vapour)}$$

DTA analysis indicates that a considerable liquid phase is formed, which contributes to the melting of the blast furnace slag in the ceramic matrix [110]. So, the sintering process must be carried out by other mechanisms. These changes can be seen as a liquid phase sintering mechanism. This mechanism involves the dissolution of solids in the liquid phase and the growth of crystalline phases [2]. The trapped gas generates the closed pores, while the crystallization process generates the micro pores [111]. Blast furnace slag has no major influence on the thermal properties of sanitary ceramics bodies.

3.5 Effect of blast furnace slag on the physical properties of fired samples

The partial substitution of feldspar by blast furnace slag affects the physical properties of fired sanitary ware bodies. Figure 63 shows the results of changes of total porosity and bulk density of the ceramic bodies. The porosity is reduced by the addition of 10 wt.% of blast furnace slag, while the density increases; this is mainly due to the formation of a liquid phase resulting from the mixing of alkali oxides (Na_2O + K_2O) in the feldspar with the alkaline earth oxides (CaO + MgO), present in the blast furnace slag. The formation of the liquid phase enhances condensation, accelerates the sintering reaction and closes the space between the crystalline phases. Subsequently, the density of the samples decreased as the total porosity increased when the addition of blast furnace slag is more than 10% wt. %. The increase in porosity may be due to the low alkali content of the BFS containing samples, which prevents the formation of the liquid phase [64, 65, 112].

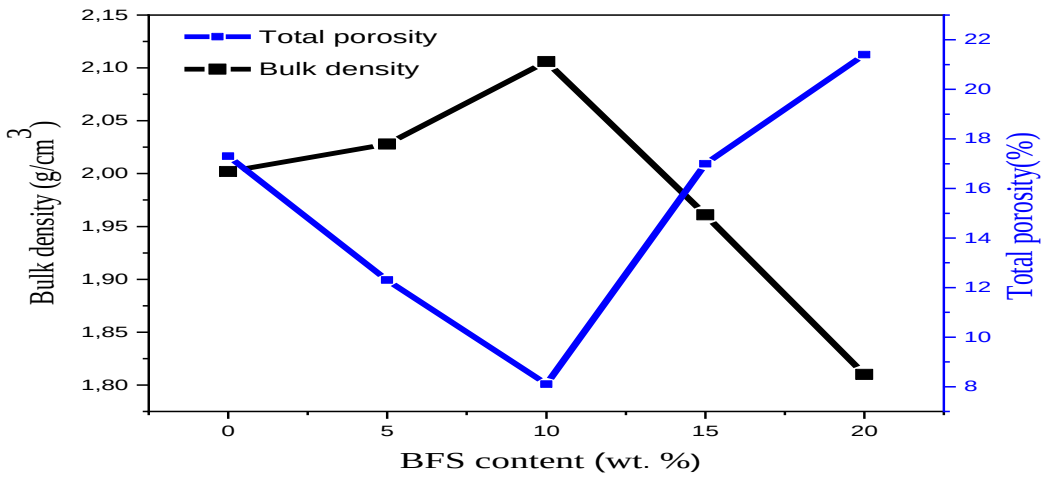

Figure 63: Variation of bulk density and total porosity for a ceramic heated at 1230◦C.

Generally, all physical properties of sanitary ceramic bodies are related to each other, such as the inverse correlation between density and total porosity on the one hand, and firing shrinkage to water absorption on the other.

Furthermore, shrinkage values are related to the amount of liquid phase produced, as shrinkage increases in the presence of a large amount of liquid phase filling the spaces between the crystalline phases and closing the pores. This leads to a decrease in the total porosity and consequently the percentage of water absorption in the samples [83]. Figure 64 shows the changes in firing shrinkage and water absorption with the increasing of blast furnace slag in the composition. The decrease in the water absorption in the case of less than10 wt. % of the slag addition, is attributed to the formation of the liquid phase in sufficient quantity to fill the pores due to the presence of alkali feldspar oxides. However, when the substitution of feldspar by blast furnace slag exceeds 10 wt. % in the composition, the amount of alkali oxides decreases as the amount of alkaline earth oxides in the slag is increased. The decrease in alkali oxides, directly affects the formation of the liquid phase. The lower amount of liquid phase in the composition leads to an increase the formation of pores and the opening of voids between the crystalline phases; this which increases water absorption and reduces shrinkage [113]. According to the production requirements of sanitary ware bodies and (ASTM C: 326-82), the maximum value of final shrinkage is usually less than 12%, thus, improving the properties of the final products. In addition, according to ASTM C 373-88, low water absorption, below 0.5% is a significant requirement to ensure hygiene throughout the lifetime of the product [83, 98, 114].

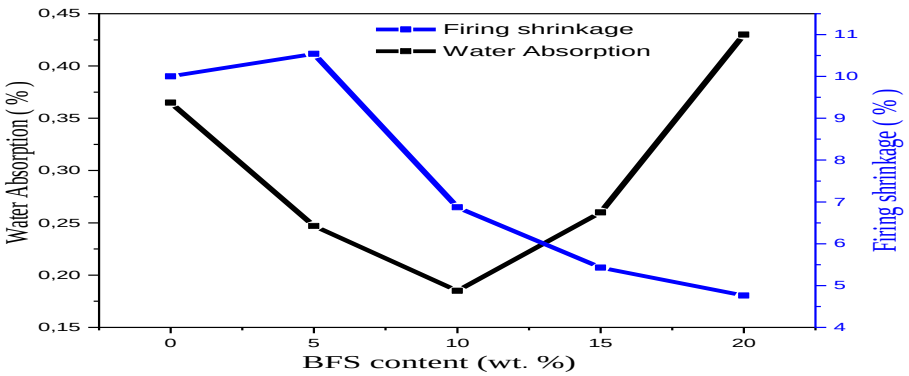

Figure 64: Variation of water absorption and firing shrinkage for a ceramic heated at 1230◦C.

3.6 Flexural strength of fired samples

Flexural strength is a mechanical property of the material and represents the maximum value of the flexural stress before the rupture of the sample. Ceramic bodies are affected by the flexural strength applied to them according to their chemical composition and their physical and thermal properties acquired during firing. The effect of the addition of blast furnace slag to the composition of sanitary bodies, on the flexural strength, is illustrated in Figure 65. An increase in flexural strength was observed for ceramic bodies containing 10 wt.% blast furnace slag (41MPa) compared to standard ceramics (33 MPa), This can be attributed to the higher pre-stress resulting from the difference in thermal expansion coefficients between the formed anorthite grains, the vitreous matrix and other crystalline phases (mullite and quartz) during the cooling process. Many authors in earlier studies have reported similar findings [39, 60].

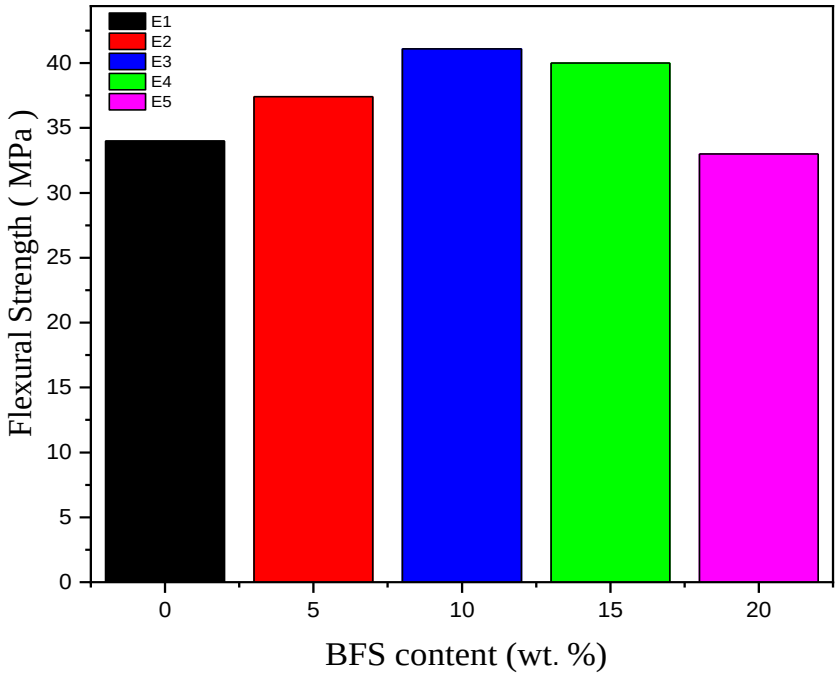

Figure 65: Evolution of the flexural strength in the case of a ceramic heated at 1230◦C.

3.7 X-ray Diffraction analysis

The substitution process in the chemical composition affects directly the different crystalline phases within the ceramic matrix. The presence of mullite, increases mechanical resistance due to its high strength, as it has a bending strength of up to 400 MPa, in addition to its low thermal expansion coefficient. This one, contributes to the chemical stability of the ceramic body [115]. Quartz's role is to adapt the plasticity of the clay slip and to reduce the firing shrinkage of the ceramic body during the firing stage. The vitreous phase is formed by the solid phase reaction of amorphous silica with molten feldspar at high temperature; its role is to increase the densification and reduces the water absorption rate[116]. Figure 66 shows the X-ray diffraction analysis of the ceramic bodies fired at 1230 °C. From the XRD peaks, mullite and quartz are the main phases in the reference sample E1. The gradual addition of blast furnace slag, leads to a decrease in the mullite peaks intensity; while the quartz peaks remains constant. This is consistent with the gradual appearance of the anorthite phase, which becomes the dominant phase, with that of quartz, in the samples containing 20 wt. % slag. The source of the formation of anorthite phase is the high calcium oxide content in blast furnace slag, compared to feldspar. The growth of the anorthite phase in ceramics E4 and E5 could be the cause of the reduced density of the fired samples, resulting from the low theoretical density of the anorthite phase ~2.7g/cm^3 compared to the mullite phase ~3.2g/cm^3 [65, 117, 118].

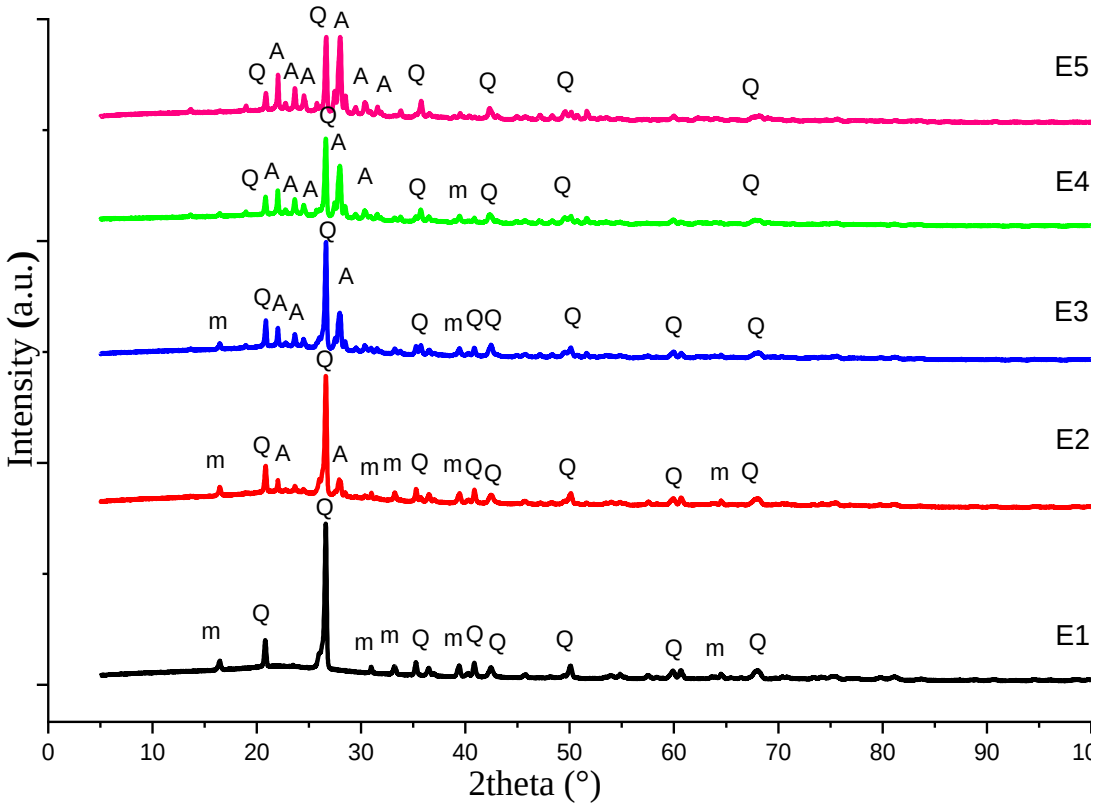

Figure 66: XRD patterns for heated samples contained BFS at 1230 °C (m: mullite,Q: quartz, A: anorthite).

3.8 SEM Analysis

The microstructure of ceramic bodies controls physical and mechanical properties of the body. Therefore, scanning electron microscopy analysis is usually used to characterise the material that make up the body: the glass matrices, and the various types of pores. Figures 67, 68 and 69 show the microstructure obtained for different blast furnace slag mixtures (0, 10 and wt. 20%) treated at 1230°C. In the reference (commercial) sanitary porcelain body sample, it is clear that there is a glassy matrix containing a mass of crystals of different shapes and sizes [119]. Quartz represents the predominant component, as appears in the EDS analysis. The reference sample, also shows some pure clay particles in addition to dissolved clay infiltrated with feldspar, inside the glass matrix. Besides, a small amount of pores appears in the ceramic matrix [120].

In sample E3 (10 wt. % BFS), the addition of blast furnace slag instead of feldspar leads to an increase in the percentage of calcium oxide within the ceramic body, which leads to

the formation of the anorthite phase; this appears clearly with quartz grains, as confirmed by EDS analysis. The presence of alkaline earth oxides in feldspar, in combination with earth oxides present in feldspar, leads to the formation of the early glassy phase. We have also the beginning of the formation of open pores inside the matrix.

In E5 samples (20wt. % BFS), anorthite becomes the predominant phase within the ceramic matrix, as confirmed by EDS analysis. There are also quartz grains and some scattered mullite crystals with a clear porosity on the surface of the crystals; these results are very consistent with the XRD analyses[121].

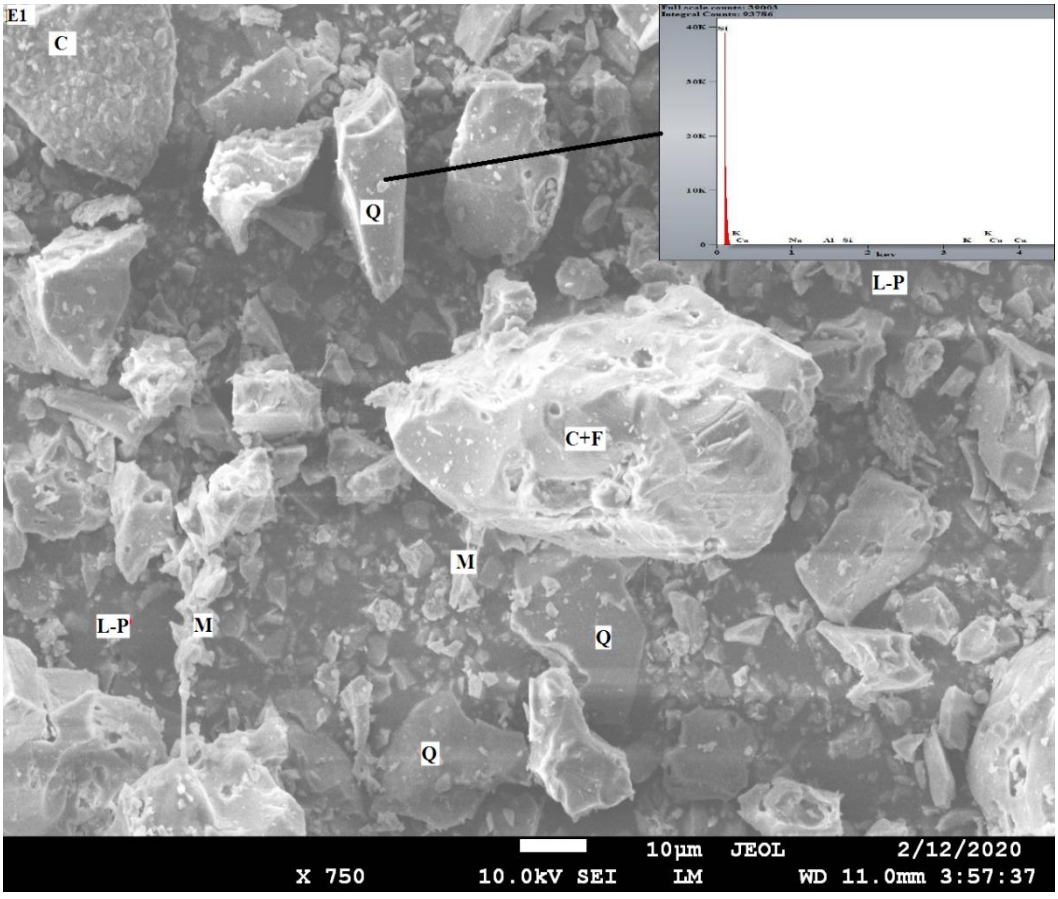

Figure 67: SEM-EDS analysis for E1 sample at 1230 °C. (M: mullite,Q: quartz, C: pure clay, C+F: clay+ melted feldspar, L-P: liquid phase).

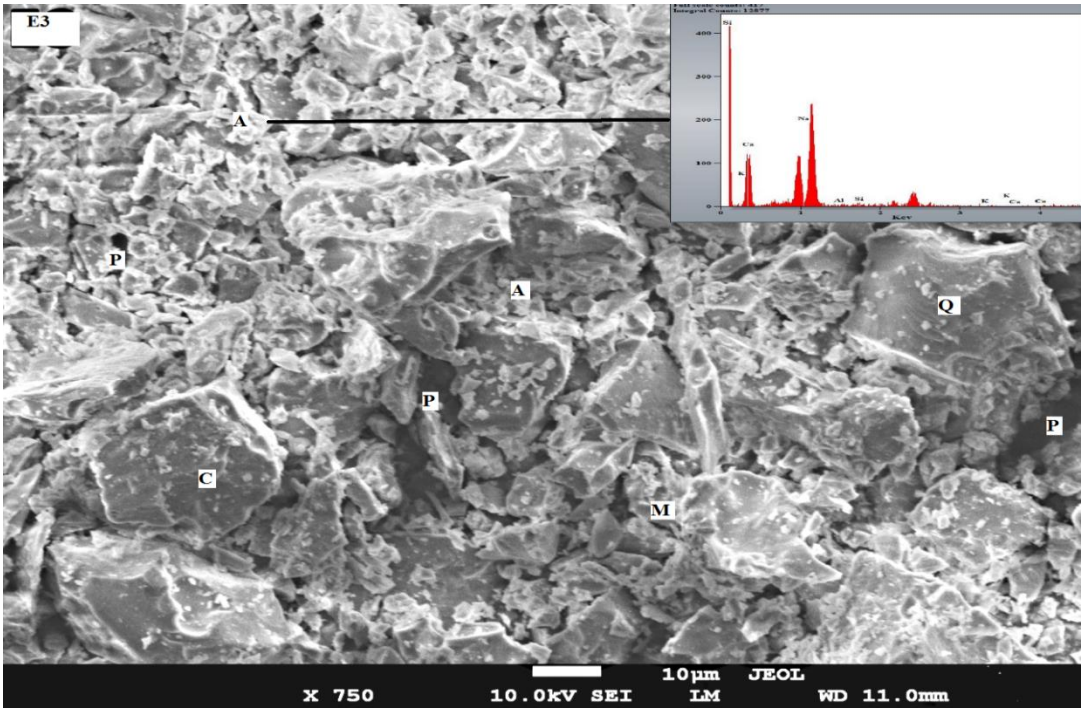

Figure 68: SEM-EDS analysis for E3 sample at 1230 °C. (M: mullite,Q: quartz, C: pure clay, A:anorthite, C+F: clay+ melted feldspar, L-P: liquid phase, p: pores).

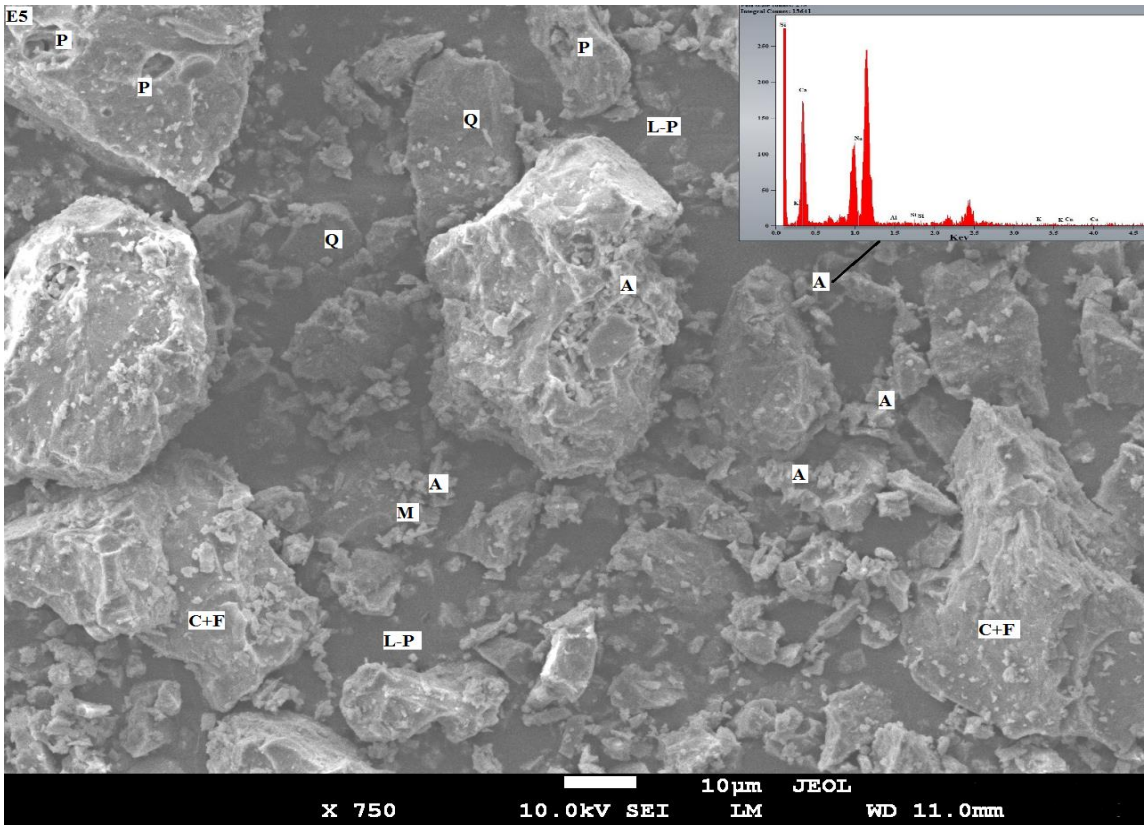

Figure 69: SEM-EDS analysis for E5 sample at 1230 °C. (M: mullite,Q: quartz, C: pure clay, A:anorthite, C+F: clay+ melted feldspar, L-P: liquid phase, p: pores).

3.9 Infrared spectroscopic study

To provide a comprehensive characterisation of clay minerals, it is useful to examine a sample measured with the KBr. Figure 70 shows the absorption bands in the range 500-4000 cm-1. Infrared spectrometry analyses allow the identification of the chemical bonds present in the ceramic body. The spectra of ceramics (0, 5, 10, 15 and 20wt. % blast furnace slag) corresponding to the main chemical bonds after firing at 1230°C .

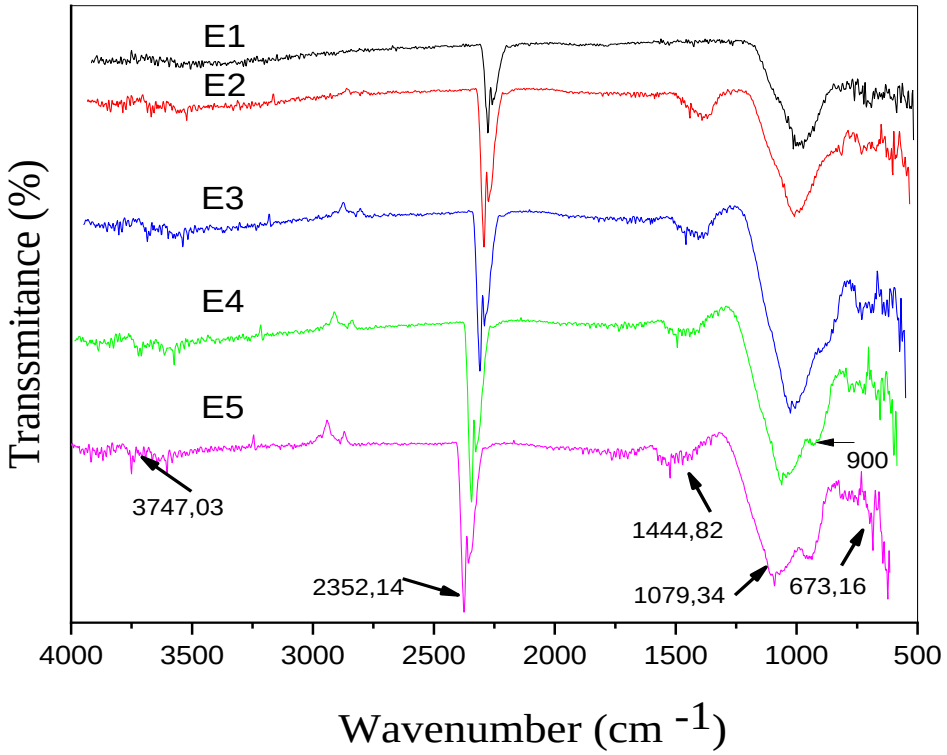

Figure 70: FTIR spectra of the ceramics E1.E2.E3.E4 and E5.

The bending vibrations Si-O located at 673cm^{-1} in all specimens, indicate the presence of quartz and assert its stability after firing of the clay; this band may also be created by the stretching effect of the Al-O vibration in the octahedral distribution [122, 123]. The 900 cm-1 absorption bands identified in samples containing slag are attributed to the asymmetric stretching of the AlO_4 groups in the vitreous phases [116, 124, 125]. The bands at 1079 cm-1 can be assigned to Si-O and (Si-O-Si) vibrations of siloxane bonds [126, 127]. The wavenumbers located at 1444 cm^{-1} are attributed to the Si-O-Ca bands, which signals the anorthite phase formation from the CaO oxide in the BFS-containing samples; they can also be related to the formation of calcite [128, 129]. Absorption bands at 2352 cm^{-1} are

assigned to the presence of –OH group in the ceramics [130]. Further peaks at 3747 cm^{-1} are attributed to OH stretching vibrations originating from Si-OH groups, which indicate the transformation of kaolinite to metakaolinite [122, 125].

3.10 Conclusion

We investigated the effect of the substitution of feldspar by Algerian blast furnace slag from the El-Hadjar steel factory, on the properties of commercial sanitary ceramic bodies. This experimental work aimed to find the optimal combination. We can summarise the results obtained as follows:

- The rheological behaviour of the slip containing BFS can be improved by using Na-electrolytes at a ratio Na_2CO_3/Na_2SiO_3=1.5 and a combined amount of 0.375 wt.% to get optimized results.
- According to TDA/TGA analysis, there is no significant effect on loss mass and kaolinite dehydroxylation and mullite crystallisation peaks.
- The use of BFS increases the formation of anorthite according to the XRD, SEM and FTIR analyses.
- The addition of BFS (10 wt. %) in sanitary ceramic bodies composition, improves flexural strength (33 to 38 MPa) and reduces water absorption (0.35 to 0.10 %).

Sanitary ceramic bodies can be produced by incorporating 10 wt. % of the blast furnace slag (BFS), while they gain in quality and allow waste recycling.

4.EFFECT OF SODA-LIME GLASS WASTE ON SANITARY CERAMIC BODIES

4.1 Introduction

Glass waste has been the subject of many technical studies in the near past. The aim is the valorisation and recycling of this solid waste into various construction materials. The use of glass waste in industrial applications is based on the knowledge of Physical, chemical and technological properties [68].

Algeria has a large production of glass waste, particularly soda-lime glass waste (SLGW). Recent studies have focused on its integration as an alternative material in the formulation of various ceramic materials. The importance of SLGW in the ceramic industry results from their chemical composition rich in SiO_2, Na_2O and CaO. In addition, it has alow melting temperature [51, 68].

This chapter is devoted to study of the integration of SLGW in the preparation of sanitary ceramic bodies to test the effect of these wastes on the rheological, thermal, physical-mechanical and structural properties.

4.2 Preparation of sanitary bodies from Soda-lime glass waste

The preparation of our sanitary bodies from SLGW, is based on the same process described in chapter III; we replacethe feldspar (Na and K) with SLGW. The different formulations are summarised in the Table 16, while the chemical composition of raw materials are presented in table 17. As in the chapter III, the reference formulation represents the composition of the slip of the sanitary ceramic factory of El-Milia - Jijel. Algeria.

Table 16: Formulations (in wt. %) of batch compositions VC, C2, C3, C4 and C5.

Raw material	VC	C2	C3	C4	C5
Clay (Hycast VC)	28	28	28	28	28
Par Kaolin	12	12	12	12	12
kaolin RMB	12	12	12	12	12
Sodium feldspar	12	9.5	7	4.5	2
Potassium feldspar	11	8.5	6	3.5	1
Quartz	25	25	25	25	25
SLGW	0	5	10	15	20

Table 17: Chemical composition of raw materials

Oxides	clay Hycast VC	Par Kaolin	Kaolin RMB	Sodium feldspar	Potassium feldspar	Quartz	SLGW
SiO_2	52	48	48	70.44	69.5	96.35	70.25
Al_2O_3	31	37	37	17.92	17.3	0.52	1.71
TiO_2	1	0.06	0.05	0.26	0	0.05	0
CaO	0,2	0.07	0.07	0.5	0.5	1.19	13.43
MgO	0.4	0.3	0.3	0.2	0.2	0.08	0.52
K_2O	2.1	1.9	1.5	0.4	9	0.17	0.28
Na_2O	0.2	0.1	0.1	9.6	3.1	0.08	13.43
Fe_2O_3	1	0.19	0.8	0.08	0.1	0.24	0.33
L. O. I	12	11.8	12.1	0.5	0.4	1.29	0.1

4.3 The melting behavior of feldspar and SLGW

A better understanding of the properties of glass waste added to the composition, can help explain its effect on the different behaviours of the ceramic body during sintering. Melting behaviour is one of the most important factors in the identification of raw materials for the traditional ceramic industry, especially the raw materials that act as fluxes within the ceramic composition [131]. The partial replacement of feldspar by the SLGW in the composition of sanitary ceramics makes the study of the melting behaviour of these materials very important. The cones are made of different types of feldspar, on the one hand, and SLGW on the other. The samples are fired in a tunnel kiln at 1230°C, as shown in figure 71. SLGW has a fast melting behaviour compared to the two types of feldspar; this is due to the presence of the mixed effect of the alkaline Na_2O and the alkaline earth CaO, which helps reduce the firing temperature and accelerate the growth kinetics of the mullite phase [21, 84, 132].

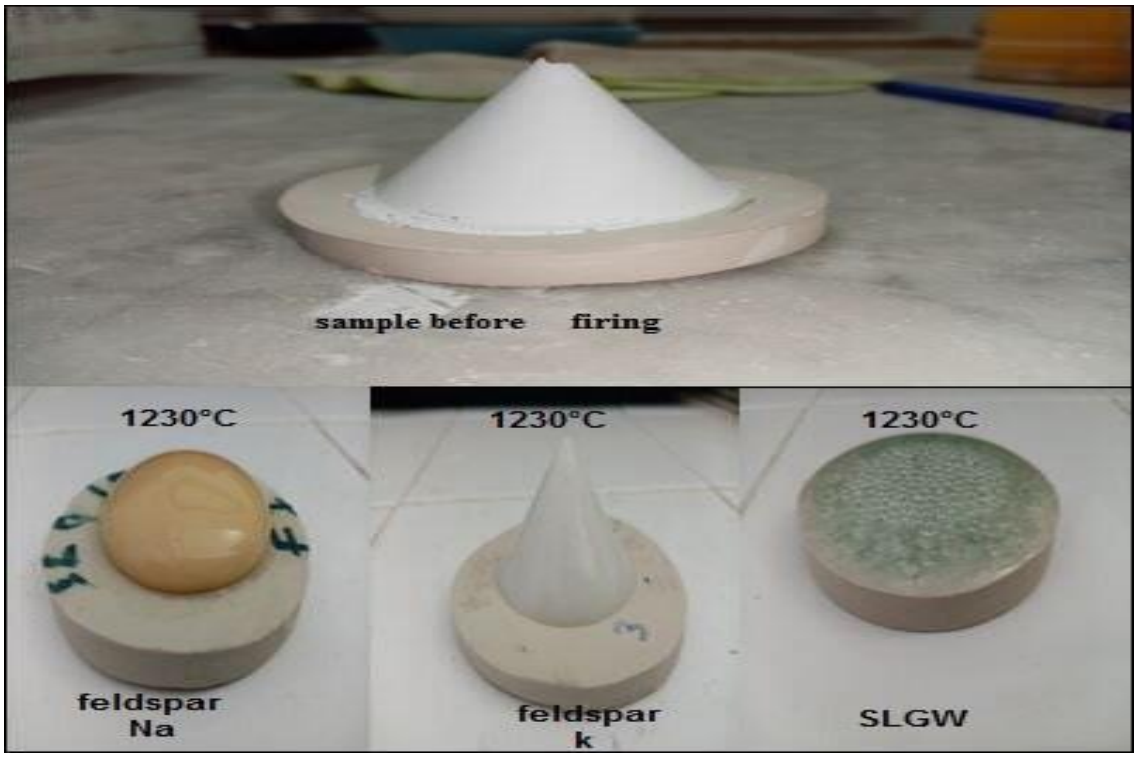

Figure 71: Melting of feldspar and SLGW at 1230°C.

4.4 SLGW effect on the rheological bahaviour of sanitary slip

The rheological properties of each slip are shown in the following table:

Table 18: Rheological properties of slip compositions.

	VC	C2	C3	C4	C5
Slip density (g/cm^3)	1.77	1.78	1.78	1.77	1.78
fluidity (s)	16	14	11	12	11
residue on sieve (63µm)	1.7	1.9	1.8	1.5	1.9
Viscosity (°G)	300	305	309	299	300
Drying shrinkage (%)	4.11	7.19	7.87	7.98	8.30
Thixotropy after 5 min (°G)	52	32	9	15	10
Thixotropy after 15 min (°G)	87	55	22	19	17
Thickness after 1 h (mm)	6.7	7.8	6.50	6.80	6.10
Sodium silicate deflocculated (%)	0.1				
Sodium carbonate deflocculated (%)	0.075				

The results listed in table 18, show that all the slips have very similar values for residue on the sieve, density and viscosity; also, the values for thixotropy and thickness are within the specified range. The chemical composition of SLGW, rich in silica and sodium oxides, acts as a deffloculant agent to accelerate slip fluidity. Therefore, the use of SLGW does not require the use of sodium silicate. The slip viscosity significantly affects the superficial charge of particles, thus creating a change in the pH of the material [106]. However, the integration of SLGW leads to the formation of calcium and sodium hydroxides, because of the excessive amount of Ca^{+} and Na^{+} cations in the mixture, causing a decrease of the diffusion layer thickness [37, 132].

4.5 Effect of soda-lime glass waste on the physical properties of fired ceramics

Figures 72 and 73, show the findings for total porosity, bulk density, firing shrinkage and water absorption of fired samples. The integration of SLGW in the composition of the sanitary bodies, reduces significantly the porosity of the industrial ceramic VC. The ceramic containing 20 wt.% SLGW, has a total porosity of 2.8%; whereas the industrial ceramic VC body has a porosity of more than 10%. The characteristic composition of waste glass, rich in alkali and alkaline earth oxides (Na_2O and CaO), makes it play the role of a classic flux (Albite and Anorthite feldspar). The presence of these oxides, contributes to the extensive formation of the liquid phase that fills the pores and voids between the crystals of the ceramic material; this leads to an increase in density and a decrease in the total porosity. It also transforms open porosity into closed porosity, which decreases the total volume of the body (increase in shrinkage); it also, reduces water absorption [113]. Generally. The linear shrinkage values do not exceed 12% and the amount of water absorption does not exceed 0.5% in all fired samples. All these results are consistent with the requirements of sanitary ware production according to (ASTM C: 326-82 and ASTM C 373-88) [97, 98, 132].

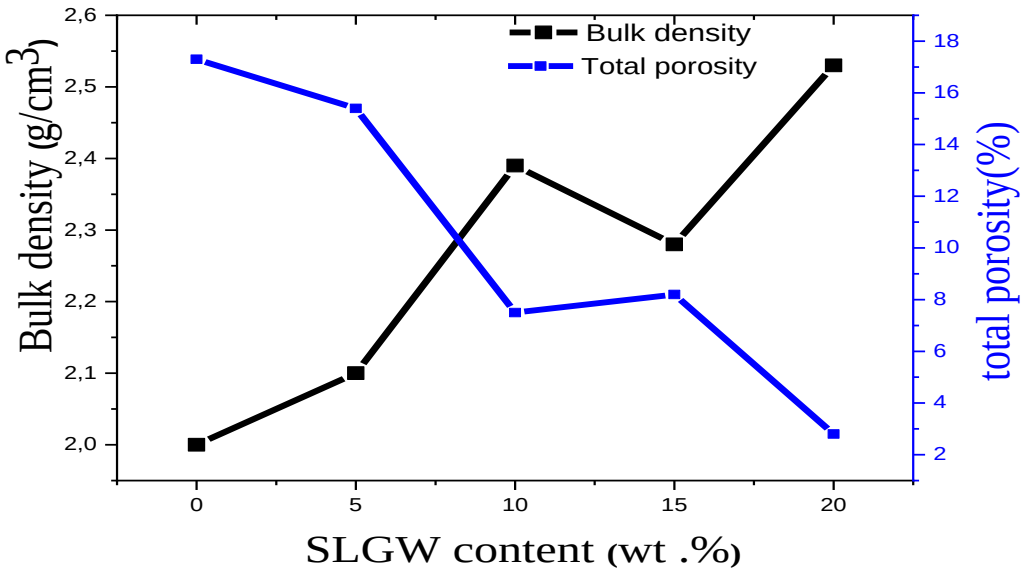

Figure 72: Bulk density and total porosity of the sintered samples.

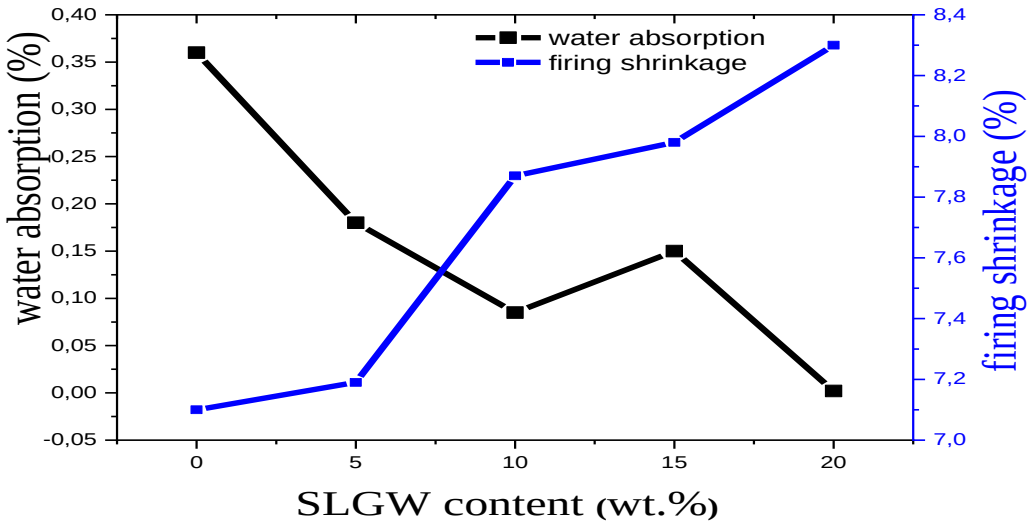

Figure 73: Water absorption and firing shrinkage of the sintered samples.

4.6 Effect of SLGW on the flexural strength of fired ceramics

Figure 74 shows the effect of SLGW on the flexural strength of sanitary ceramic samples. As mentioned before, all the ceramic bodies of different compositions have a good degree of densification, as crystalline phases such as mullite and quartz are dispersed in the glassy phase; we may add that with a low porosity, the flexural strength values go up. The flexural strength of sample C5 (20 wt.% SLGW) is the highest (51 MPa), compared to the standard VC ceramics (33 MPa). A small increase in the flexural strength of ceramics C2,

C3 and C4, can also, be observed. The presence of calcium oxide in the composition of SLGW, contributes to the formation of the anorthite phase inside the glassy matrix. The difference in the coefficient of thermal expansion between the formed anorthite crystals, mullite, quartz and the liquid phase increases the prestressing during the cooling process, thus, enhancing the flexural strength of the ceramic body [39, 60]. It is interesting to note that the flexural strength of all samples range from 33 to 51 MPa. These values are satisfactory for unglazed sanitary wares [113, 133].

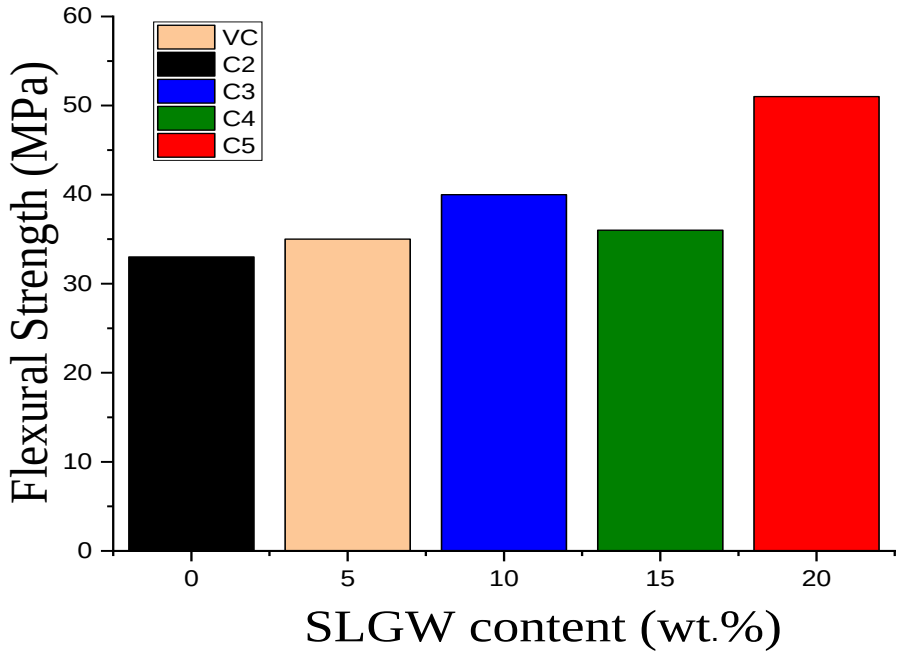

Figure 74: Evolution of the flexural strength of samples fired at 1230◦C.

4.7 X-ray Diffraction analysis

Traditional triaxial ceramics (kaolinite, feldspar and quartz) generally have a heterogeneous structure. The crystalline phases (mainly quartz and mullite) and a certain level of porosity are dispersed in the glass matrix [60]. Figure 75 shows the X-ray diffractograms corresponding to the fired samples. Quartz and mullite are the main phases in the standard ceramic sample. The partial replacement of the feldspar by soda-lime glass waste leads to the gradual formation of the anorthite phase, which is mainly caused by the high calcium oxide content (CaO >13 %) in the SLGW [134]. In addition, the mixed alkali and alkaline earth, result in the formation of a glassy phase and mullite; while, the sharp quartz peaks can be attributed to the strong presence in all samples of (SiO_2 > 70%) [132, 135].

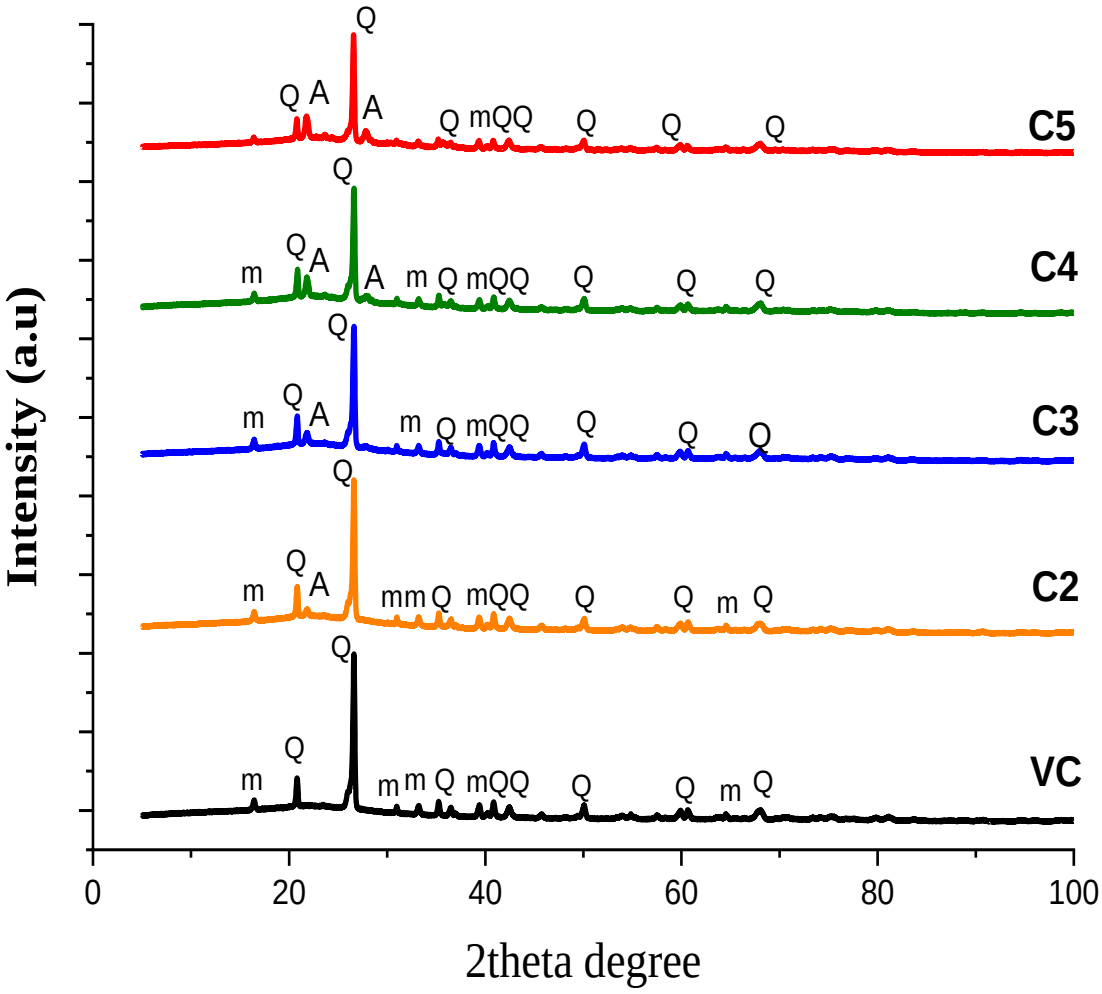

Figure 75: XRD patterns for heated samples contained SLGW at 1230 °C (m: mullite,Q: quartz, A: anorthite).

4.8 SEM Analysis

Microstructural observations of VC, C2, C3, C4 and C5 ceramics with different SLGW incorporation ratios are presented in figures 76, 77, 78, 79 and 80. All samples have a similar morphology. The ceramic matrix contains agglomerations of feldspar-infiltrated clay residues, as well as agglomerations of pure clay in addition to quartz. The pure clay residues are the main source of primary mullite, while the feldspar-infiltrated clay residues are the source of secondary mullite [120, 136]. The gradual emergence of the anorthite phase, results from the incorporation of SLGW, which is rich in calcium oxide. The porosity decreases significantly in sample C5 (20wt. % SLGW) [132].

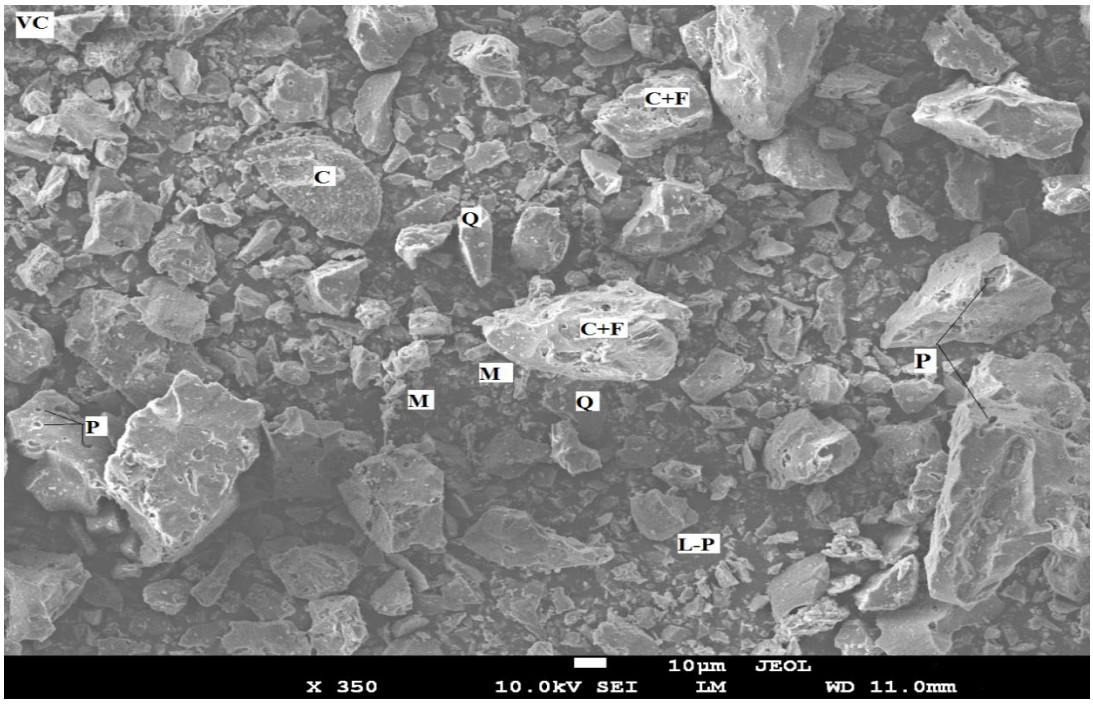

Figure 76: SEM analysis for VC sample at 1230 °C (M: mullite,Q: quartz, C: pure clay, C+F: clay+ melted feldspar, L-P: liquid phase, P: pores).

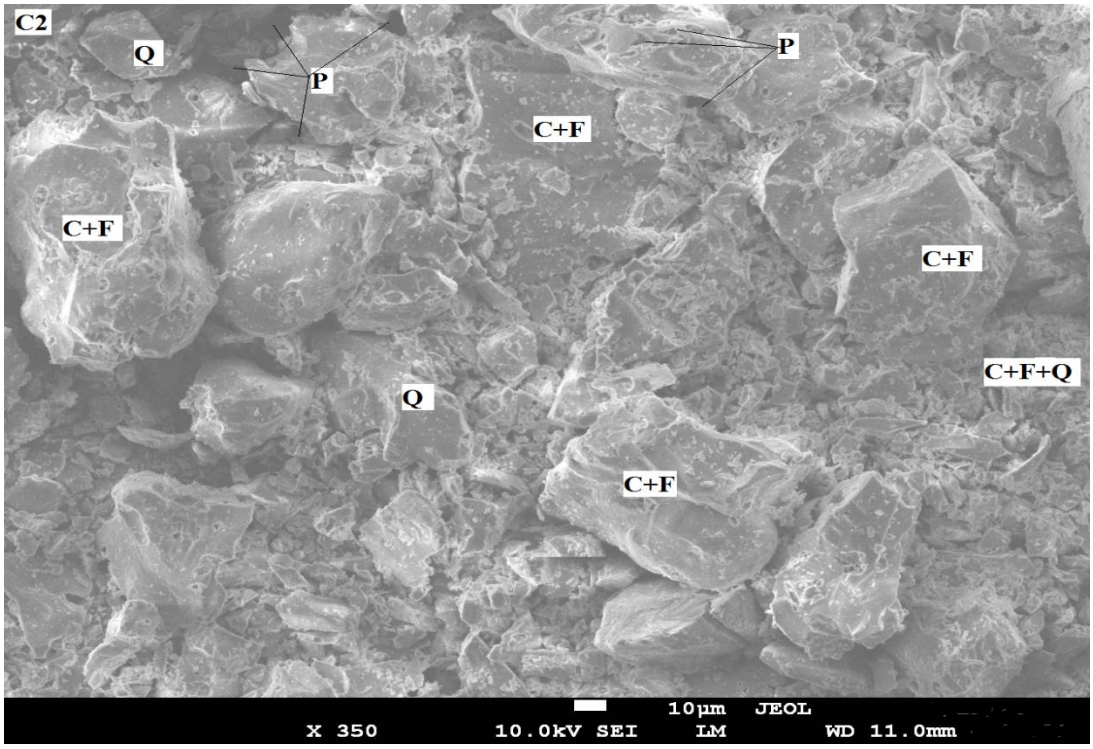

Figure 77: SEM analysis for C2 sample at 1230 °C (Q: quartz, C: pure clay, C+F: clay+ melted feldspar, L-P: liquid phase, P: pores).

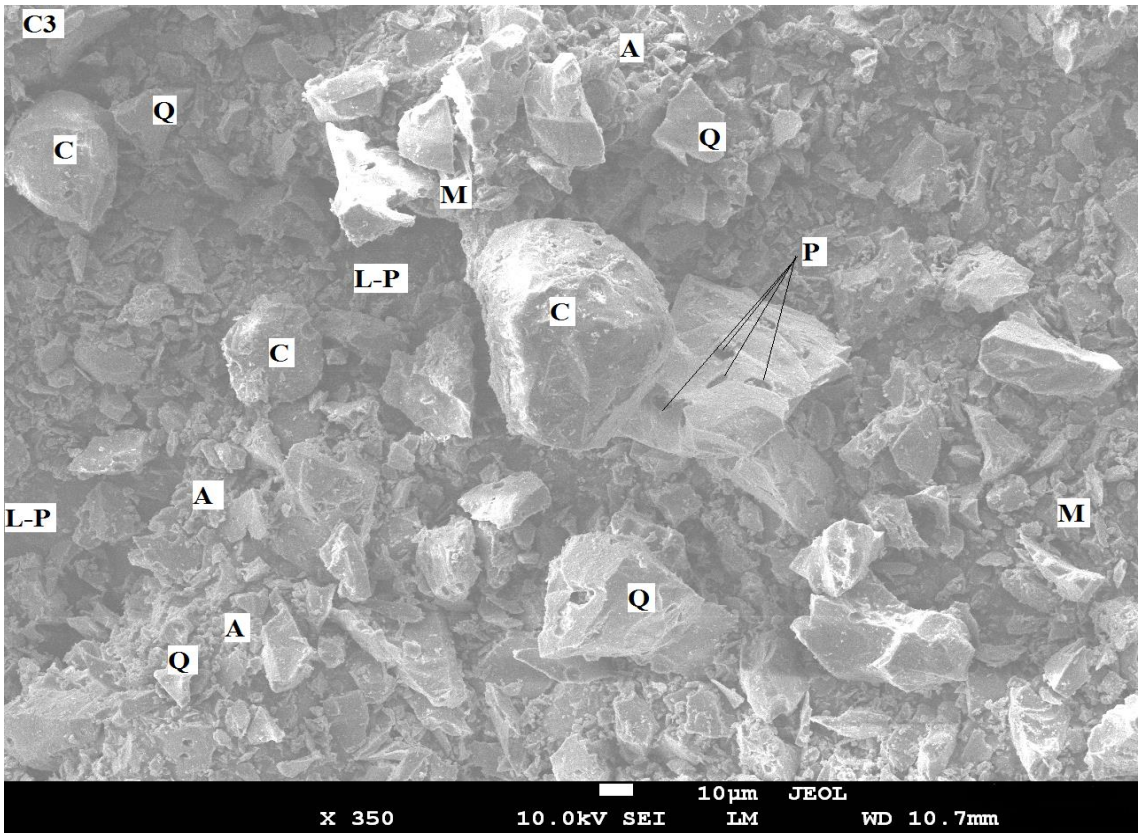

Figure 78: SEM analysis for C3 sample at 1230 °C (M: mullite,Q: quartz, C: pure clay, C+F: clay+ melted feldspar, L-P: liquid phase, P: pores).

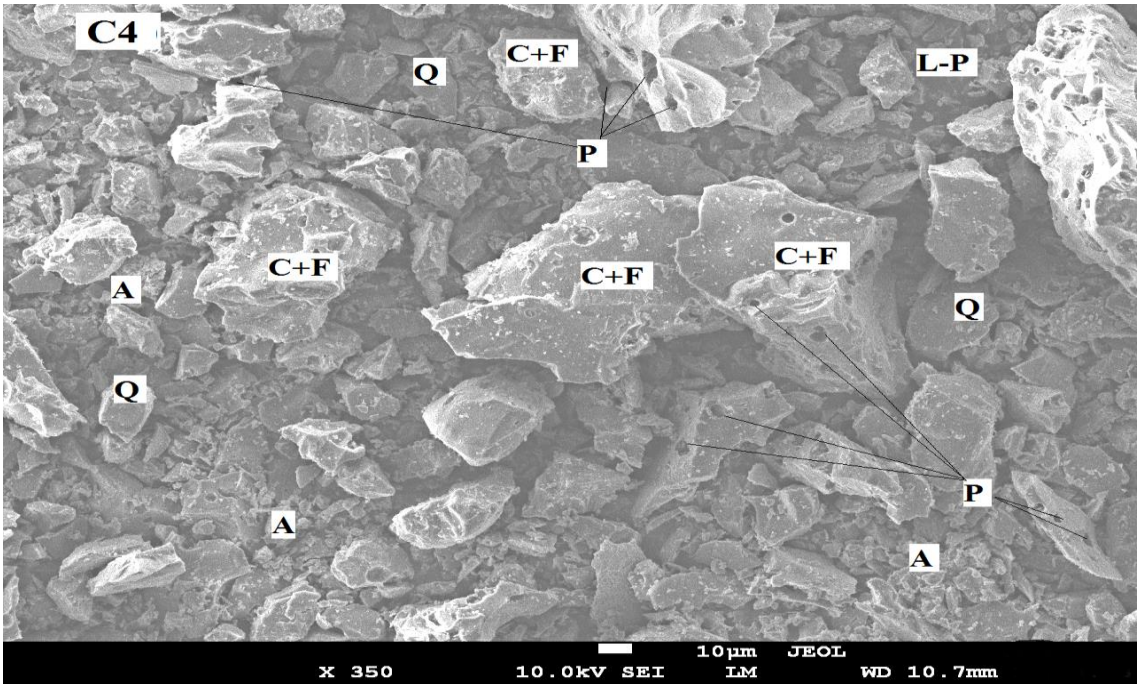

Figure 79: SEM analysis for C4 sample at 1230 °C (Q: quartz, C: pure clay, C+F: clay+ melted feldspar, L-P: liquid phase, P: pores).

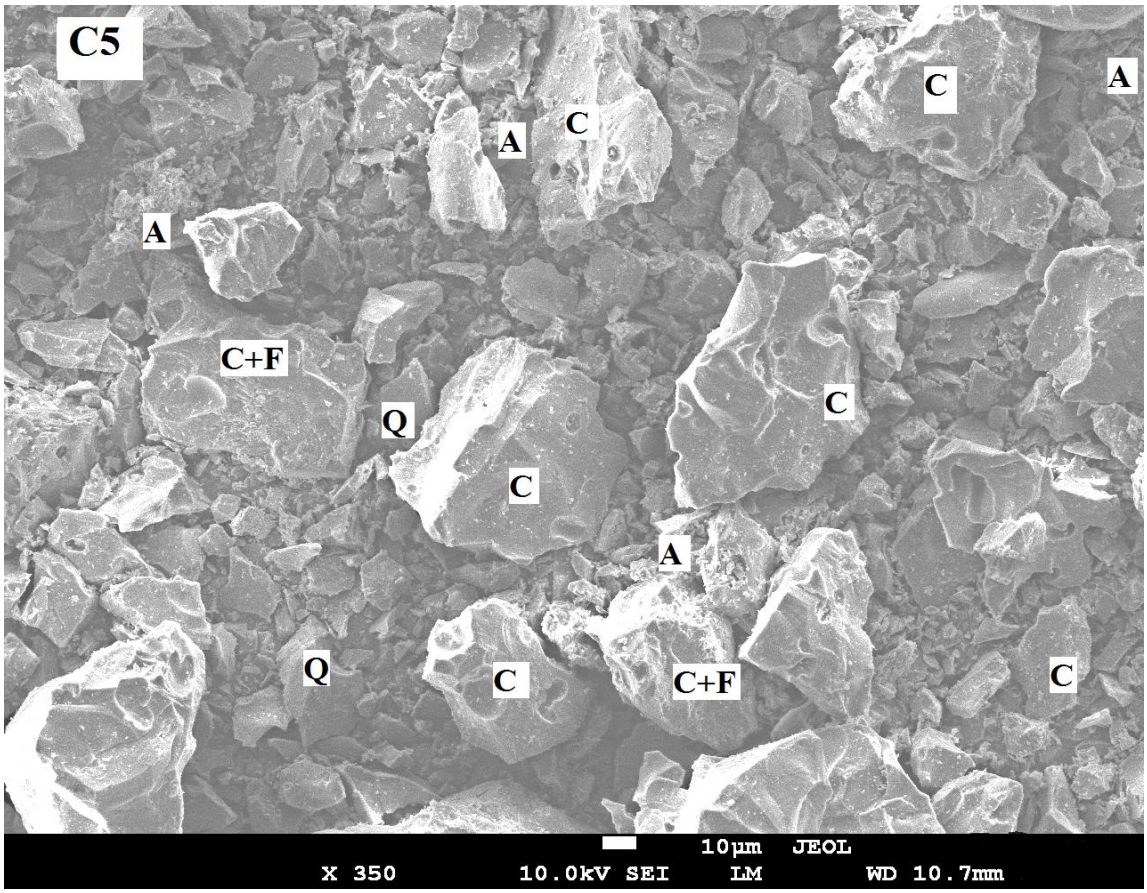

Figure 80: SEM analysis for C5 sample at 1230 °C (Q: quartz, C: pure clay, C+F: clay+ melted feldspar, L-P: liquid phase, P: pores).

4.9 Thermal analysis

Figures 81, 82 and 83 present the TGA/DTG curves of samples VC, C2 and C4, which contain 0, 5 and 15 wt. % SLGW. In the three ceramic samples, we note the first loss of mass in the interval 20°C - 100°C; it is attributed to the elimination of the water present in the raw materials. The second mass loss from 400 to 600°C is attributed to kaolin dehydroxylation to form metakaolin ($A1_2O_3.2SiO_2$); this is consistent with the peaks seen in the DTG analysis curves as they appear at 480 °C for the VC sample and 500 °C for ceramic bodies containing 5 and 15 wt. %SLGW [115]. As the temperature increases, the mass loss continues; in fact, DTG analysis indicates three minor peaks at 1099, 1047 and 1107 °C, for samples with 0, 5 and 15 wt.% of SLGW, respectively. These small peaks are attributed to the crystallisation of the mullite phase [39, 137]. The values of total mass loss in the ceramics 0, 5, and 15 wt. % SLGW are: 8.83, 8.12 and 8.56%, respectively. The addition of SLGW reduces mass loss in sanitary ceramic bodies, it could be related to the

lower ignition loss that SLGW has (0.1 wt. %), compared to potassium feldspar (0.4 wt. %) and sodium feldspar (0.5 wt. %) [84, 132].

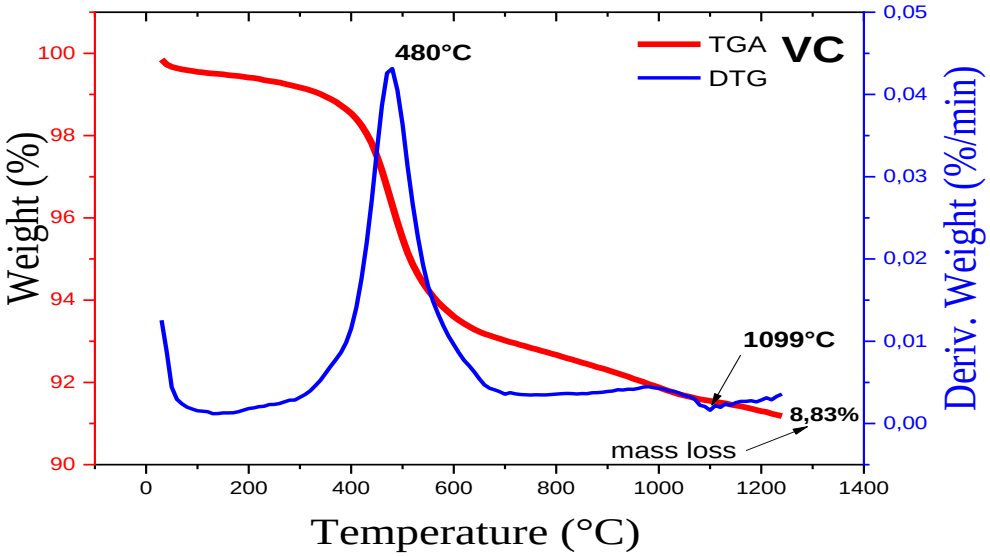

Figure 81: TGA/DTG analysis of the mixture, with 0% of SLGW.

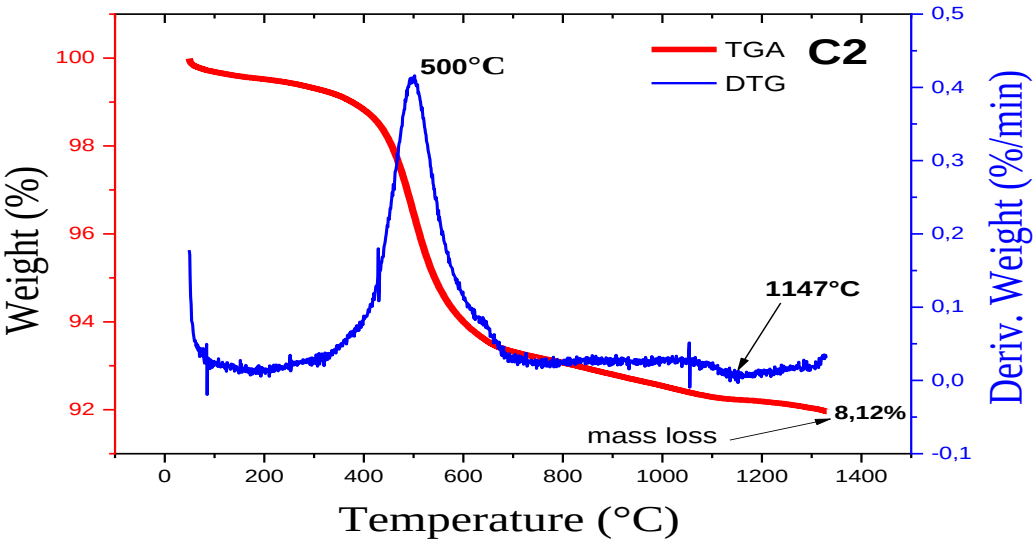

Figure 82 : TGA/DTG analysis of the mixture, with 5% of SLGW.

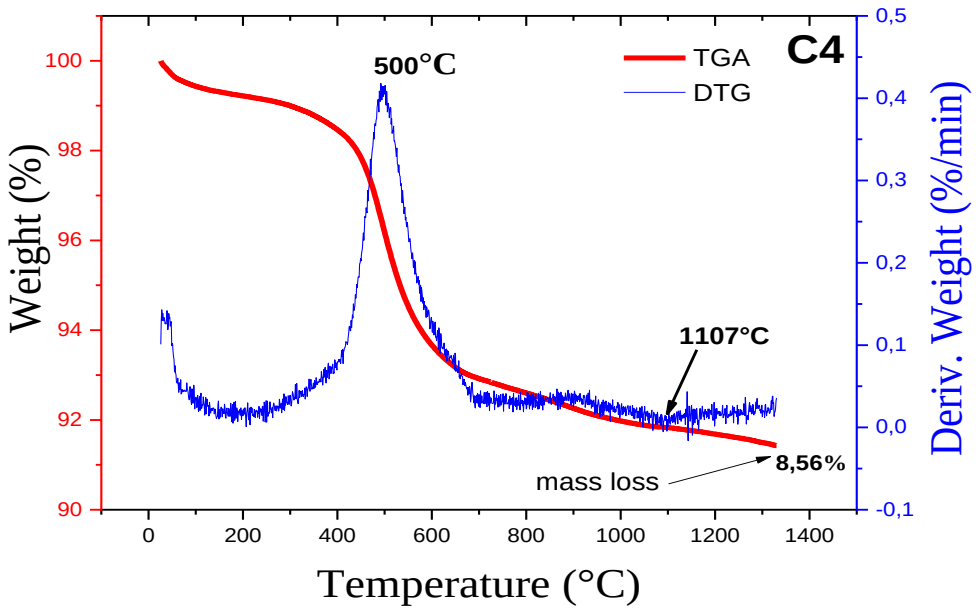

Figure 83 : TGA/DTG analysis of the mixture, with 15% of SLGW.

4.10 FTIR Spectroscopy

Figure 84 shows the FTIR spectra of the studied ceramic samples. Most of the bands are narrow and sharp, which indicates the regular structure of the ceramic body. The peak that appears at 715cm^{-1} can be assigned to the (Al-O-Si) bending vibration bond [138]. A band at 1079cm^{-1} may be related to (Si-O-Si) stretching vibrations of the siloxane bonds and Si-O vibrations [127]. The weak bands appearing at 1580cm^{-1} in samples containing SLGW indicates the presence of bound water in the cordierite-mullite structure[139-141]. The sharp band that appears in all samples at 2352cm^{-1} are to be assigned to –OH group in the ceramics [127, 130]. Moreover, very small bands appear at 3232cm^{-1}, indicating the absorption of calcium-silicate hydrate (Ca-Si-H) compounds [142].

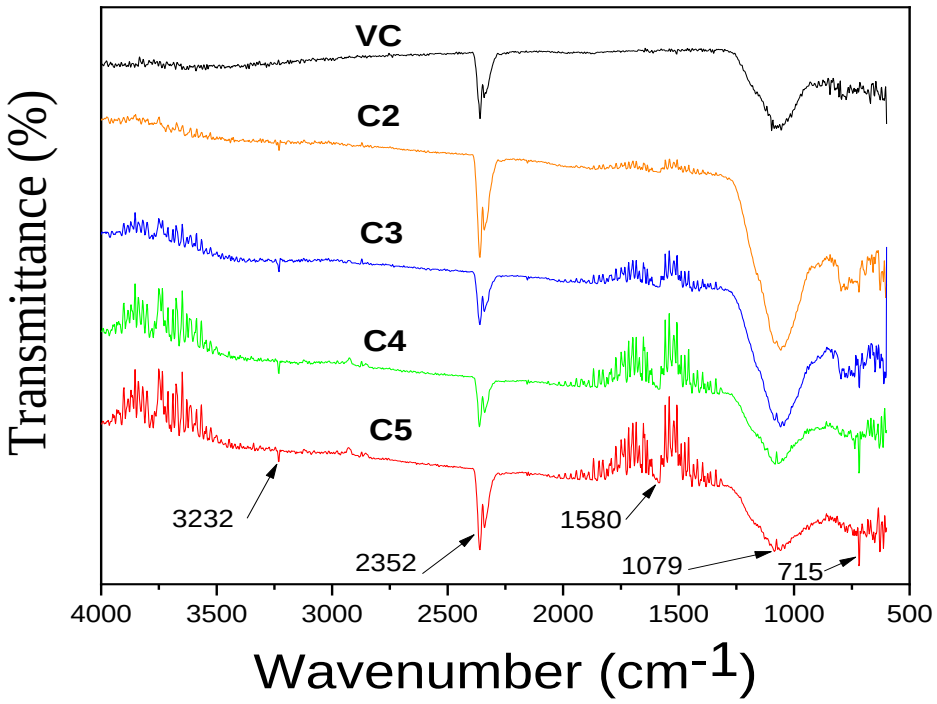

Figure 84: FTIR analysis of the mixtures with 0, 5, 10, 15and 20 % SLGW.

4.11 Conclusion

We studied the effect of replacing feldspar with soda-lime glass waste originating from the factory of the African Glass Company (Jijel, Algeria), on the properties of commercial sanitary-ware bodies. The findings can be resumed as follows:

- SLGW powder has improved many slip properties without needing a large amount of Na-electrolytes (0.075 wt. % Na_2CO_3 and 0.1 wt. % Na_2SiO_3).
- From the TGA/DTG curves, SLGW reduces mass loss in sanitary bodies as a result of its lower ignition loss, compared to both types of feldspar.
- The addition of SLGW (20 wt. %) improves physical-mechanical properties, including bulk density (2-2.52 g/cm^3), flexural strength (33-51 MPa) and reduced water absorption (0.35 to 0.02 %).
- According to XRD, SEM and FTIR analyses, quartz and mullite are the main crystalline phases present, with a gradual appearance of anorthite due to SLGW additions.

To conclude, satisfactory sanitary ceramics products can be prepared with the incorporation of 20wt. % of soda-lime glass waste (SLGW).

5.EFFECT OF SANITARY CERAMIC WASTE ON THE PROPERTIES OF THEIR UNGLAZED BODIES

5.1 Introduction

Sanitary ceramic is a necessary material commonly used in buildings. The increase in the production of various sanitary ware automatically leads to an increase in their waste production resulting from various deformations such as shrinkage, as it generates from 20 to 30 tons every month from each sanitary factories [85, 143].

Sanitary ceramic waste (SCW) is of much important, since it can be incorporated into various construction materials. The growing interest in the valorisation of this waste means more research on its physical, chemical and technological properties [89].

Many recent studies have been conducted to include SCW in the preparation of various ceramic materials, for industrial applications. The rich chemical composition of Al_2O_3 and SiO_2 in SCW makes it a good and material in the ceramic industry. This chapter focuses on the effect of partial replacement of feldspar with SCW on the different properties of sanitary ceramic bodies [144].

5.2 Preparation of sanitary ceramic bodies using their glazed waste

This preparation of sanitary ceramic bodies from SCW follows the same steps as in chapter III; we substituted the feldspar (K and Na) with SCW. We present in table 19 the different compositions of the ceramic samples, while table 20 shows the chemical composition of the SCW and raw materials.

Table 19: Formulations (in wt. %) of ceramic compositions for VC, VC5, VC10, VC15 and VC20 samples.

Raw materials	***VC***	***VC5***	***VC10***	***VC15***	***VC20***
Clay (Hycast VC)	28	28	28	28	28
Parkaolin	12	12	12	12	12
kaolin RMB	12	12	12	12	12
Sodium feldspar	12	9.5	7	4.5	2
Potasium feldspar	11	8.5	6	3.5	1
Silica Sand	25	25	25	25	25
SCW	0	5	10	15	20

Table 20: Chemical analysis of SCW and raw materials.

Oxides (%)	***Clay Hycast VC***	***PAR KAOLIN***	***Kaolin RMB***	***Sodium feldspar***	***Potassium feldspar***	***Quartz***	***SCW***
SiO_2	52	48	48	70.44	69.5	96.35	69.2
Al_2O_3	31	37	37	17.92	17.3	0.52	22
TiO_2	1	0.06	0.05	0.26	0	0.05	0.439
CaO	0,2	0.07	0.07	0.5	0.5	1.19	1.14
MgO	0.4	0.3	0.3	0.2	0.2	0.08	0.279
K_2O	2.1	1.9	1.5	0.4	9	0.17	3.17
Na_2O	0.2	0.1	0.1	9.6	3.1	0.08	1.64
Fe_2O_3	1	0.19	0.8	0.08	0.1	0.24	1.42
ZnO	0	0	0	0	0	0	0.,181
ZrO_2	0	0	0	0	0	0	0.406
L. O. I	12	11.8	12.1	0.5	0.4	1.29	0.8

5.3 The effect of SCW on rheological properties of slip

The SCW is found to be undamaging the slip properties. To improve rheological behaviour of the slip, the addition of some electrolytes is necessary. Indeed, a combined amount of sodium silicate and sodium carbonate was added, with a ratio $\frac{Na_2CO_3}{Na_2SiO_3} = 0.25$ and with a total combined quantity of 0.375 wt. %; we found that it positively affect the fluidity of the various slips; this combination quantity of electrolytes is stable in all preparations as shown in table 21[144].

The addition of SCW powder with a small amount of sodium electrolytes reduces the liquidity time (fluidity). The added amount of sodium contributes to the formation of an excessive amount of Na^+ cations in the slip mixture, which reduces the diffusion layer thickness [37]. The particles size affects the slip properties; especially the residue on the sieve (63 µm) (%), which reduced by adding SCW. This is mainly due to the small size of the SCW particles compared to feldspar particles [88, 145].

Table 21: Evolution of the fluidity, residue on sieve and density of slip as a function of added SCW concentration.

	VC	VC5	VC10	VC15	VC20
$\frac{Na_2CO_3}{Na_2SiO_3}$	0.25				
$\frac{Na_2CO_3}{Na_2SiO_3}$ (wt.%)	0.375				
Density (g/cm^3)	1.771	1.780	1.773	1.776	1.775
Residue on sieve (63 µm) (%)	1.6	0.6	0.9	0.6	0.5
fluidity(s)	30	25	24	24	20
Drying shrinkage (%)	5.7	8.56	7.59	8.44	8.97

5.4 Effect of SCW on the physical properties of the fired ceramics

Figure 85 presents the results of bulk density and total porosity measurements of the ceramic samples. The higher density was observed in specimen VC5 where the feldspar is substituted by 5 wt.% SCW. Similarly, the addition of 10 wt.% SCW makes the VC10 ceramic body most dense than the standard VC body; this may be attributed mainly to the formation of the liquid phase from the mixing of alkali oxides (K_2O + Na_2O) in the feldspar with the alkaline earth oxide (CaO) from SCW. The increase of SCW in the ceramic mixture leads to a reduced liquid phase because of the decrease of alkaline oxides (K_2O + Na_2O) in the feldspar, while the content of viscous molten SiO_2 in the SCW increases. For this reason, the porosity values are higher in VC15 and VC20 [64, 65, 112]. Figure 86 shows the change in water absorption and shrinkage values of the fired ceramics. Typically, the decrease in alkali content in the ceramic body, leads to a decrease in the liquid phase, which increases porosity and water absorption while reducing the shrinkage values [83, 144]. SCW has a lower coefficient of thermal expansion than both types of feldspar, as it contains a lower percentage of quartz. Thus, the addition of SCW to the composition of ceramic bodies contributes to the stability of the dimensions (shrinkage and deformation) of the final ceramic body [90]. Besides, water absorption values are less than 0.5%; linear shrinkage has values smaller than 12% in all fired ceramics; this makes these findings compliant with the recommendations for sanitary ware manufacturing (ASTM C 373-88 and ASTM C: 326-82) [97, 98].

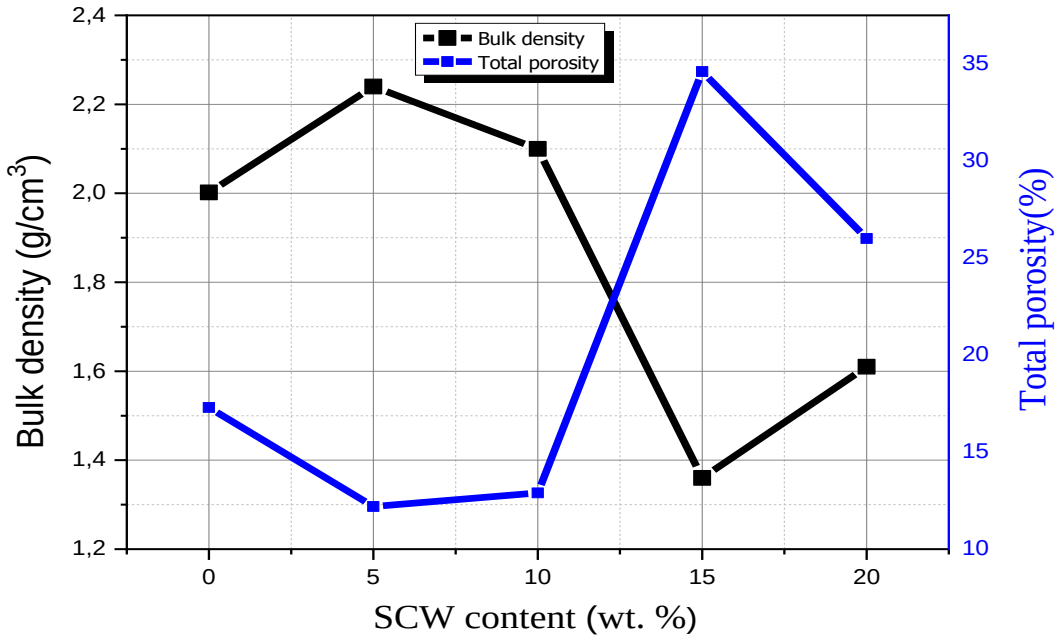

Figure 85 : Variation of bulk density and total porosity with SCW content, for a ceramic heated at 1230◦C.

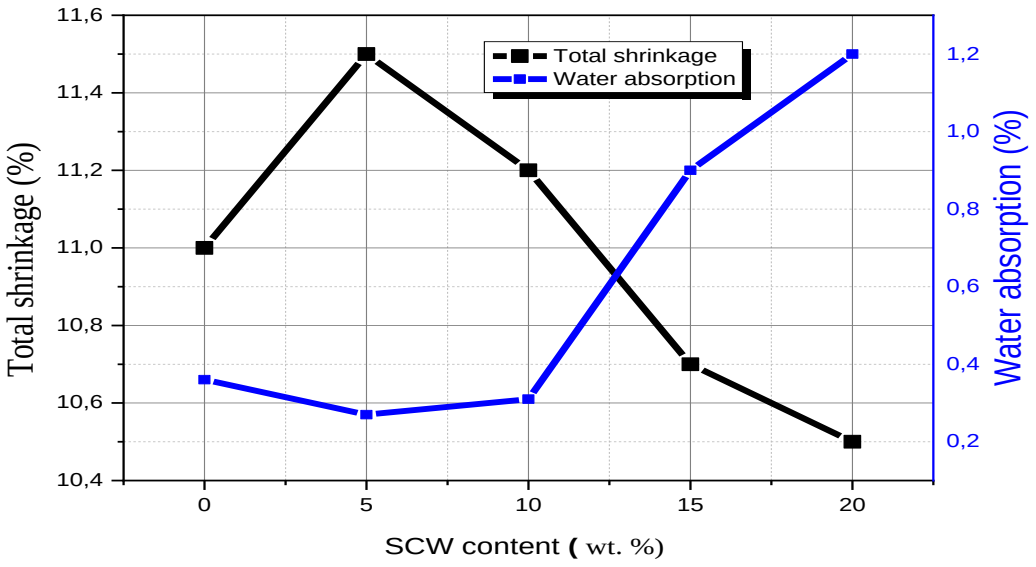

Figure 86 : Variation of water absorption and total shrinkage with SCW content, for a ceramic heated at 1230◦C.

5.5 Effect of SCW on the flexural strength of fired ceramics

Figure 87 shows the effect of SCW on the flexural strength of ceramic bodies; a clear improvement is found with the addition of 5 wt.% SCW. The VC10 samples have a higher flexural strength (44 MPa) than the standard ceramics (33 MPa). This is mainly due to the

formation of the liquid phase as well as the increased growth of the mullite phase; this is the source of strength resulting from the high content of SiO_2 and Al_2O_3 in the SCW[89]. However, as the replacement of feldspar with SCW exceeds 10 wt%, the flexural strength reduces as the amount of alkali oxides (K_2O + Na_2O) is lower, which reduces the liquid phase and increases porosity [90, 144].

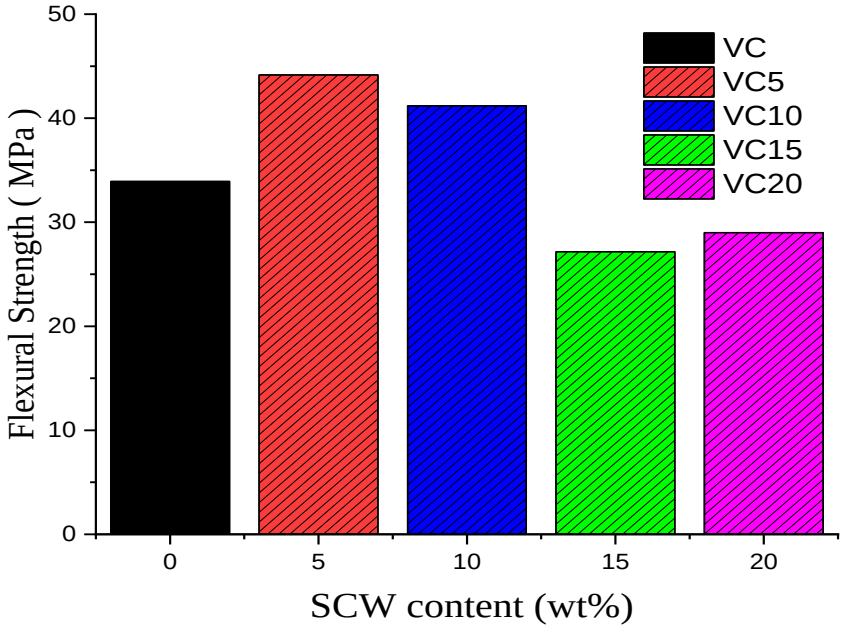

Figure 87 : Variation of flexural strength with SCW content for the samples heated at 1230°C.

5.6 X-ray analysis of fired ceramics

Figure 88 presents the X-ray diffraction analysis of the ceramic bodies, heated at 1230 °C. All samples contain mullite and quartz as the main crystal phases with the liquid phase. The high Al_2O_3 content in the SCW, with the presence of alkali oxides (K_2O + Na_2O) from feldspar, favour the formation of the mullite phase, while the high SiO_2 content leads to a higher peak intensity of the quartz. Albite is mostly invisible due to its dissolution to form a liquid phase above 1100°C [90, 146]. The mullite phase obtained, increases the flexural strength of ceramic bodies when the SCW amount does not exceed 10 wt. % [144].

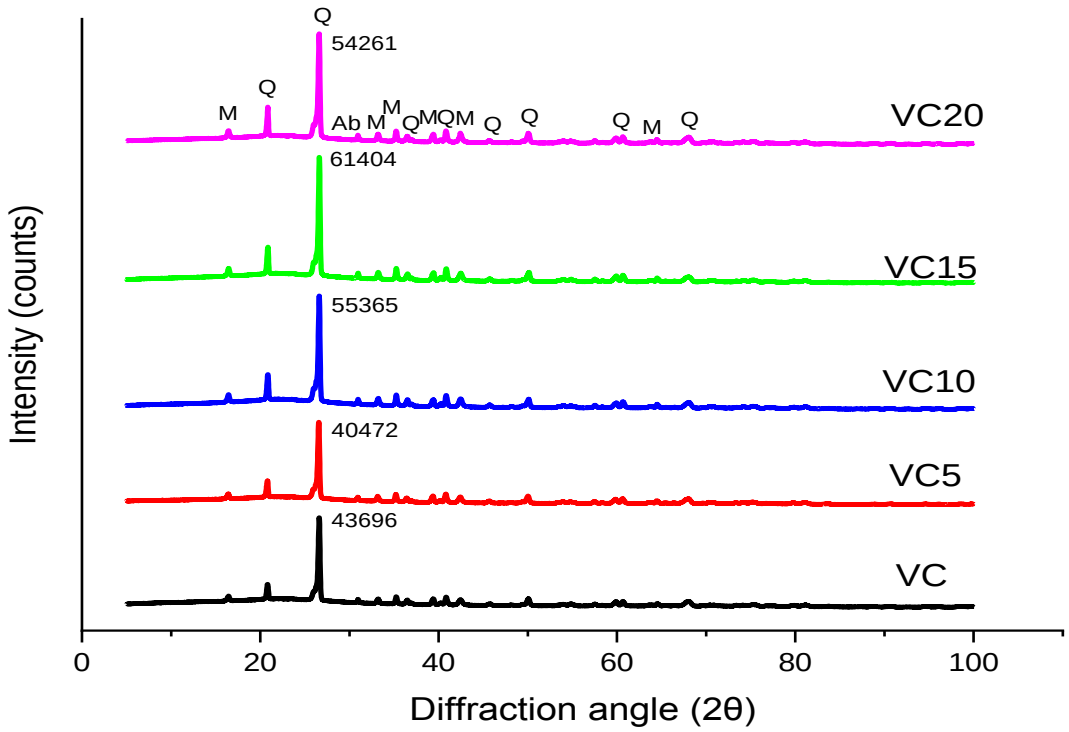

Figure 88 : XRD patterns for heated samples at 1230 °C (M: mullite, Q: quartz , Ab: albite).

5.7 SEM Analysis

To study the relation between physical-mechanical properties and microstructural characterizations, SEM analyses were carried out. Figure 89 shows the SEM micrographs of the fired samples at 1230°C. The ceramic bodies contain a heterogeneous group of crystals within the glass matrix; it consists in mullite and quartz. The pure clay forms the primary mullite, while the clay penetrated by dissolved feldspar forms the secondary mullite. The rich content of SiO2 in SCW and all raw materials used leads to the formation of the quartz phase. The glassy phase is attributed to feldspar melting. The combination of SCW with feldspar leads to presence of more alkali oxides (K_2O + Na_2O) with a smaller amount of alkaline earth oxides (CaO+MgO), enhancing the formation of the liquid phase. The latter closes the pores and spaces between the crystals, thus giving a higher density to sample VC5. We can note that, the morphology of VC10 is more dense than that of the standard body [121, 147]. The increase in SCW content reduces the amount of alkali oxides in the VC15 and VC20 compositions. This reduces the generation of the liquid phase and causes the opening of the pores, as shown clearly on the surface of the grains. These

findings are well confirmed by the physical-mechanical measurements and the XRD analyses.

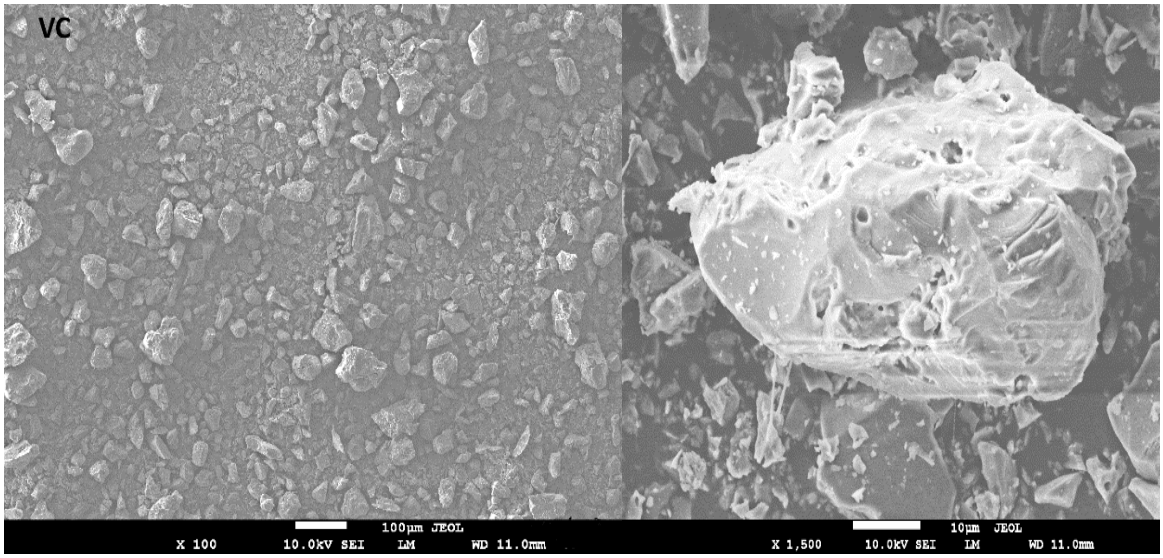

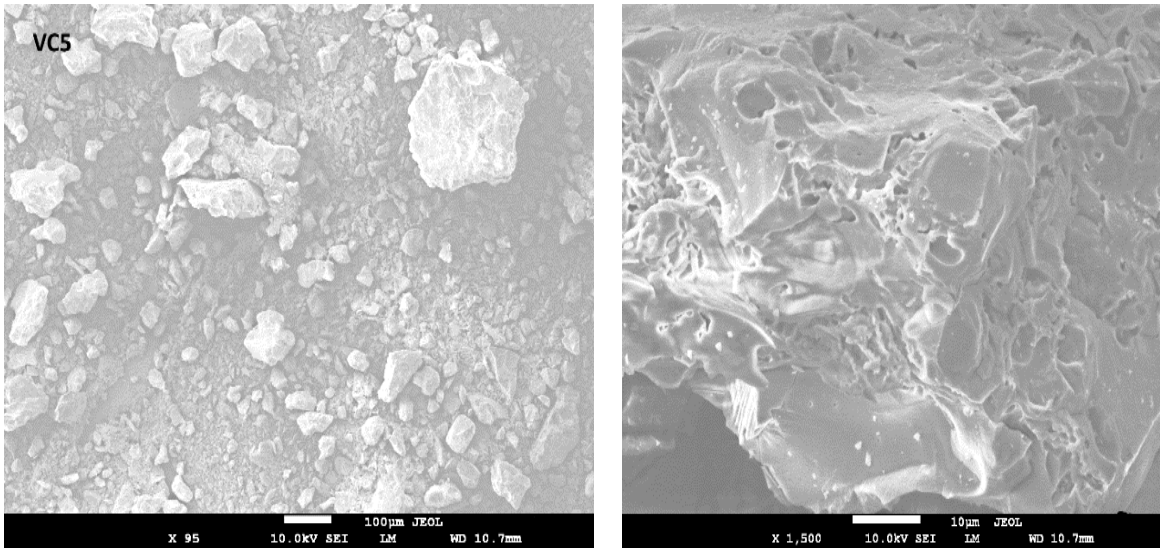

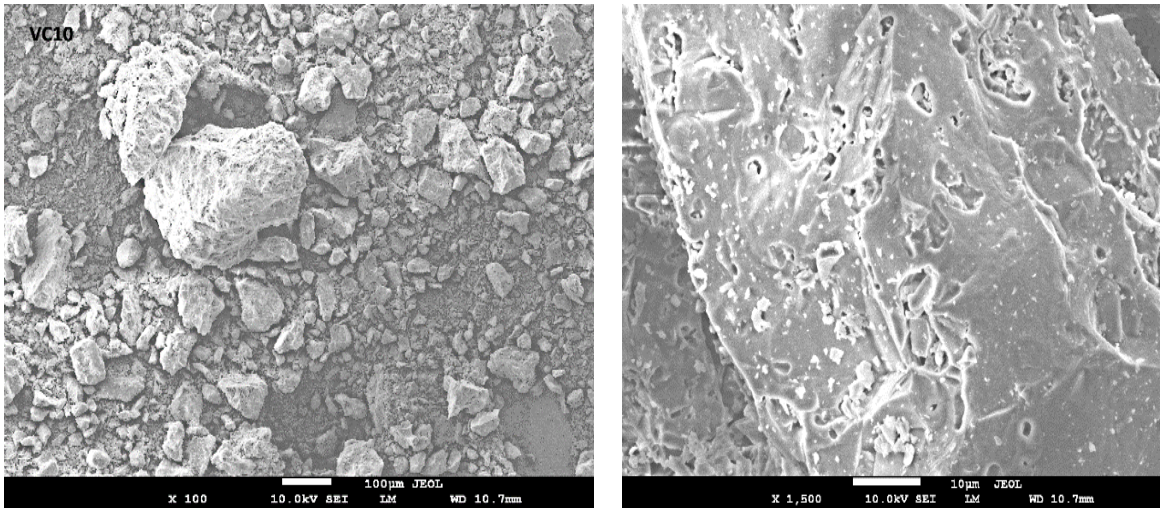

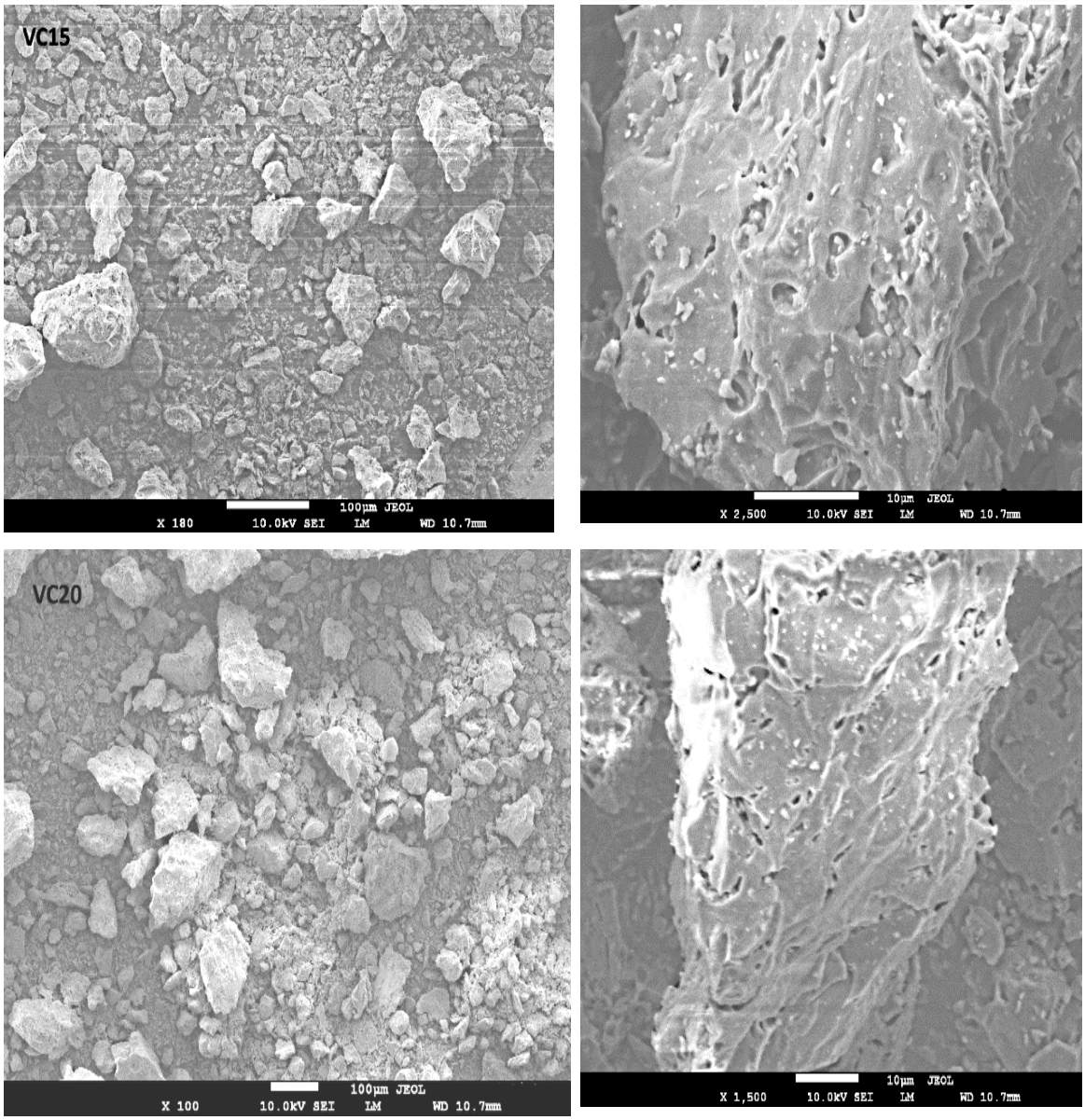

Figure 89 : SEM micrographs of VC, VC5, VC10, VC15 and VC20 samples.

5.8 FTIR Spectroscopy

FTIR analysis of the samples is shown in figure 90. As appear in chapters three and four, all ceramic samples have the same structure with small new bands formed by SCW addition. The bands at 781 cm^{-1}, in all samples, are attributed to Si-O-Al vibrations [148]. The Si-O-Si asymmetric stretching vibration is found at 1084 cm^{-1}; which is attributed to the quartz-rich content due to SCW addition [126, 127]. At 1620 and 3460 cm^{-1}, the absorption bands make their appearance, they are specific to the H-O- H bending vibrations from the H_2O adsorbed molecules [149, 150]. The located bands that show up in VC and VC5 ceramics, at 2853 and 2918 cm^{-1} can be ascribed to the symmetrical Si-O and Al-O stretching

vibrations, which means the formation of mullite and thus, improves the strength of VC5 [123, 151].

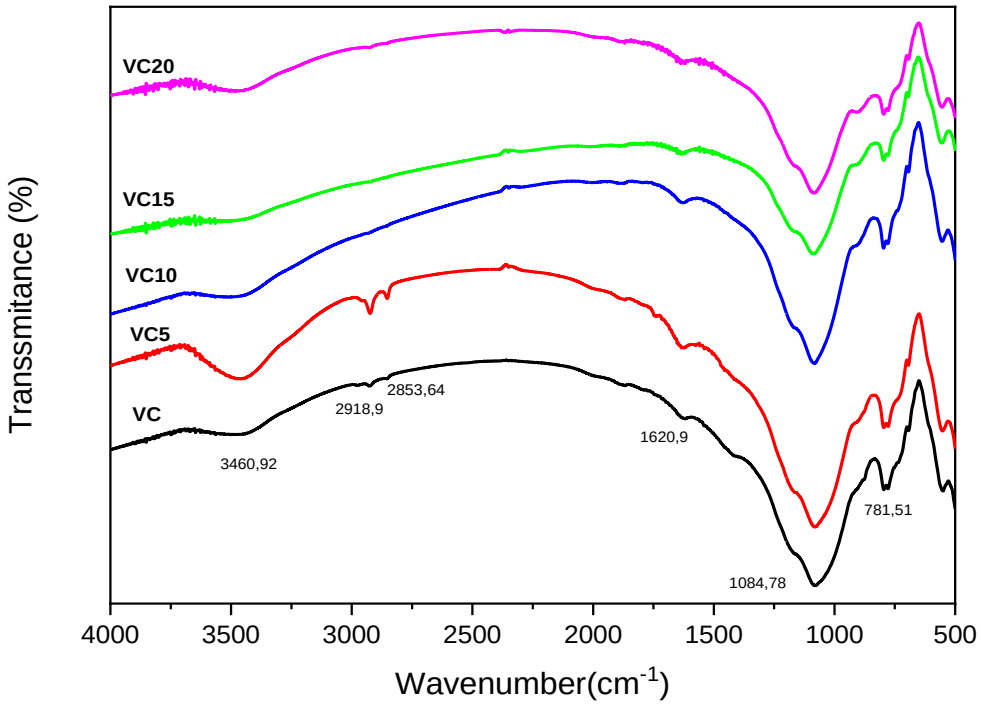

Figure 90: FTIR analysis of the ceramics with 0, 5, 10, 15 and 20 wt. % SCW.

5.9 Conclusion

We have studied the effect of the integration of sanitary ceramic waste (SCW) (from the sanitary ceramic factory of El-milia-Jijel) on the properties of their unglazed sanitary ware. The results obtained can be summarized as follows:

- The combination ratio $\frac{Na_2CO_3}{Na_2SiO_3} = 0.25$, with a combined total amount of 0.375 wt. % has a positive effect on the rheological behaviour of the different slips containing SCW.
- According to XRD, SEM and FTIR analyses, the use of SCW increases the peaks intensities of the mullite and quartz phases.
- A high density was recorded in sample VC5 containing 5 wt. % SCW (2.24 g/cm^3) with a lower water absorption (0.18 %).
- The flexural strength is improved (33 to 44 MPa) while total porosity is reduced (18 to 12 %) in the ceramics containing 5 wt. % SCW.

Although the VC5 ceramic samples shows the best physical-mechanical results, the use of 10 wt. % SCW give better results than the standard ceramic. This makes us conclude that the incorporation of 10 wt. % SCW in the unglazed sanitary ceramic composition provides technical, economical and environmental benefits.

GENERAL CONCLUSION AND FUTURE PROSPECTS

The choice of a composition for the preparation of sanitary ceramic bodies must take into account various characteristics, including: rheological behaviour, physical-mechanical properties, structural properties (evolution of crystalline phases) and economic considerations (quality and production cost).

In this context, we carried out this experimental work in the sanitary ceramic company (SCS) of El-Milia, Jijel-Algeria. The aim is to propose solutions for developing and improving the quality of sanitary ceramic products based on the valorization of industrial solid wastes.

For the realisation of this thesis, we have divided our research work in three main parts:

The first part is based on the effect of blast furnace slag (from Al-Hadjar steel factory, Annaba-Algeria) on the properties of sanitary ceramic bodies. The conclusions to be drawn are as follows:

- The rheological study of the ceramic slip showed a slow rheological behaviour following the incorporation of slag. The idea of using some electrolytes, Na-electrolytes in the optimum ratio Na_2CO_3/Na_2SiO_3=1.5 and a combined amount of 0.375 wt. %, was effective in improving the rheological behaviour of the slip.

- Differential thermal analysis (DTA) of green ceramics, has provided a lot of information on the physical-chemical reactions during the firing cycle.

- XRD and SEM analyses identified quartz and mullite as the main phases, with the gradual appearance of the anorthite phase. In order to confirm these phases, the FTIR spectrum was used; it revealed vibrational bands attributed to quartz, mullite and anorthite.

- The experimental results showed that replacing the feldspar mixture (sodium and potassium) with blast furnace slag 10 wt. %, was the optimal composition, as it results in a flexural strength of 38 MPa and a water absorption of 0.1%.

The second part is also focused on the valorisation of solid wastes, through the evaluation of the integration of soda-lime glass waste in the preparation of sanitary ceramic bodies. We can conclude with the following points:

- 0.075 wt. % Na_2CO_3 and 0.1 wt. % Na_2SiO_3 electrolytes were sufficient to incorporate SLGW in the slip composition with many improvements in various properties.

- The TGA thermal analysis allowed us to know the amount of mass loss when firing sanitary ceramic bodies; we observed a reduced mass loss by SLGW addition.

- XRD and SEM analysis, identified the presence of quartz and mullite with a slight gradual appearance of anorthite, this was confirmed using FTIR spectroscopy, where vibrational bands of mullite quartz and, to a lesser extent, anorthite were detected.

- The incorporation of soda–lime glass waste instead of feldspar (sodium and potassium) by 20 wt. % result in many technical improvements in various properties of sanitary ceramic bodies. In addition, enhanced rheological behaviour of the slip by using a very small amount of electrolytes, leads to a significant increase in flexural strength (33 to 51MPa) and a considerable reduction in water absorption (0.35 to 0.02%).

The third part deals with the general topic of this thesis, which is the recycling of the sanitary ceramic waste in the formulation of unglazed bodies; we can conclude with the following:

- The different slips containing sanitary ceramic waste have optimal properties when using the combination ratio $Na_2CO_3 / Na_2 SiO_3$=0.25, with a total amount of 0.375 wt. %.

- XRD and FTIR analyses proved the high intensity of quartz and mullite peaks in samples containing SCW.

- The VC5 body (5 wt. % SCW) has the best physical-mechanical results as it has a flexural strength of 44 MPa and water absorption of 0.18 %. Moreover, the VC10 body sample has better physical-mechanical properties than the standard ceramic sample. Therefore, we can say that sanitary waste can be recycled in the manufacture of their unglazed ceramic bodies with up to 10 wt. % contribution.

According to the results of these three studies, we can consider that the success of the integration of these solid industrial wastes in the compositions of sanitary ceramic bodies is mainly related to the chemical composition controlling the rheological properties and their effect on the behaviour of the slip and the physical-mechanical properties after sintering. Based on this consideration, soda-lime glass waste was found that with an integration of waste by an amount of 20 wt. %,it gives the best results; followed by sanitary ceramic waste and blast furnace slag with a proportion of 10 wt. %, we optimize the product.

The work carried out has provided some answers to the problem of exploitationas of industrial solid waste rich in aluminosilicate and its incorporation in the composition of sanitary ceramic bodies. Some interesting points are to be proposed for future research work:

- In order to save energy and protect the environment, it will be interesting to study the effect of the reduction of the firing temperature from 1200, 1150, 1050 to 1100 °C, on the properties of the sanitary body, as this waste has been pre-fired. Its incorporation may lead to a lower melting point.

- To consider the option of new sanitary ceramics based on the mixture of specific proportions of these wastes according to stoichiometry parameters.

- Valorise these wastes in the production of sanitary ceramic glaze and use them as alternative materials to feldspar, dolomite or calcium carbonate according to the appropriate chemical composition of the mixture.

REFERENCES

[1] Hamadouche, M., Sedel, L. Ceramics in orthopaedics. The Journal of Bone and Joint Surgery. British volume. 2000, 82, 1095-9.
[2] Boussak, H. Thèse de doctorat. Effet de la température sur les performances des céramiques contenant la bentonite de Maghnia. , ; 2015.
[3] Bernasconi, A. Sanitary-ware: from the industrial macro characterization to the atomic scale analysis. 2013.
[4] Sglavo, V.M., Maurina, S., Conci, A., Salviati, A., Carturan, G., Cocco, G. Bauxite 'red mud' in the ceramic industry. Part 2: production of clay-based ceramics. Journal of the European Ceramic Society. 2000, 20, 245-52.
[5] Chen, A.-N., Li, M., Xu, J., Lou, C.-H., Wu, J.-M., Cheng, L., et al. High-porosity mullite ceramic foams prepared by selective laser sintering using fly ash hollow spheres as raw materials. Journal of the European Ceramic Society. 2018, 38.
[6] El-Fadaly, E. Characterization of porcelain stoneware tiles based on solid ceramic wastes. International Journal of Science and Research (IJSR) ISSN. 2013, 2319-7064.
[7] Kim, K., Kim, K., Hwang, J. Characterization of ceramic tiles containing LCD waste glass. Ceramics International. 2016, 42, 7626-31.
[8] Karamanova, E., Avdeev, G., Karamanov, A. Ceramics from blast furnace slag, kaolin and quartz. Journal of the European Ceramic Society. 2011, 31, 989-98.
[9] Ozturka, Z., Yildizb, B. The E ect of Different Fluxes on Thermal Behavior of Floor Tile Glazes.
[10] Darweesh, H.H.M. Recycling of glass waste in ceramics—part I: physical, mechanical and thermal properties. SN Applied Sciences. 2019, 1, 1274.
[11] Krahl, R. Chinese ceramics in the late Tang Dynasty. Shipwrecked: Tang Treasures and Monsoon Winds. 2010, 45-74.
[12] Ferreira, W.M., Cruz, A.S., de Azevedo, A.R., Marvila, M.T., Monteiro, S.N., Vieira, C.M.F. Perspective of the application of ash from the ceramic industry in the development of alkali-activated roof tiles. Ceramics International. 2022, 48, 6250-7.
[13] Carty, W.M., Senapati, U. Porcelain—raw materials, processing, phase evolution, and mechanical behavior. Journal of the American Ceramic Society. 1998, 81, 3-20.
[14] Jean-Marie HAUSSONNE, J.L.B., Paul BOWEN, Claude Paul CARRY. CÉRAMIQUES ET VERRES, PRINCIPES ET TECHNIQUES D'ÉLABORATION. Presses polytechniques et universitaires romandes, Presses polytechniques et universitaires romandes, 2005.
[15] Silvestri, L., Forcina, A., Silvestri, C., Ioppolo, G. Life cycle assessment of sanitaryware production: A case study in Italy. Journal of Cleaner Production. 2020, 251, 119708.
[16] Sanad, M., Rashad, M., Abdel-Aal, E., El-Shahat, M. Mechanical, morphological and dielectric properties of sintered mullite ceramics at two different heating rates prepared from alkaline monophasic salts. Ceramics International. 2013, 39, 1547-54.
[17] Aliprandi, G. Matériaux réfractaires et céramiques techniques, Éditions Septima, 1979.
[18] Page Consulté le 07/06/2020, Smart. Conseil, Émaillage et tension superficielle [en ligne], AdresseURLhttps://www.substech.com/dokuwiki/doku.php?id=general_classification_of_ceramics.

[19] Aklouche, N. Thése de doctorat. Préparation et étude des composés corierite et anorthite. 2009.

[20] Heinrich, Jürgen G. Gomes, Cynthia M. Introduction to Ceramics Processing. 2014.
[21] Aydin, T., Casin, E. Mixed Alkali and Mixed Alkaline-Earth Effect in Ceramic Sanitaryware Bodies Incorporated with Blast Furnace Slag. Waste and Biomass Valorization. 2021, 12, 2685-702.
[22] Tarhan, B. Usage of fired wall tile wastes into fireclay sanitaryware products. Journal of the Australian Ceramic Society. 2019, 55, 737-46.

[23] İssi, A., Derin Coşkun, N., Tiryaki, V., Uz, V. Casting and sintering of a sanitaryware body containing fine fire clay (FFC). Journal of the Australian Ceramic Society. 2017, 53, 157-62.
[24] Benkacem, S. These de doctorat. Développement et caractérisation d 'un émail de la céramique sanitaire d'El Milia - Jijel. 2020.
[25] Brulon, D.G. Les diverses céramiques définitions, origines, compositions, techniques.P. 1–6, 1995.
[26] Huggett., J.M. Clay minerals. Encyclopedia of Geology. 2005, P. 358-65.
[27] Bultel, F. Prise en compte du gonflement des terrains dans le dimensionnement des revêtements des tunnels Ecole Nationale des Ponts et Chaussées; 2001.
[28] Heinrich, J.G., Gomes., C.M. Introduction to Ceramics Processing2014.
[29] Worrall, W.E. Ceramic raw materials. 2ed. The institue of ceramics, Pergamon Press, P. 17, 1982. 1982.

[30] F. Singer, S.S.S. Industrial Ceramics. 1ed. Chapman. Hall, P. 27, 1963. 1963.
[31] Avgustinik, A.I. Ceramics (2nd ed.). Stroiizdat, Leningrad, [in Russian]. 1975.
[32] Pakhomova, A., Simonova, D., Koemets, I., Koemets, E., Aprilis, G., Bykov, M., et al. Polymorphism of feldspars above 10 GPa. Nature Communications. 2020, 11, 2721.
[33] Geller, R., Creamer, A. Investigation of feldspar and its effect in pottery bodies. Journalofthe American Ceramic Society. 1931, 14, 30-71.
[34] Dove, M. Rigid Unit Modes in Framework Silicates. Mineralogical Magazine - MINER MAG. 1995, 59, 629-39.
[35] Santos, F.D., da Conceição, L.R.V., Ceron, A., de Castro, H.F. Chamotte clay as potential low cost adsorbent to be used in the palm kernel biodiesel purification. Applied Clay Science. 2017, 149, 41-50.
[36] Beheary, M., El-matary, F. Management of heat stress in sanitary ware industry. 2012.
[37] Evcin, A. Investigation of the effects of different deflocculants on the viscosity of slips. Scientific Research and Essays. 2011, 6, 2302-5.
[38] Hammadi, L. Improving of the mechanical and rheological properties of slip of ceramic. Construction and Building Materials. 2018, 173, 118-23.
[39] Pal, M., Das, S., Gupta, S., Das, S.K. Thermal analysis and vitrification behavior of slag containing porcelain stoneware body. Journal of Thermal Analysis and Calorimetry. 2016, 124, 1169-77.
[40] Zanelli, C., Raimondo, M., Guarini, G., Dondi, M. The vitreous phase of porcelain stoneware: composition, evolution during sintering and physical properties. Journal of Non-CrystallineSolids. 2011, 357, 3251-60.
[41]https://www.google.com/search?q=traditional+ceramics&tbm=isch&ved=2ahUKEwjolNXL0tv_AhXericCHR6zAm4Q2-cCegQIABAA&oq=traditional+ceramics&gs_lcp=CgNpbWcQAzIHCAAQExCABDIHCAAQExCABDIICAAQBxAeEBMyCAgAEAcQHhATMggIABAHEB4QEzIICAAQBxAeEBMyCAgAEAcQHhATMggIABAHEB4QEzIICAAQBxAeEBM6BggAEAcQHlCiF1icPGDqQmgAcAB4AIABtgGIAd4PkgEEMC4xMpgBAKABAaoBC2d3cy13aXotaW1nwAEB&sclient=img&ei=UL6WZOisFN7dnsEPnuaK8AY&bih=657&biw=1349&hl=ar. SANITARYWARE TECHNICAL Physical and Chemical Reaction during Firing of Sanitaryware [online], URL : https://ceramicninja.com/physical-chemical-reaction-firing-sanitaryware/

[42] Makhlouf, A.S.H., Ali, G.A. Waste Recycling Technologies for Nanomaterials Manufacturing, Springer Nature, 2021.
[43] Pertiwi, I.G.A.I.M., Winaya, N.A.P., Andayani, K.W., Kristinayanti, W.S. Waste management system on Badung River area in Bali. IOP Conference Series: Earth and Environmental Science. 2019, 351, 012005.

[44] Andreola, F., Barbieri, L., Lancellotti, I., Leonelli, C., Manfredini, T. Recycling of industrial wastes in ceramic manufacturing: State of art and glass case studies. Ceramics International. 2016, 42.
[45] Diah, N. The Effect of Addition of Plastic Waste and Styrofoam Waste Against Powerful Concrete Brick Press. In: First International Conference on Health, Social Sciences and Technology (ICOHSST 2020), Atlantis Press, 2021, pp. 212-5.
[46] Eddine, B.T., Salah, M.M. Solid waste as renewable source of energy: current and future possibility in Algeria. International Journal of Energy and Environmental Engineering. 2012, 3, 1-12.
[47] Djemaci, B., Chertouk, MAZ La gestion intégrée des déchets solides en Algérie. Contrainteset limites de samise enœuvre. International Centre of Research and Information on the Public. http://www.ciriec.ulg.ac.be (2011).Accessed. April 2011.

[48] Kehila, Y., Mezouari, F., Matejka, G. Impact de l'enfouissement des déchets solidesurbainsen Algérie: expertise de deux centres d'enfouissement technique (CET) à Alger et Biskra. Déchets Sciences et Techniques. 2009, 56, 29-38.
[49] Hans Breukelman, R.v.S. Business opportunities in waste management in Algeria. 2018.
[50] Rakhimova, N.R. Recent advances in blended alkali-activated cements: a review. European Journal of Environmental and Civil Engineering. 2020, 1-23.
[51] Alioui, H., Chiker, T., Saidat, F., Lamara, M., Aggoun, S., Hamdi, O.M. Investigation of theeffect of commercial limestone on alkali-activated blends based on Algerian slag-glasspowder.European Journal of Environmental and Civil Engineering. 2021, 1-24.
[52] Liu, H., Lu, H., Chen, D., Wang, H., Xu, H., Zhang, R. Preparation and properties of glass–ceramics derived from blast-furnace slag by a ceramic-sintering process. Ceramics International. 2009, 35, 3181-4.
[53] Hayet, C., Khadidja, A.M. Characterization of blast furnace slag to formulate a road material.
[54] MEKTI, z. Thèse de doctorat. Comportement du laitier de l'usine sidérurgique d'El-Hadjarsur le mélange clinker : Cas ERCE Hadjar-Soud, Skikda. 2018.
[55] Jiang, C., Li, K., Zhang, J., Qin, Q., Liu, Z., Sun, M., et al. Effect of MgO/Al2O3 ratio on the structure and properties of blast furnace slags: A molecular dynamics simulation. Journal of Non-Crystalline Solids. 2018, 502, 76-82.
[56] Cyr, M., Andre, L. Synergic effects of activation routes of ground granulated blast-furnaceslag (GGBS) used in the precast industry. In: Congrès International de Géotechnique–Ouvrages–Structures, Springer, 2017, pp. 588-97.
[57] Francis, A. Conversion of blast furnace slag into new glass-ceramic material. Journal of the European Ceramic Society. 2004, 24, 2819-24.
[58] Zhao, Y., Chen, D., Bi, Y., Long, M. Preparation of low cost glass–ceramics from molten blast furnace slag. Ceramics International. 2012, 38, 2495-500.
[59] Ma, J., Shi, Y., Zhang, H., Ouyang, S., Deng, L., Chen, H., et al. Crystallization of CaO–MgO–Al2O3–SiO2 glass ceramic derived from blast furnace slag via one-step method. Materials Chemistry and Physics. 2021, 261, 124213.
[60] Dana, K., Das, S.K. Partial substitution of feldspar by BF slag in triaxial porcelain: Phase and microstructural evolution. Journal of the European Ceramic Society. 2004, 24, 3833-9.
[61] Mostafa, N.Y., Shaltout, A.A., Abdel-Aal, M.S., El-Maghraby, A. Sintering mechanism of blast furnace slag–kaolin ceramics. Materials & Design. 2010, 31, 3677-82.
[62] Siddiqui, A., Pal, M., Bhattacharya, D., Das, S. Iron and steel slag: an alternative source of raw materials for porcelain ceramics. Global NEST Journal. 2014, 16, 587-96.
[63] Ghosh, S., Das, M., Chakrabarti, S., Ghatak, S. Development of ceramic tiles from commonclay and blast furnace slag. Ceramics International. 2002, 28, 393-400.
[64] Ozdemir, I., Yilmaz, S. Processing of unglazed ceramic tiles from blast furnace slag. Journal of materials processing technology. 2007, 183, 13-7.

[65] Dana, K., Dey, J., Das, S.K. Synergistic effect of fly ash and blast furnace slag on the mechanical strength of traditional porcelain tiles. Ceramics International. 2005, 31, 147-52.
[66] Ozturk, Z.B., Gultekin, E.E. Preparation of ceramic wall tiling derived from blast furnace slag. Ceramics International. 2015, 41, 12020-6.
[67] Lopez-Perales, J., Contreras, J.E., Vazquez-Rodríguez, F., Gómez-Rodríguez, C., Diaz-Tato, L., Banda-Muñoz, F., et al. Partial replacement of a traditional raw material by blast furnace slag in developing a sustainable conventional refractory castable of improved physical-mechanical properties. Journal of Cleaner Production. 2021, 306, 127266.
[68] Silva, R.V., de Brito, J., Lye, C.Q., Dhir, R.K. The role of glass waste in the production of ceramic-based products and other applications: A review. Journal of Cleaner Production. 2017, 167, 346-64.
[69] Francis, A., Rawlings, R., Boccaccini, A. Glass-ceramics from mixtures of coal ash and soda-lime glass by the petrurgic method. Journal of materials science letters. 2002, 21, 975-80.
[70] Zhang, W., Liu, H. A low cost route for fabrication of wollastonite glass–ceramics directly using soda-lime waste glass by reactive crystallization–sintering. Ceramics International. 2013, 39, 1943-9.
[71] Ponsot, I., Bernardo, E., Bontempi, E., Depero, L., Detsch, R., Chinnam, R.K., et al. Recycling of pre-stabilized municipal waste incinerator fly ash and soda-lime glass into sintered glass-ceramics. Journal of Cleaner Production. 2015, 89, 224-30.
[72] Almasri, K.A., Matori, K.A., Zaid, M.H.M. Effect of sintering temperature on physical, structural and optical properties of wollastonite based glass-ceramic derived from waste soda lime silica glasses. Results in physics. 2017, 7, 2242-7.
[73] Jusoh, W.N.W., Matori, K.A., Zaid, M.H.M., Zainuddin, N., Khiri, M.Z.A., Rahman, N.A.A., et al. Effect of sintering temperature on physical and structural properties of Alumino-Silicate-Fluoride glass ceramics fabricated from clam shell and soda lime silicate glass. Results in physics. 2019, 12, 1909-14.
[74] Bootkul, D., Intarasiri, S. Development of glass-ceramics from Soda lime silica glass waste with addition of kaolin and coloring oxide for Turquoise's imitation. Vibrational spectroscopy. 2022, 123, 103467.
[75] Rambaldi, E., Carty, W.M., Tucci, A., Esposito, L. Using waste glass as a partial flux substitution and pyroplastic deformation of a porcelain stoneware tile body. Ceramics International. 2007, 33, 727-33.
[76] Youssef, N., Abadir, M., Shater, M. Utilization of soda glass (cullet) in the manufacture of wall and floor tiles. Journal of the European Ceramic Society. 1998, 18, 1721-7.
[77] Matteucci, F., Dondi, M., Guarini, G. Effect of soda-lime glass on sintering and technological properties of porcelain stoneware tiles. Ceramics International. 2002, 28, 873-80.
[78] Luz, A., Ribeiro, S. Use of glass waste as a raw material in porcelain stoneware tile mixtures. Ceramics International. 2007, 33, 761-5.
[79] Owoeye, S.S., Toludare, T.S., Isinkaye, O.E., Kingsley, U. Influence of waste glasses on the physico-mechanical behavior of porcelain ceramics. Boletín de la Sociedad Española de Cerámica y Vidrio. 2019, 58, 77-84.
[80] Bragança, S., Bergmann, C. Waste glass in porcelain. Materials Research-ibero-american Journal of Materials - MATER RES-IBERO-AM J MATER. 2005, 8.
[81] Yürüyen, S., Toplan, H.Ö. The sintering kinetics of porcelain bodies made from waste glass and fly ash. Ceramics International. 2009, 35, 2427-33.
[82] Marinoni, N., Diella, V., Confalonieri, G., Pavese, A., Francescon, F. Soda-lime-silica-glass/quartz particle size and firing time: Their combined effect on sanitary-ware ceramic reactions and macroscopic properties. Ceramics International. 2017, 43, 10895-904.
[83] Martini, E., Fortuna, D., Fortuna, A., Rubino, G., Tagliaferri, V. Sanitser, an innovative sanitary ware body, formulated with waste glass and recycled materials. Cerâmica. 2017, 63, 542-8.

[84] Marinoni, N., D'Alessio, D., Diella, V., Pavese, A., Francescon, F. Effects of soda–lime–silica waste glass on mullite formation kinetics and micro-structures development in vitreousceramics. Journal of environmental management. 2013, 124, 100-7.
[85] Mostari, M.S., Haque, J. Recycling of Post Sintered Sanitaryware Waste in Its Formulation. International Journal of Technical Research & Science. 2020, 5, 27-34.
[86] Reig, L., Soriano, L., Borrachero, M.V., Monzó, J.M., Payá, J. Potential use of ceramic sanitary ware waste as pozzolanic material. Boletín de la Sociedad Española de Cerámica y Vidrio. 2021.
[87] Khater, G., Abdel-Motelib, A., El Manawi, A., Safiah, M.A. Glass-ceramics materials from basaltic rocks and some industrial waste. Journal of Non-Crystalline Solids. 2012, 358, 1128-34.
[88] ElFadaly, E. Incorporation of Sanitaryware. Ceramic Forum International. 2021.
[89] Tarhan, M., Tarhan, B., Aydin, T. The effects of fine fire clay sanitaryware wastes on ceramic wall tiles. Ceramics International. 2016, 42, 17110-5.
[90] Tarhan, B., Tarhan, M., Aydin, T. Reusing sanitaryware waste products in glazed porcelain tile production. Ceramics International. 2017, 43, 3107-12.
[91] Silva, T., Castro, A., Valente, F., Soares, M., De Resende, D., Bezerra, A. Recycling ceramic waste as a raw material in sanitary ware production. Cerâmica. 2019, 65, 426-31.
[92] Silva, T.H., de Resende, M.C., de Resende, D.S., Junior, P.R.R.S., da Silva Bezerra, A.C. Valorization of ceramic sludge waste as alternative flux: A way to clean production in the sanitary ware industry. Cleaner Engineering and Technology. 2022, 7, 100453.
[93] Brown, M.E. Handbook of thermal analysis and calorimetry, Principales and practice. Vol. 1, ed. Elsevier Science B.V, P. 12, 20,. 1998.

[94] Kloss., W.S. Differential Thermal Analysis. Application and results in mineralogy. ed. Springer Verlag Berlin Heidelberg New York. P. 1, . 1974.

[95] Page Consulté le 08/06/2020, Smart. Conseil, Émaillage et tension superficielle [en ligne], Adresse URL http://smart2000.pagesperso-orange.fr/tension_superficielle_email.htm.

[96] M. Sugai, S.S. Measurement of density, viscosity and surface tension of the melt of thesystem SiO2–TiO3–Al2O3 at 1600°C. Yogyo Kyokaishi. 90, 262–269. 1982.

[97] ASTM, C. 373-88: Standard Test Method for Water Absorption. Bulk Density, Apparent Porosity, and Apparent Specific Gravity of Fired Whiteware Products. 2006, 1-2.
[98] ASTM, A. C326—Test Method for Drying and Firing Shrinkage of Ceramic Whiteware Clays. In: American Society for Testing and Materials, 1997.
[99] C, A. – FLEXURAL STRENGTH TESTING OF ADVANCED CERAMICS 1161.

[100] Marsh, A., Heath, A., Patureau, P., Evernden, M., Walker, P. Phase formation behaviour in alkali activation of clay mixtures. Applied Clay Science. 2019, 175, 10-21.
[101] Olupot, P.W., Jonsson, S., Byaruhanga, J.K. Electroporcelains from Raw Materials in Uganda: A Review. In: Proceedings from the International Conference on Advances in Engineering and Technology, Mwakali, J.A., Taban-Wani, G. Eds., Elsevier Science Ltd, Oxford, 2006, pp. 454-64.
[102] S.J. Schneider Jr., e.a. « Glass and Ceramics», Engineering Materials Handbook ASM International,. 1987.

[103] C. Vittel. « Pates et Glacures Céramiques », Edition Delta S. A CH-1800 VEVEY. 1986.

[104] J Chevalier. « What future for zirconia as biomaterial ». Biomaterials. 27 (4), 535-43 2006.

[105] J. Poujade. M, Z.C., D. Serre, . « Céramiques dentaires ». Encyclopédie MédicoChirurgicale ; Odontologie, 23-065-G-10. 2003.

[106] El-Fadaly, E.A., Askar, A.S., Aly, M.H., Ibrahim, D.M. Rheological, physico-mechanical and microstructural properties of porous mullite ceramic based on environmental wastes. Boletín de la Sociedad Española de Cerámica y Vidrio. 2020.
[107] Eygi, M.S., Ateşok, G. An investigation on utilization of poly-electrolytes as dispersant for kaolin slurry and its slip casting properties. Ceramics International. 2008, 34, 1903-8.
[108] Celik, H. Technological characterization and industrial application of two Turkish claysforthe ceramic industry. Applied Clay Science. 2010, 50, 245-54.
[109] Oluseyi, A., Aladesuyi, O., Pal, M., Das, S. Evaluation of Nigerian Source of Kaolin as A Raw Material for Mullite Synthesis. Oriental Journal of Chemistry. 2016, 32, 1571-82.
[110] Aydin, T., Casin, E. Mixed Alkali and Mixed Alkaline-Earth Effect in Ceramic Sanitaryware Bodies Incorporated with Blast Furnace Slag. Waste and Biomass Valorization. 2020, 1-18.
[111] García R, A., Domínguez-Ríos, C., Bocanegra-Bernal, M.H., Aguilar-Elguézabal, A. Use of thermally treated bentonitic clay in the formulation of ceramic tiles. Applied Clay Science. 2009, 46, 271-6.
[112] Zhao, L., Li, Y., Zhou, Y., Cang, D. Preparation of novel ceramics with high CaO content from steel slag. Materials & Design. 2014, 64, 608-13.
[113] Salman, M.M., Nhabih, H.T. Assessment of the partial and total replacement of feldspar by waste glass on por-celain properties. Journal of Ceramic Processing Research. 2020, 21, 371-7.
[114] ASTM, C. Standard test method for water absorption, bulk density, apparent porosity, and apparent specific gravity of fired whiteware products. West Conshohocken, Pennsylvania, US: ASTM International. C373-88. 2006.
[115] Anggono, J. Mullite Ceramics: Its Properties, Structure, and Synthesis. Jurnal Teknik Mesin. 2005, 7.
[116] Boulaiche, K., Boudeghdegh, K., Roula, A., Alioui, H., Hamdi, O.M. Potential use of Algerian metallurgical slag in the manufacture of sanitary ceramic bodies and its effect on the physical-mechanical and structural properties. Iranian Journal of Chemistry and Chemical Engineering (IJCCE). 2022.
[117] Ismail, M., Nakai, Z., Sōmiya, S. Microstructure and mechanical properties of mullite prepared by the sol-gel method. Journal of the American Ceramic Society. 1987, 70, C-7-C-8.
[118] Kurama, S., Ozel, E. The influence of different CaO source in the production of anorthite ceramics. Ceramics International. 2009, 35, 827-30.
[119] Romero, M., Perez, J.M. Relation between the microstructure and technological properties of porcelain stoneware. A review. Materiales de Construcción. 2015, 65, e065.
[120] Iqbal, Y., Lee, W.E. Microstructural evolution in triaxial porcelain. Journal of the American Ceramic Society. 2000, 83, 3121-7.
[121] Carbajal, L., Rubio-Marcos, F., Bengochea, M., Fernandez, J. Properties related phase evolution in porcelain ceramics. Journal of the European Ceramic Society. 2007, 27, 4065-9.
[122] Adeniyi, F.I., Ogundiran, M.B. Synthesis of geopolymer binders and mortars from Ijero-Ekiti calcined clay, blast furnace slag and river sand. Earthline Journal of Chemical Sciences. 2020, 4,15-34.
[123] Roy, J., Bandyopadhyay, N., Das, S., Maitra, S. Studies on the Formation of Mullite from Diphasic Al2O3-SiO2 Gel by Fourier Transform Infrared Spectroscopy. Iranian Journal of Chemistry and Chemical Engineering (IJCCE). 2011, 30, 65-71.
[124] Ismail, I., Bernal, S.A., Provis, J.L., San Nicolas, R., Hamdan, S., van Deventer, J.S. Modification of phase evolution in alkali-activated blast furnace slag by the incorporation of fly ash. Cement and Concrete Composites. 2014, 45, 125-35.
[125] Gören, R., Ersoy, B., Özgür, C., Alp, T. Colloidal stability–slip casting behavior relationship in slurry of mullite synthesized by the USP method. Ceramics International. 2012, 38, 679-85.
[126] Nilforoushan, M.R., Otroj, S., Talebian, N. The Study of Ion Adsorption by Amorphous Blast Furnace Slag. Iranian Journal of Chemistry and Chemical Engineering (IJCCE). 2015, 34, 57-64.

[127] Joni, I.M., Nulhakim, L., Vanitha, M., Panatarani, C. Characteristics of crystalline silica (SiO 2) particles prepared by simple solution method using sodium silicate (Na 2 SiO 3) precursor. Journal of Physics: Conference Series. 2018, 1080, 012006.
[128] Raizada, P., Shandilya, P., Singh, P., Thakur, P. Solar light-facilitated oxytetracycline removal from the aqueous phase utilizing a H2O2/ZnWO4/CaO catalytic system. Journal of Taibah University for Science. 2016, 11.
[129] Ghadami Jadval Ghadam, A., Idrees, M. Characterization of CaCO3 Nanoparticles Synthesized by Reverse Microemulsion Technique in Different Concentrations of Surfactants. Iranian Journal of Chemistry and Chemical Engineering (IJCCE). 2013, 32, 27-35.
[130] Balachander, L., Ramadevudu, G., Shareefuddin, M., Sayanna, R., Venudhar, Y. IR analysis of borate glasses containing three alkali oxides. ScienceAsia. 2013, 39, 278-83.
[131] Kronberg, T., Hupa, L. Melting behaviour of raw glazes. Journal of the European Ceramic Society. 2019, 39, 4404-16.
[132] Boulaiche, K., Boudeghdegh, K., Haddad, S., Roula, A., Alioui, H. Valorisation of Industrial Soda-Lime Glass Waste and Its Effect on the Rheological Behavior, Physical-Mechanical and Structural Properties of Sanitary Ceramic Vitreous Bodies. In: Annales de Chimie-Science des Matériaux, 2022, Vol. 46, pp. 147-54.
[133] Martini, E., Fortuna, D., Fortuna, A., Rubino, G., Tagliaferri, V. Sanitser, an innovative sanitary ware body, formulated with waste glass and recycled materials. Cerâmica. 2017, 63, 542-8.
[134] Wang, S., Li, X., Wang, C., Bai, M., Zhou, X., Zhang, X., et al. Anorthite-based transparent glass-ceramic glaze for ceramic tiles: Preparation and crystallization mechanism. Journal of the European Ceramic Society. 2022, 42, 1132-40.
[135] Albhilil, A.A., Kozánková, J., Palou, M. Thermal and Microstructure Stability of Cordierite – Mullite Ceramics Prepared from Natural Raw Materials. ARABIAN JOURNAL FOR SCIENCE AND ENGINEERING. 2014, 39, 67-73.
[136] Kunduraci, N., Aydin, T. The Effect of Nepheline Syenite Addition on Sanitaryware Body. Uluslararası Muhendislik Arastirma ve Gelistirme Dergisi. 2015, 7, 16-9.
[137] Boussak, H., Chemani, H., Serier, A. Characterization of porcelain tableware formulation containing bentonite clay. International Journal of Physical Sciences. 2015, 10, 38-45.
[138] Zawrah, M., Gado, R., Khattab, R. Optimization of slag content and properties improvement of metakaolin-slag geopolymer mixes. The Open Materials Science Journal. 2018, 12.
[139] Zakaly, H.M.H., Saudi, H.A., Tekin, H.O., Rashad, M., Issa, S.A.M., Rammah, Y.S., et al. Glass fabrication using ceramic and porcelain recycled waste and lithium niobate: physical, structural, optical and nuclear radiation attenuation properties. Journal of Materials Research and Technology. 2021, 15, 4074-85.
[140] Michailova, I., Radev, L., Aleksandrova, V., Colova, I., Salvado, I., Fernandes, M. Carbonate-apatite forming ability of polyphase glass-ceramics in the CaO - MgO - SiO2 system, Journal of Chemical Technology and Metallurgy, 50 (2015) 4, 502-511. Journal of Chemical Technology and Metallurgy. 2015, 50, 502-11.
[141] Vakhula, O., Pona, M., Solokha, I., Poznyak, I. Research of corrosive destruction mechanism of cordierite-mullite refractory materials. 2010.
[142] Monich, P., Rincón, A., Vollprecht, D., Bernardo, E. Porous glass-ceramics from alkali activation and sinter-crystallization of mixtures of waste glass and residues from plasma processing of municipal solid waste. Journal of Cleaner Production. 2018, 188.
[143] Cuviella-Suárez, C., Borge-Diez, D., Colmenar-Santos, A. Introduction to Ceramic Sanitary-Ware Manufacturing. In: Water and Energy Use in Sanitary-ware Manufacturing, Springer, 2021, pp. 1-12.
[144] Khaled, B., kamel, b., Abdelmalek, R., hichem, A., Oussama, M. Reuse of sanitary ceramic waste in the production of vitreous china bodies. Iranian Journal of Chemistry and Chemical Engineering. 2022.

[145] Eygi, M., Ateşok, G. Effect of Electrolyte Type on the Rheological Behavior of Kaolins for Production of Sanitaryware2007.
[146] Souza, A., Pinheiro, B., Holanda, J. Sintering behavior of vitrified ceramic tiles incorporated with petroleum waste. Sinter Appl. 2013.
[147] Romero, M., Perez, J.M. Relación entre la microestructura y las propiedades tecnológicasen gres porcelánico. Revisión bibliográfica. Materiales de Construcción. 2015, 65, e065.
[148] Budhathoki, P., Paudyal, G., Oli, R., Duwal, N., Bhattarai, J. Assessment on the characterization of mineralogical phase of ceramic tiles available in Kathmandu valley (Nepal) using XRD and FTIR analyses. International Journal of Applied Sciences and Biotechnology. 2018, 6, 238-43.
[149] Benkacem, S., Boudeghdegh, K., Zehani, F., Hamidouche, M., Belhocine, Y. Preparation, Microstructure Studies and Mechanical Properties of Glazes Ceramic Sanitary Ware Based on Kaolin. Science of Sintering. 2021, 53.
[150] Rezende, J.C.T., Ramos, V.H.S., Oliveira, H., Oliveira, R., De Jesus, E. Removal of Cr(VI) from Aqueous Solutions Using Clay from Calumbi Geological Formation, N. Sra. Socorro, SE State, Brazil. Materials Science Forum. 2018, 912, 1-6.
[151] Roy, J., Maitra, S. Non-Isothermal Dehydration Kinetics of Diphasic Mullite Precursor Gel. Iranian Journal of Chemistry and Chemical Engineering (IJCCE). 2019, 38, 91-100.

ANNEXES

A.1 Data files of raw materials and electrolytes

A.1 .1 Technical file for Hycast VC clay

BALL CLAY

Hycast VC

APPLICATION
Sanitaryware

PRODUCT SPECIFICATION

CHEMICAL ANALYSIS (%)	Min.	Value	Max.
SiO_2	50	53	55
Al_2O_3	28	30	32
Fe_2O_3	1.0	1.2	1.4
TiO_2	0.9	1.0	1.3
K_2O	1.8	2.0	2.3
L.O.I.	11.0	12.2	13.5
PHYSICAL PROPERTIES			
M.B.I. ($mg.g^{-1}$)	20	25	30
CASTING DATA			
Casting concentration (mass % solids)	65.5	66.5	68.0
M75 sodium silicate + Na_2CO_3 demand (mass %) 7 poise	0.60	0.75	0.90
M75 sodium silicate + Na_2CO_3 demand (mass %) 5 poise	0.90	1.05	1.20
Thixotropy V60 @ 7 poise	1	100	200

TYPICAL PROPERTIES

CHEMICAL ANALYSIS (%)	Value
Na_2O	0.2
CaO	0.2
MgO	0.3
Carbon	2.2
PARTICLE SIZE ANALYSIS (%)	
> 125 µm	1.5
> 53 µm	2.5
< 5 µm	91
< 2 µm	77
< 1 µm	67
< 0.5 µm	54
CHEMICAL PROPERTIES (%)	
Water soluble salts	0.15
MODULUS OF RUPTURE ($MN.m^{-2}$)	
Dried at 110 °C	5.5

FIRED PROPERTIES (%)	1120°C	1180°C	1240°C
Brightness	70	62	56
Water absorption	9.0	5.5	3.0
Linear contraction	11.0	13.0	14.0

PRODUCT FORM & STANDARD PACKAGING
Powder, shredded, slurry
Big bag, 25-50 kg bags, bulk

December 2014

Tenth Edition
This version supersedes the version dated October 2014

Production Site
Imerys Minerals Ltd
Higher Brocks Plantation,
Old Newton Road,
Teigngrace,
Newton Abbot,
TQ12 6QZ, Devon, United Kingdom

Tel. +44 (0) 1626 83 2366
Fax: +44 (0) 1626 83 5683

Email
info@imerys-ceramics.com

Website
www.imerys-ceramics.com

IMERYS Ceramics

A.1 .2 Technical file for Remblend kaolin

Kaolin

Remblend

APPLICATION(S)
Sanitaryware, Tableware, Electrical Porcelain

PRODUCT SPECIFICATION

CHEMICAL ANALYSIS (%)	Min.	Value	Max.
Fe_2O_3	1.05	1.17	1.29
K_2O	2.05	2.25	2.45
PARTICLE SIZE ANALYSIS (%)			
> 53 µm	-	-	0.25
> 8 µm	14	19	24
< 2 µm	34	39	44
CASTING DATA			
Casting concentration (mass % solids)	64.5	66.5	68.5
Casting rate ($mm^2.min^{-1}$)	0.90	1.90	2.90

TYPICAL PROPERTIES

CHEMICAL ANALYSIS (%)	Value
SiO_2	48.0
Al_2O_3	36.5
TiO_2	0.05
Na_2O	0.10
CaO	0.07
MgO	0.30
L.O.I.	12.0
MODULUS OF RUPTURE ($MN.m^{-2}$)	
At 80 % RH	0.50
CASTING DATA (mass %)	
P84 demand	0.48

FIRED PROPERTIES (%)	AT 1180°C	AT 1280°C
Brightness	82.0	83.0
Water absorption	16.5	9.5
Linear contraction	7.0	10.5
PRODUCT FORM & STANDARD PACKAGING		
Powder, lumps		
Big bag, 25-50 kg bags, bulk		

Typical data values do not represent a specification. The data quoted are determined by the use of Imerys Standard Test Methods, copies of which will be supplied on request. Every precaution is taken in production to ensure the products conform to our published data. Since the products are based on naturally occurring materials, we reserve the right to change these data should it become necessary. Sales are in accordance with our "Conditions of Sale", copies of which will be supplied on request.

Production Site
Imerys Minerals Ltd
Par Moor Centre
Par Moor Road
Par, Cornwall
PL24 2SQ, UK

Tel. +44 (0) 1726 81 8000
Fax: +44 (0) 1726 81 1200

Email
info@imerys-ceramics.com

Website
www.imerys-ceramics.com

bsi. ISO 9001 Quality Management
FM 14752

IMERYS Ceramics

A.1 .3 Technical file for Parkaolin

KAOLIN

Parkaolin

APPLICATION(S)
Sanitaryware

TYPICAL PROPERTIES

CHEMICAL ANALYSIS (%)	Value
SiO_2	49
Al_2O_3	36
Fe_2O_3	1.1
TiO_2	0.05
K_2O	2.3
Na_2O	0.15
CaO	0.06
MgO	0.29
L.O.I.	11.62

PARTICLE SIZE ANALYSIS (%)	
> 8 µm	17
< 2 µm	44

PHYSICAL PROPERTIES (%)	
Moisture	12

CASTING DATA ($mm^2.min^{-1}$)	
Casting rate	1.3

PRODUCT FORM & STANDARD PACKAGING
Powder, lumps
Big bag, 25-50 kg bags, bulk

These values do not represent a specification. The data quoted are determined by the use of Imerys Standard Test Methods, copies of which will be supplied on request. Every precaution is taken in production to ensure the products conform to our published data. Since the products are based on naturally occurring materials, we reserve the right to change these data should it become necessary. Sales are in accordance with our "Conditions of Sale", copies of which will be supplied on request.

October 2014

Third Edition
This version supersedes the version dated September 2011

Production Site
Imerys Minerals Ltd
Par Moor Centre
Par Moor Road
Par, Cornwall
PL24 2SQ, UK

Tel. +44 (0) 1726 818 000
Fax: +44 (0) 1726 811 200

Email
info@imerys-ceramics.com

Website
www.imerys-ceramics.com

bsi. ISO 9001 Quality Management
FM 14752

IMERYS Ceramics

A.1 .4 Technical file for Sodium feldspar

kaltun
IBERICA, S.L

KALTUN IBERICA, S.L
Muelle de la Ceramica s/n
12100 Grao - CASTELLON
ESPAÑA
Tel. 00 34 964 73 70 50
Fax 00 34 964 28 62 65
E-mail: mangel@kaltun.com

FELDESPATO SODICO STD 63

Origen producto ; Çine – AYDIN - Turquía

Materia ; Feldespato sódico de alta pureza, con bajo contenido en Fe_2O_3 y TiO_2 , procedente de los depósitos de la región de Çine. Material no flotado.

Embalaje ; Granel / cisterna

Analisis Químico

; Elemento	%	Típico
SiO_2	69,00	
Al_2O_3	17,00 – 19,00	17,80
Fe_2O_3	< 0,15	0,10
TiO_2	< 0,35	0,31
CaO	0,75	
MgO	0,10	
Na_2O	9,5 – 10,50	10,10
K_2O	0,25	
P_2O_5	0,20	
L.O.I	0,32	
Humedad	< 1,00	

Tamaño partícula ; Residuo sobre tamiz 63 micras < 1,0 % 0,5 %
Método: Tamiz vía seca

These figures are average values from numerous measurements.

A.1 .4 Technical file for Potassium feldspar

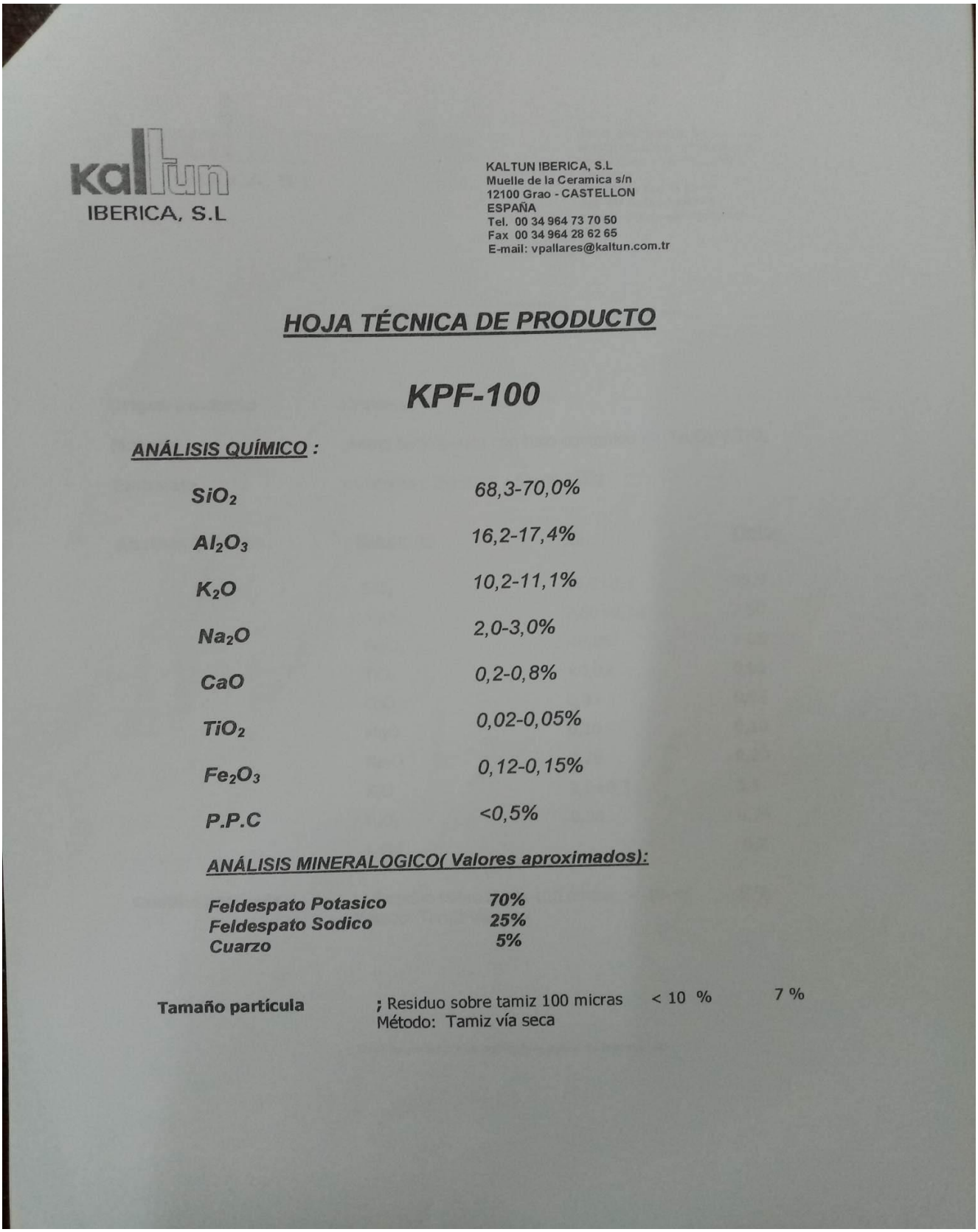

kaltun
IBERICA, S.L

KALTUN IBERICA, S.L
Muelle de la Ceramica s/n
12100 Grao - CASTELLON
ESPAÑA
Tel. 00 34 964 73 70 50
Fax 00 34 964 28 62 65
E-mail: vpallares@kaltun.com.tr

HOJA TÉCNICA DE PRODUCTO

KPF-100

ANÁLISIS QUÍMICO :

SiO_2	68,3-70,0%
Al_2O_3	16,2-17,4%
K_2O	10,2-11,1%
Na_2O	2,0-3,0%
CaO	0,2-0,8%
TiO_2	0,02-0,05%
Fe_2O_3	0,12-0,15%
P.P.C	<0,5%

ANÁLISIS MINERALOGICO(Valores aproximados):

Feldespato Potasico	70%
Feldespato Sodico	25%
Cuarzo	5%

Tamaño partícula	; Residuo sobre tamiz 100 micras Método: Tamiz vía seca	< 10 %	7 %

A.1 .4 Technical file for Quartz of Bir El Ater

SARL SABLATLAS
ALLOUANE BELGACEM
CITE EL ATIK BIR EL ATER 12001
RC n° 058 25 99 B 01
TEL/FAX : 037 64 60 73
MOBILE : 0659 91 91 51
E-MAIL : sable_tlas@yahoo.com

Fiche Technique

* Sable blanc brut pour Céramique :

Elément	Formule	%
Silice Totale	SiO_2	97.60
Oxyde d'Aluminium	Al_2O_3	0.83
Oxyde de fer	Fe_2O_3	0.30
Oxyde de calcium	CaO	0.60
Oxyde de Maghésium	MgO	0.70
Oxyde de potassium	K_2O	0.50
Oxyde de sodium	Na_2O	0.10
Oxyde de titane	TiO_2	0.049
Oxyde de chrome	Cr_2O3	0.037
Oxyde de manganèse	MnO	0.011
Anhydride phosphorique	P_2O5	0.086
Anhydride sulfurique	SO_3	0.26
Perte au feu	/	0.38

Granulométries disponibles :
- 0.8 à 1.25 mm : silex de filtration
- 0.8 à 1.80 mm : silex de filtration
- 1.5 à 2.60 mm : support de filtration
- 3 à 5.6 mm : support de filtration

Conditionnement :
- Big Bags de 2 tonnes.
- Sacs de 25 et 50 Kg.

A.1 .5 Technical file for Sodium carbonate

DISTRIM,S.p.a.

CARBONATE DE SOUDE LEGER

+ CARACTERISTIQUES

- Nom chimique	$NaZCO3$
- degrés de pureté	98 à 100% après dessiccation
- insolubilité dans l'eau	0.02%

+ COMPOSITION CHIMIQUE

Na_2CO_3	99.3%
Na CI	0.25 à 0.35%
Na_2SO_4	0.03%
Fe_2O_3	0.002%
CaO	0.01%
MgO	0.01%
Perte de dessiccation	0.3%

+ ANALYSES GRANULOMETRIQUES

>0.250mm	5 à 10% en poids
0.250 à 0.125mm	30%
0.125 à 0.062mm	40%
<0.062 mm	20%

Distrim Annaba : Zone indistruelle de Maboudja Sidi Amar -Annaba
Tél.038.52.47.47 ou 038.52.46.48 **Fax**.038.52.49.00

A.1 .6 Technical file for Sodium silicate

EP ECOPRO CHIMICALS

FICHE TECHNIQUE SILICATE DE SOUDIUM LIQUIDE

Nom de produit : Silicate de sodium liquide

-Formule brute : nSiO2, Na2O.x H2O (avec n >2)

Caractéristiques physiques :

N	Caractéristiques	Spécifications
01	Aspect	Liquide limpide incolore à pâle
02	Odeur	Inodore
03	Pression de vapeur à 20°C	23 hPa
04	Densité à 20 °C	1,467 à 1.509 g/cm³
05	Solubilité dans/miscibilité avec l'eau	Entièrement miscible
06	Viscosité à 20°C	Env. 100 mPas

Caractéristiques chimiques :

N	Caractéristiques	Spécifications	
		(MIN%)	(MAX%)
01	Matière sèche	40	43
02	Rapport pondéral Sio2/Na2O	1.90	2.10

A.2 HighScore files of the crystalline phases

A.2. 1 HighScore file of Mullite

Name and formula

Reference code:	98-009-9327
Mineral name:	Mullite
Compound name:	Mullite
Common name:	Mullite
Chemical formula:	$Al_{4.44}O_{9.78}Si_{1.56}$

Crystallographic parameters

Crystal system:	Orthorhombic
Space group:	P b a m
Space group number:	55
a (Å):	7.5350
b (Å):	7.6830
c (Å):	2.8830
Alpha (°):	90.0000
Beta (°):	90.0000
Gamma (°):	90.0000
Calculated density (g/cm^3):	3.18
Volume of cell (10^6 pm^3):	166.90
Z:	1.00
RIR:	0.78

Subfiles and quality

Subfiles:	User Inorganic User Mineral
Quality:	User From Structure (=)

Comments

Creation Date:	01/04/2005
Modification Date:	30/12/1899
Original ICSD space group:	PBAM. Surface layer of Al-based ceramic. X-ray diffraction (powder)
Structure type:	Al4.8Si1.2O9+x. Temperature factors available. Rietveld profile refinement applied

The structure has been assigned a PDF number (calculated powder diffraction data): 01-074-4143

Compound with mineral name:	Mullite
Structure type:	Al4.8Si1.2O9+x
Recording date:	4/1/2005
Mineral origin:	synthetic
ANX formula:	A3X5

Z: 1
Calculated density: 3.18
R value: 0.08
Pearson code: oP16
Wyckoff code: h4 g d a
Structure TIDY: TRANS Origin 1/2 0 1/2
Publication title: Crystallographical analysis of surface layers of refractory ceramics formed using combined flame spray and simultaneous laser treatment
ICSD collection code: 99327
Structure: Al4.8Si1.2O9+x
Chemical Name: Aluminium Silicon Oxide (4.44/1.56/9.78)
Second Chemical Formula: Al4.44 Si1.56 O9.78

References

Structure: Stott, F.H.;Li, L.;Li, J.F., *Journal of the European Ceramic Society*, **24**, 3129 - 3138, (2004)

Peak list

No.	h	k	l	d [A]	2Theta[deg]	I [%]
1	1	1	0	5.37961	16.465	40.7
2	0	2	0	3.84150	23.135	0.0
3	2	0	0	3.76750	23.596	2.0
4	1	2	0	3.42239	26.015	84.1
5	2	1	0	3.38269	26.326	100.0
6	0	0	1	2.88300	30.994	18.0
7	2	2	0	2.68981	33.282	31.8
8	1	1	1	2.54110	35.292	43.7
9	1	3	0	2.42477	37.045	24.3
10	3	1	0	2.38734	37.648	2.0
11	0	2	1	2.30586	39.031	0.3
12	2	0	1	2.28956	39.320	18.2
13	1	2	1	2.20493	40.896	48.9
14	2	1	1	2.19420	41.105	0.9
15	2	3	0	2.11799	42.654	15.4
16	3	2	0	2.10221	42.990	1.7
17	2	2	1	1.96674	46.116	1.6
18	0	4	0	1.92075	47.287	1.6
19	4	0	0	1.88375	48.274	4.7
20	1	4	0	1.86123	48.896	0.1
21	1	3	1	1.85569	49.051	0.1
22	3	1	1	1.83875	49.534	8.2
23	4	1	0	1.82956	49.799	1.0
24	3	3	0	1.79320	50.880	2.5
25	2	4	0	1.71120	53.507	4.4
26	2	3	1	1.70689	53.653	0.4
27	3	2	1	1.69859	53.936	2.9
28	4	2	0	1.69134	54.186	9.1
29	0	4	1	1.59848	57.619	12.5
30	4	0	1	1.57696	58.480	4.6
31	1	4	1	1.56368	59.026	0.5
32	4	1	1	1.54476	59.822	0.7
33	3	4	0	1.52574	60.645	0.0
34	3	3	1	1.52269	60.780	27.6
35	4	3	0	1.51746	61.012	0.0
36	1	5	0	1.50561	61.543	0.3
37	5	1	0	1.47882	62.784	0.4
38	2	4	1	1.47151	63.131	0.8

39	4	2	1	1.45883	63.744	5.4
40	0	0	2	1.44150	64.603	11.9
41	2	5	0	1.42281	65.557	2.0
42	5	2	0	1.40291	66.607	4.1
43	1	1	2	1.39238	67.177	0.7
44	0	2	2	1.34961	69.606	0.0
45	3	4	1	1.34854	69.669	0.3
46	2	0	2	1.34632	69.801	0.0
47	4	4	0	1.34490	69.885	1.9
48	4	3	1	1.34281	70.010	0.0
49	1	5	1	1.33458	70.506	5.3
50	1	2	2	1.32847	70.879	2.9
51	2	1	2	1.32611	71.024	3.4
52	5	1	1	1.31581	71.665	2.0
53	3	5	0	1.31076	71.984	1.5
54	5	3	0	1.29882	72.751	0.7
55	0	6	0	1.28050	73.964	0.5
56	2	5	1	1.27589	74.276	8.0
57	2	2	2	1.27055	74.641	2.5
58	1	6	0	1.26240	75.206	0.2
59	5	2	1	1.26148	75.270	5.3
60	6	0	0	1.25583	75.668	2.3
61	6	1	0	1.23939	76.854	1.2
62	1	3	2	1.23908	76.877	2.9
63	3	1	2	1.23400	77.252	0.9
64	4	4	1	1.21881	78.397	0.7
65	2	6	0	1.21239	78.893	0.4
66	6	2	0	1.19367	80.380	0.4
67	3	5	1	1.19322	80.416	0.0
68	2	3	2	1.19168	80.541	0.7
69	4	5	0	1.19070	80.621	0.7
70	3	2	2	1.18885	80.772	0.2
71	5	4	0	1.18563	81.038	0.1
72	5	3	1	1.18419	81.156	0.9
73	0	6	1	1.17026	82.330	0.1
74	1	6	1	1.15640	83.537	0.0
75	0	4	2	1.15293	83.845	0.1
76	6	0	1	1.15134	83.987	0.2
77	4	0	2	1.14478	84.580	0.4
78	3	6	0	1.14080	84.944	0.0
79	1	4	2	1.13967	85.048	0.0
80	6	1	1	1.13863	85.144	0.0
81	4	1	2	1.13228	85.736	0.2
82	6	3	0	1.12756	86.181	0.3
83	3	3	2	1.12350	86.570	0.3
84	2	6	1	1.11759	87.142	0.6
85	6	2	1	1.10287	88.605	0.4
86	2	4	2	1.10246	88.647	0.8
87	4	5	1	1.10053	88.843	1.0
88	4	2	2	1.09710	89.195	1.5
89	5	4	1	1.09652	89.255	0.4

Structure

No.	Name	Elem.	X	Y	Z	Biso	sof	Wyck.
1	O1	O	0.45300	0.37600	0.00000	4.4000	0.1120	4g
2	O2	O	0.00000	0.00000	0.00000	5.5000	0.6600	2a
3	O3	O	0.12700	0.26600	0.50000	4.4000	1.0000	4h
4	O4	O	0.35190	0.07100	0.00000	4.4000	1.0000	4g

5	AL1	Al	0.28300	0.28000	0.00000	1.5000	0.1120	4g
6	SI1	Si	0.15090	0.15860	0.00000	3.7000	0.3870	4g
7	AL2	Al	0.15090	0.15860	0.00000	3.7000	0.5000	4g
8	AL3	Al	0.00000	0.50000	0.50000	3.1000	1.0000	2d

Stick Pattern

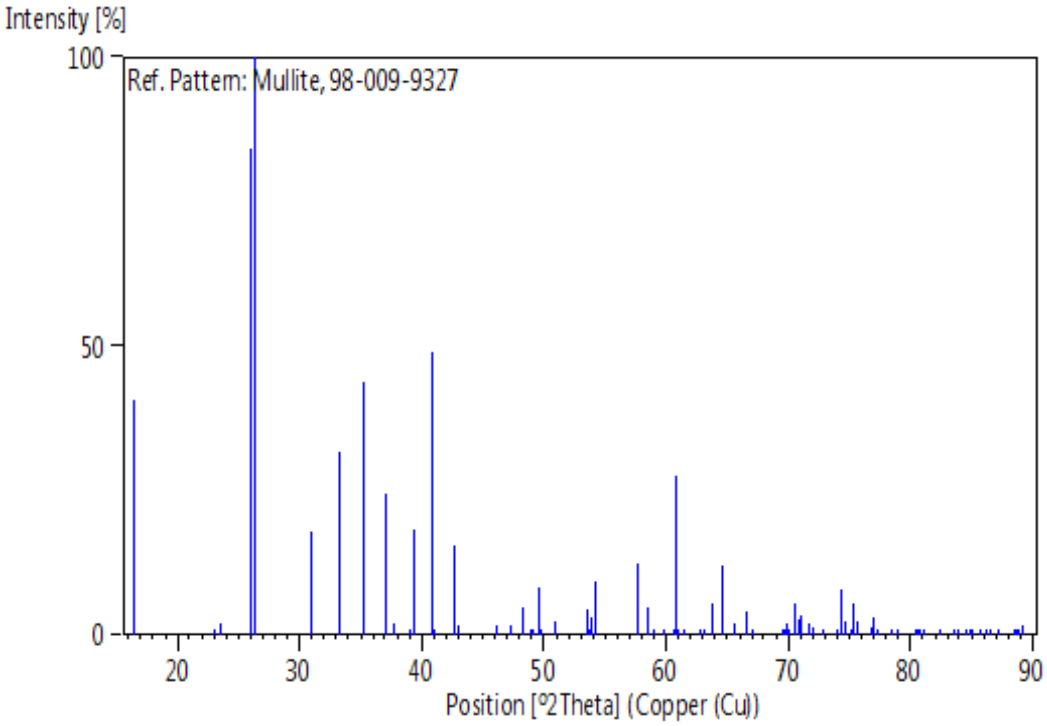

A.2. 2 HighScore file of Quartz

Name and formula

Reference code:	98-015-6196
Mineral name:	Quartz
Compound name:	Quartz
Common name:	Quartz
Chemical formula:	O_2Si_1

Crystallographic parameters

Crystal system:	Hexagonal
Space group:	P 31 2 1
Space group number:	152
a (Å):	4.9230
b (Å):	4.9230
c (Å):	5.4090
Alpha (°):	90.0000
Beta (°):	90.0000

Gamma (°):	120.0000
Calculated density (g/cm^3):	2.64
Volume of cell (10^6 pm^3):	113.53
Z:	3.00
RIR:	3.10

Subfiles and quality

Subfiles:	User Inorganic User Mineral
Quality:	User From Structure (=)

Comments

Creation Date:	01/08/2007
Modification Date:	30/12/1899
Original ICSD space group:	P3221. z-coordinate of Si corrected from 0 into 0.6667 to fit positions.. The coordinates given in the paper contain an error. The values in the database have been corrected.. X-ray diffraction from single crystal
Structure type:	Quartz,low. Temperature factors available
Compound with mineral name:	Quartz
Structure type:	Quartz,low
Recording date:	8/1/2007
Mineral origin:	Yangkou meta-igneous complex, Sulu UHP terrain, eastern China
ANX formula:	AX2
Z:	3
Calculated density:	2.64
R value:	0.0866
Pearson code:	hP9
Wyckoff code:	c a

Structure TIDY: TRANS -a,-b,-c
Structure TIDY: REMARK Transformed from enantiomorphic space group.
Publication title: First in situ X-ray identification of coesite and retrograde quartz on a glass thin section of an ultrahigh-pressure metamorphic rock and their crystal structure details
ICSD collection code: 156196
Structure: Quartz,low
Chemical Name: Silicon Oxide
Second Chemical Formula: Si O2

References

Structure: Tamada, O.;Downs, R.T.;Rakovan, J.F.;Ito, K.;Hirajima, T.;Banno, S.;Kawame, N.;Ikuta, D., *American Mineralogist*, **92**, 57 - 63, (2007)

Peak list

No.	h	k	l	d [A]	2Theta[deg]	I [%]
1	0	1	0	4.26344	20.818	13.4
2	0	1	1	3.34836	26.600	100.0

3	1	1	0	2.46150	36.473	9.1
4	1	0	2	2.28377	39.424	8.7
5	1	1	1	2.24042	40.219	4.3
6	0	2	0	2.13172	42.366	3.2
7	2	0	1	1.98326	45.710	2.4
8	1	1	2	1.82040	50.067	15.7
9	0	0	3	1.80300	50.584	0.4
10	0	2	2	1.67418	54.788	4.4
11	0	1	3	1.66061	55.274	1.6
12	2	1	0	1.61143	57.113	0.2
13	1	2	1	1.54435	59.839	5.8
14	1	1	3	1.45454	63.955	2.3
15	3	0	0	1.42115	65.643	0.2
16	1	2	2	1.38433	67.620	4.2
17	2	0	3	1.37663	68.050	5.7
18	0	3	1	1.37450	68.170	4.4
19	1	0	4	1.28897	73.398	1.5
20	3	0	2	1.25803	75.513	1.8
21	2	2	0	1.23075	77.493	1.7
22	2	1	3	1.20149	79.751	1.9
23	2	2	1	1.20008	79.864	0.8
24	1	1	4	1.18518	81.074	2.2
25	1	3	0	1.18247	81.300	1.5
26	1	3	1	1.15518	83.644	1.2
27	2	0	4	1.14188	84.844	0.3
28	2	2	2	1.12021	86.887	0.0
29	3	0	3	1.11612	87.286	0.3

Structure

No.	Name	Elem.	X	Y	Z	Biso	sof	Wyck.
1	O1	O	0.41400	0.15000	0.12133	2.2108	1.0000	6c
2	SI1	Si	0.53200	0.00000	0.33333	1.7370	1.0000	3a

Stick Pattern

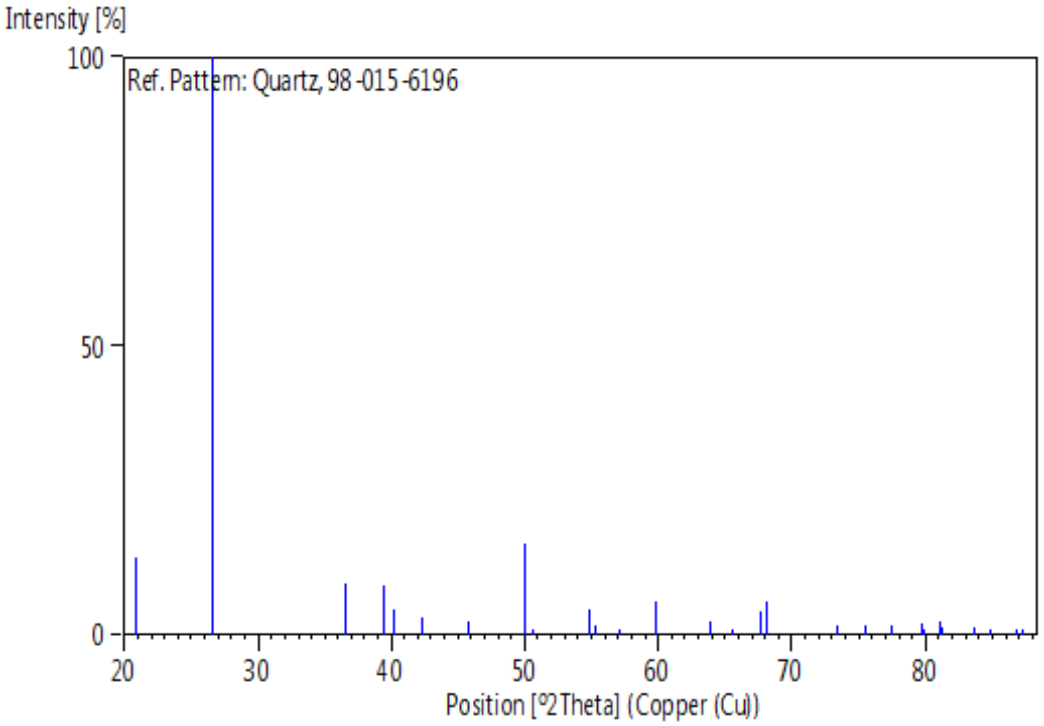

A.2. 3 HighScore file of Anorthite

Name and formula

Reference code:	98-000-9330
Mineral name:	Anorthite
Compound name:	Anorthite
Common name:	Anorthite
Chemical formula:	$Al_2Ca_1O_8Si_2$

Crystallographic parameters

Crystal system:	Monoclinic
Space group:	P 1 21 1
Space group number:	4
a (Å):	4.8270
b (Å):	8.6210
c (Å):	8.2280
Alpha (°):	90.0000
Beta (°):	90.0000
Gamma (°):	90.0000
Calculated density (g/cm^3):	2.70
Measured density (g/cm^3):	2.69
Volume of cell (10^6 pm^3):	342.40
Z:	2.00

RIR: 1.23

Subfiles and quality

Subfiles: User Inorganic
User Mineral
Quality: User From Structure (=)

Comments

Creation Date: 01/01/1980
Modification Date: 01/04/2003
Original ICSD space group: P1211. Only minor deviation from P21/n (~ 1/2+x 1/2-y 1/2+z)
av.T-O: 1.733, 1.732, 1.640, 1.619. The coordinates are those given in the paper but the atomic distances do not agree with those calculated during testing.The coordinates are probably correct.. Deviation of the charge sum from zero tolerable.. X-ray diffraction from single crystal. Temperature factors available

Temperature in Kelvin: 291
The structure has been assigned a PDF number (experimental powder diffraction data): 46-1266
The structure has been assigned a PDF number (calculated powder diffraction data): 01-071-0788
Compound with mineral name: Anorthite
Recording date: 1/1/1980
Modification date: 4/1/2003
Mineral origin: synthetic
ANX formula: AB2C2X8
Z: 2
Authors density: 2.69
Calculated density: 2.7
R value: 0.05
Pearson code: mP26
Wyckoff code: a14
PDF code: 00-046-1266
Structure TIDY: TRANS c,-b,a origin 1/2 .12860 1/2
Publication title: The crystal structure of monoclinic Ca Al2 Si2 O8. A case of monoclinic structure closely simulating orthorhombic symmetry
ICSD collection code: 9330
Chemical Name: Calcium Tecto-dialumodisilicate
Second Chemical Formula: Ca (Al2 Si2 O8)

References

Structure: Ito, J.;Haga, N.;Takeuchi, Y., *Zeitschrift fuer Kristallographie, Kristallgeometrie, Kristallphysik, Kristallchemie (-144,1977)*, **137**, 380 - 398, (1973)

Peak list

No.	h	k	l	d [A]	2Theta[deg]	I [%]
1	0	0	1	8.22800	10.744	0.0
2	0	1	-1	5.95216	14.872	1.5

3	1	0	0	4.82700	18.365	0.2
4	0	2	0	4.31050	20.588	3.7
5	1	1	0	4.21175	21.077	4.9
6	1	0	-1	4.16343	21.324	41.6
7	0	0	2	4.11400	21.583	49.0
8	0	2	1	3.81826	23.278	0.4
9	1	1	1	3.74912	23.713	24.9
10	0	1	2	3.71290	23.948	0.1
11	1	2	0	3.21514	27.724	100.0
12	1	0	-2	3.13108	28.484	0.2
13	1	2	1	2.99463	29.811	0.7
14	0	2	-2	2.97608	30.001	13.5
15	1	1	2	2.94299	30.347	24.5
16	0	0	3	2.74267	32.623	0.1
17	0	3	-1	2.71296	32.990	14.5
18	0	1	3	2.61359	34.283	2.2
19	1	2	2	2.53329	35.405	8.2
20	1	3	0	2.46922	36.355	0.8
21	2	0	0	2.41350	37.225	0.6
22	1	0	-3	2.38462	37.692	4.7
23	1	3	1	2.36502	38.017	3.2
24	0	3	2	2.35585	38.170	0.0
25	2	1	0	2.32414	38.712	5.3
26	2	0	-1	2.31592	38.855	0.1
27	0	2	3	2.31397	38.889	0.0
28	1	1	3	2.29832	39.164	2.3
29	2	1	-1	2.23662	40.291	5.0
30	0	4	0	2.15525	41.882	1.0
31	1	3	2	2.11715	42.672	4.0
32	2	2	0	2.10587	42.912	1.2
33	1	2	-3	2.08660	43.328	20.3
34	0	4	1	2.08491	43.365	0.0
35	2	0	2	2.08171	43.435	2.4
36	0	0	4	2.05700	43.984	8.5
37	2	2	-1	2.04011	44.367	3.5
38	2	1	2	2.02356	44.750	1.2
39	0	1	4	2.00083	45.286	0.0
40	0	3	-3	1.98405	45.691	0.1
41	1	4	0	1.96799	46.085	13.4
42	1	4	-1	1.91400	47.463	0.1
43	0	4	-2	1.90913	47.592	1.0
44	1	0	-4	1.89234	48.041	0.0
45	2	2	-2	1.87456	48.526	0.1
46	0	2	-4	1.85645	49.030	1.1
47	1	1	4	1.84834	49.260	0.4
48	2	3	0	1.84815	49.265	3.1
49	1	3	3	1.83508	49.639	0.1
50	2	0	-3	1.81186	50.319	0.0
51	2	3	1	1.80322	50.577	1.1
52	1	4	-2	1.77532	51.430	3.2
53	2	1	3	1.77313	51.498	0.2
54	1	2	4	1.73272	52.791	1.0
55	0	4	3	1.69462	54.073	0.0
56	0	5	1	1.68755	54.318	1.6
57	2	3	2	1.68585	54.377	0.4
58	0	3	4	1.67264	54.842	0.1
59	2	2	3	1.67030	54.926	10.8
60	0	0	5	1.64560	55.822	0.0
61	1	5	0	1.62372	56.641	1.0
62	0	1	5	1.61642	56.920	0.0

63	3	0	0	1.60900	57.207	0.0
64	2	4	0	1.60757	57.262	4.3
65	1	4	3	1.59895	57.600	4.2
66	1	5	-1	1.59300	57.835	1.2
67	0	5	-2	1.59019	57.947	0.0
68	3	1	0	1.58169	58.289	0.4
69	1	3	-4	1.58045	58.339	0.2
70	3	0	-1	1.57909	58.394	1.0
71	2	4	-1	1.57774	58.449	2.8
72	2	0	4	1.56554	58.949	0.1
73	1	0	-5	1.55757	59.280	5.9
74	3	1	-1	1.55325	59.462	0.3
75	2	1	-4	1.54035	60.011	0.2
76	0	2	5	1.53738	60.139	0.3
77	1	1	5	1.53276	60.339	4.0
78	1	5	2	1.51034	61.330	0.5
79	3	2	0	1.50741	61.462	1.0
80	3	0	-2	1.49847	61.869	0.0
81	2	4	2	1.49732	61.922	0.2
82	0	4	-4	1.48804	62.351	0.2
83	3	2	-1	1.48273	62.599	0.1
84	3	1	2	1.47634	62.901	0.6
85	2	2	-4	1.47149	63.132	0.6
86	1	2	-5	1.46487	63.451	1.3
87	0	5	3	1.45971	63.701	0.0
88	0	6	0	1.43683	64.838	7.9
89	0	3	-5	1.42803	65.288	3.7
90	1	4	-4	1.42200	65.599	0.5
91	3	2	2	1.41539	65.945	2.7
92	3	3	0	1.40391	66.553	8.8
93	2	5	0	1.40296	66.604	2.9
94	1	5	3	1.39722	66.914	1.9
95	3	0	3	1.38781	67.428	1.5
96	2	4	-3	1.38689	67.479	4.0
97	3	3	1	1.38391	67.643	0.2
98	2	5	1	1.38300	67.694	0.3
99	1	6	0	1.37712	68.023	0.8
100	2	3	-4	1.37477	68.155	0.1
101	0	0	6	1.37133	68.349	3.5
102	3	1	-3	1.37017	68.415	0.1
103	1	3	5	1.36936	68.461	0.8
104	2	0	-5	1.35963	69.020	0.0
105	1	6	-1	1.35823	69.102	1.4
106	0	6	-2	1.35648	69.203	1.1
107	0	1	6	1.35431	69.330	0.2
108	2	1	5	1.34303	69.997	2.4
109	3	3	2	1.32868	70.866	2.9
110	2	5	-2	1.32787	70.915	2.6
111	0	5	-4	1.32139	71.316	0.0
112	3	2	3	1.32103	71.339	0.4
113	1	0	-6	1.31913	71.457	0.0
114	0	4	5	1.30794	72.164	0.0
115	0	2	-6	1.30680	72.237	0.0
116	1	6	-2	1.30590	72.295	0.2
117	1	1	6	1.30396	72.419	0.5
118	2	2	-5	1.29666	72.892	5.0
119	3	4	0	1.28933	73.374	2.0
120	1	5	-4	1.27450	74.371	0.3
121	3	4	-1	1.27379	74.419	0.1
122	0	6	3	1.27275	74.490	0.0

123	3	0	-4	1.26734	74.862	0.0
124	2	4	4	1.26664	74.911	0.9
125	1	4	-5	1.26241	75.205	0.9
126	1	2	6	1.26139	75.277	1.6
127	3	1	4	1.25387	75.808	0.2
128	3	3	3	1.24971	76.105	0.3
129	2	5	3	1.24903	76.153	0.6
130	0	3	6	1.23763	76.983	0.0
131	2	6	0	1.23461	77.206	0.0
132	1	6	-3	1.23069	77.498	0.7
133	3	4	2	1.23033	77.525	0.8
134	2	3	5	1.22901	77.624	1.0
135	2	6	-1	1.22094	78.234	0.2
136	0	7	-1	1.21800	78.459	0.1
137	3	2	-4	1.21588	78.623	0.1
138	4	0	0	1.20675	79.334	1.1
139	1	3	-6	1.19885	79.961	1.4
140	4	1	0	1.19510	80.264	1.7
141	4	0	-1	1.19398	80.355	0.0
142	1	7	0	1.19334	80.406	1.2
143	2	0	6	1.19231	80.490	0.2
144	0	5	-5	1.19043	80.643	0.6
145	4	1	1	1.18269	81.281	0.1
146	2	6	2	1.18251	81.296	0.0
147	2	1	-6	1.18107	81.416	0.5
148	1	7	1	1.18099	81.423	0.4
149	0	7	-2	1.17984	81.519	0.0
150	0	6	-4	1.17792	81.680	0.4
151	3	5	0	1.17635	81.812	0.0
152	0	0	7	1.17543	81.890	0.0
153	3	4	3	1.16683	82.625	1.0
154	0	1	-7	1.16465	82.813	0.1
155	3	5	1	1.16451	82.825	0.1
156	4	2	0	1.16207	83.038	0.3
157	3	3	-4	1.15958	83.256	0.4
158	2	5	4	1.15905	83.303	0.1
159	4	0	-2	1.15796	83.399	0.3
160	0	4	-6	1.15699	83.485	0.1
161	1	5	5	1.15580	83.589	1.7
162	4	2	1	1.15065	84.049	0.1
163	3	0	-5	1.15046	84.066	1.7
164	2	4	-5	1.14993	84.113	3.0
165	2	2	-6	1.14916	84.183	0.1
166	4	1	2	1.14766	84.319	1.0
167	1	7	-2	1.14610	84.460	1.9
168	1	6	4	1.14434	84.619	0.2
169	1	0	7	1.14206	84.828	0.0
170	3	1	5	1.14035	84.985	0.2
171	0	2	-7	1.13402	85.572	0.0
172	1	1	7	1.13216	85.746	0.1
173	3	5	-2	1.13103	85.854	0.1
174	2	6	-3	1.12580	86.349	0.0
175	1	4	6	1.12512	86.414	0.9
176	0	7	-3	1.12350	86.570	1.1
177	4	2	2	1.11831	87.071	1.3
178	4	3	0	1.11263	87.629	0.0
179	3	2	-5	1.11155	87.736	0.0
180	4	0	-3	1.10456	88.435	0.0
181	1	2	7	1.10397	88.495	1.2
182	4	3	1	1.10259	88.634	0.3

183	2	3	-6	1.10128	88.767	0.3
184	2	7	0	1.09700	89.205	0.4
185	4	1	-3	1.09560	89.350	1.7
186	1	7	3	1.09425	89.490	0.4
187	3	4	4	1.09247	89.676	0.2

Structure

No.	Name	Elem.	X	Y	Z	Biso	sof	Wyck.
1	O1	O	0.31050	0.19520	0.05920	1.1100	1.0000	2a
2	O2	O	0.02110	0.00000	0.23360	0.8100	1.0000	2a
3	O3	O	0.74860	0.39070	0.02540	1.3000	1.0000	2a
4	O4	O	0.16040	0.57840	0.06190	0.6000	1.0000	2a
5	O5	O	0.18630	0.57400	0.45400	0.5000	1.0000	2a
6	O6	O	0.49790	0.23360	0.73860	1.4700	1.0000	2a
7	O7	O	0.76190	0.36930	0.46200	0.8800	1.0000	2a
8	O8	O	0.32630	0.18950	0.43910	1.0500	1.0000	2a
9	SI1	Si	0.10480	0.04380	0.05460	0.4500	1.0000	2a
10	SI2	Si	0.60550	0.22160	0.54970	0.2500	1.0000	2a
11	AL1	Al	0.39410	0.73410	0.06760	0.6200	1.0000	2a
12	AL2	Al	0.10240	0.03540	0.43500	0.7000	1.0000	2a
13	CA1	Ca	0.15600	0.37140	0.25020	1.4200	0.5640	2a
14	CA2	Ca	0.36420	0.39760	0.24700	0.4700	0.4030	2a

Stick Pattern

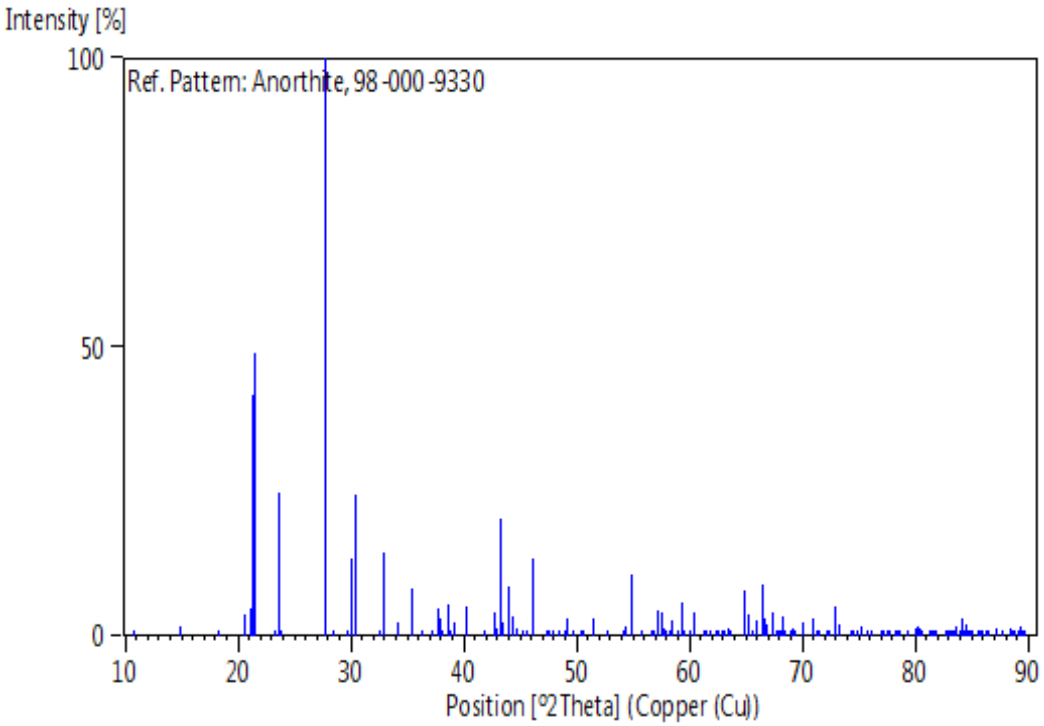

A.3. Data on particle size distribution of industrial solid wastes used

A.3. 1 particle size distribution of blast furnace slag

2018.11.18 10:45:09

HORIBA Laser Scattering Particle Size Distribution Analyzer LA-960

Nom échantillon	: BFS	Diamètre médian	: 37.39974Microns
ID#	: 201811181043353	Diamètre moyen	: 299.12244Microns
Nom des données	: 201811181043353	Ecart-type	: 393.5887Microns
Transmission(R)	: 91.0 (%)	Moyenne géo. diamétre	: 58.1427Microns
Transmission(B)	: 90.6 (%)	Ecart type géo.	: 8.6644Microns
Vitesse circulation	: 5	Diamètre Mode	: 827.8235Microns
Vitesse agitation	: 5	Span	: Non-actif
Ultra-sons	: 00:15 (7)	Diamètre pour % cumulé	: (1)5.000 (%)- 2.3496Microns
Type de distribution	: Auto		: (2)10.00 (%)- 4.0406Microns
Base de distribution	: Volume		: (3)20.00 (%)- 7.5457Microns
Indice réfraction(R)	: cim		: (4)30.00 (%)- 11.7705Microns
	[ciment(1.500 - 1.500i),water(1.333)]		: (5)40.00 (%)- 18.9692Microns
Indice réfraction(B)	: cim		: (6)60.00 (%)- 114.4730Microns
	[ciment(1.500 - 1.500i),water(1.333)]		: (7)70.00 (%)- 501.4911Microns
Matériau	: Poudre		: (8)80.00 (%)- 705.7551Microns
Source	:		: (9)90.00 (%)- 914.4434Microns
Numéro de lot	:		

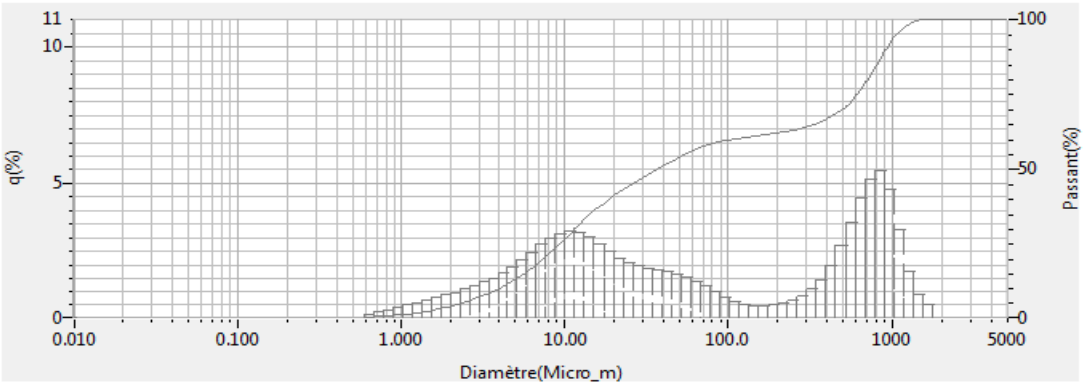

No.	Diamètre(Micro_m)	q(%)	Passant(%)
1	0.011	0.000	0.000
2	0.013	0.000	0.000
3	0.015	0.000	0.000
4	0.017	0.000	0.000
5	0.020	0.000	0.000
6	0.022	0.000	0.000
7	0.026	0.000	0.000
8	0.029	0.000	0.000
9	0.034	0.000	0.000
10	0.039	0.000	0.000
11	0.044	0.000	0.000
12	0.051	0.000	0.000
13	0.058	0.000	0.000
14	0.067	0.000	0.000
15	0.076	0.000	0.000
16	0.087	0.000	0.000
17	0.100	0.000	0.000
18	0.115	0.000	0.000
19	0.131	0.000	0.000
20	0.150	0.000	0.000
21	0.172	0.000	0.000
22	0.197	0.000	0.000
23	0.226	0.000	0.000
24	0.259	0.000	0.000
25	0.296	0.000	0.000
26	0.339	0.000	0.000
27	0.389	0.000	0.000
28	0.445	0.000	0.000
29	0.510	0.000	0.000
30	0.584	0.000	0.000
31	0.669	0.105	0.105
32	0.766	0.159	0.264
33	0.877	0.236	0.501
34	1.005	0.334	0.835
35	1.151	0.424	1.259
36	1.318	0.506	1.766
37	1.510	0.592	2.357
38	1.729	0.692	3.049
39	1.981	0.794	3.843
40	2.269	0.897	4.740
41	2.599	1.006	5.747
42	2.976	1.128	6.874
43	3.409	1.270	8.145
44	3.905	1.440	9.585
45	4.472	1.644	11.229
46	5.122	1.883	13.112
47	5.867	2.150	15.262
48	6.720	2.431	17.693
49	7.697	2.701	20.394
50	8.816	2.929	23.323
51	10.097	3.092	26.415
52	11.565	3.177	29.593
53	13.246	3.137	32.730
54	15.172	2.972	35.702
55	17.377	2.720	38.421
56	19.904	2.445	40.866
57	22.797	2.203	43.069
58	26.111	2.024	45.093
59	29.907	1.909	47.002
60	34.255	1.839	48.841
61	39.234	1.790	50.632
62	44.938	1.733	52.365
63	51.471	1.634	53.999
64	58.953	1.491	55.490
65	67.523	1.314	56.803
66	77.339	1.113	57.916
67	88.583	0.902	58.818
68	101.460	0.703	59.521
69	116.210	0.539	60.060
70	133.103	0.445	60.505
71	152.453	0.405	60.910
72	174.616	0.403	61.313
73	200.000	0.434	61.747
74	229.075	0.496	62.243
75	262.376	0.595	62.838
76	300.518	0.751	63.589
77	344.206	1.006	64.595
78	394.244	1.402	65.997
79	451.556	1.954	67.951
80	517.200	2.652	70.603
81	592.387	3.508	74.110
82	678.504	4.402	78.512
83	777.141	5.129	83.641
84	890.116	5.415	89.055
85	1019.515	4.755	93.810
86	1167.725	3.243	97.053
87	1337.481	1.698	98.751
88	1531.914	0.803	99.554
89	1754.613	0.446	100.000
90	2009.687	0.000	100.000
91	2301.841	0.000	100.000
92	2636.467	0.000	100.000
93	3019.738	0.000	100.000
94	3458.727	0.000	100.000
95	3961.532	0.000	100.000
96	4537.433	0.000	100.000
97	5000.000	0.000	100.000

A.3. 2 particle size distribution of soda-lime glass waste

2018.11.18 10:27:02

HORIBA Laser Scattering Particle Size Distribution Analyzer LA-960

Nom échantillon	: SLGW	Diamètre médian	: 38.83410Microns
ID#	: 201811181024346	Diamètre moyen	: 264.28214Microns
Nom des données	: 201811181024346	Ecart-type	: 407.7260Microns
Transmission(R)	: 88.6 (%)	Moyenne géo. diamétre	: 57.7441Microns
Transmission(B)	: 89.3 (%)	Ecart type géo.	: 6.6857Microns
Vitesse circulation	: 5	Diamètre Mode	: 10.8097Microns
Vitesse agitation	: 5	Span	: Non-actif
Ultra-sons	: 00:34 (7)	Diamètre pour % cumulé	: (1)5.000 (%)- 4.9996Microns
Type de distribution	: Auto		: (2)10.00 (%)- 6.5726Microns
Base de distribution	: Volume		: (3)20.00 (%)- 9.3158Microns
Indice réfraction(R)	: Silice		: (4)30.00 (%)- 12.5242Microns
	[Silice(2.000 - 0.000i),water(1.333)]		: (5)40.00 (%)- 18.0288Microns
Indice réfraction(B)	: Silice		: (6)60.00 (%)- 93.6769Microns
	[Silice(2.000 - 0.000i),water(1.333)]		: (7)70.00 (%)- 212.0749Microns
Matériau	: Poudre		: (8)80.00 (%)- 573.5127Microns
Source	:		: (9)90.00 (%)- 939.7905Microns
Numéro de lot	:		

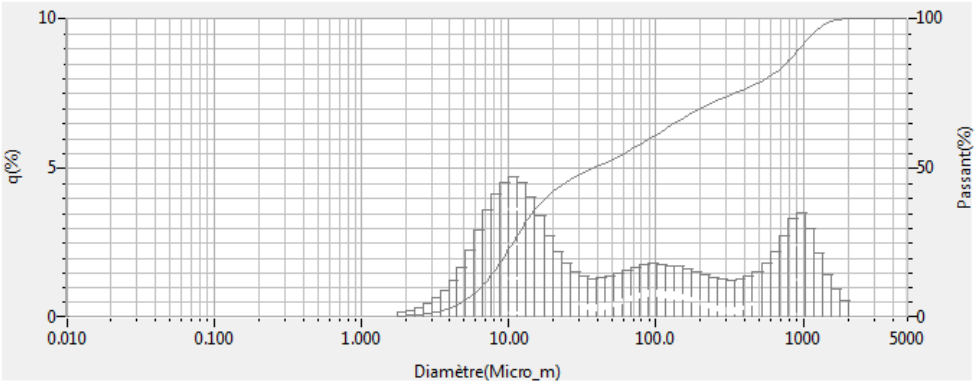

No.	Diamètre(Micro_m)	q(%)	Passant(%)
1	0.011	0.000	0.000
2	0.013	0.000	0.000
3	0.015	0.000	0.000
4	0.017	0.000	0.000
5	0.020	0.000	0.000
6	0.022	0.000	0.000
7	0.026	0.000	0.000
8	0.029	0.000	0.000
9	0.034	0.000	0.000
10	0.039	0.000	0.000
11	0.044	0.000	0.000
12	0.051	0.000	0.000
13	0.058	0.000	0.000
14	0.067	0.000	0.000
15	0.076	0.000	0.000
16	0.087	0.000	0.000
17	0.100	0.000	0.000
18	0.115	0.000	0.000
19	0.131	0.000	0.000
20	0.150	0.000	0.000
21	0.172	0.000	0.000
22	0.197	0.000	0.000
23	0.226	0.000	0.000
24	0.259	0.000	0.000
25	0.296	0.000	0.000
26	0.339	0.000	0.000
27	0.389	0.000	0.000
28	0.445	0.000	0.000
29	0.510	0.000	0.000
30	0.584	0.000	0.000
31	0.669	0.000	0.000
32	0.766	0.000	0.000
33	0.877	0.000	0.000
34	1.005	0.000	0.000
35	1.151	0.000	0.000
36	1.318	0.000	0.000
37	1.510	0.000	0.000
38	1.729	0.000	0.000
39	1.981	0.125	0.125
40	2.269	0.188	0.314
41	2.599	0.277	0.591
42	2.976	0.405	0.996
43	3.409	0.587	1.582
44	3.905	0.844	2.426
45	4.472	1.200	3.626
46	5.122	1.672	5.299
47	5.867	2.258	7.557
48	6.720	2.920	10.476
49	7.697	3.577	14.053
50	8.816	4.120	18.174
51	10.097	4.491	22.665
52	11.565	4.686	27.350
53	13.246	4.514	31.864
54	15.172	4.026	35.889
55	17.377	3.373	39.262
56	19.904	2.721	41.983
57	22.797	2.179	44.163
58	26.111	1.782	45.944
59	29.907	1.516	47.460
60	34.255	1.354	48.814
61	39.234	1.282	50.097
62	44.938	1.303	51.400
63	51.471	1.368	52.768
64	58.953	1.468	54.236
65	67.523	1.584	55.820
66	77.339	1.680	57.500
67	88.583	1.760	59.260
68	101.460	1.797	61.057
69	116.210	1.761	62.818
70	133.103	1.727	64.545
71	152.453	1.687	66.232
72	174.616	1.619	67.850
73	200.000	1.533	69.383
74	229.075	1.428	70.811
75	262.376	1.313	72.125
76	300.518	1.218	73.342
77	344.206	1.186	74.529
78	394.244	1.235	75.763
79	451.556	1.351	77.114
80	517.200	1.522	78.637
81	592.387	1.791	80.427
82	678.504	2.189	82.616
83	777.141	2.698	85.314
84	890.116	3.287	88.602
85	1019.515	3.495	92.097
86	1167.725	2.940	95.036
87	1337.481	2.134	97.170
88	1531.914	1.435	98.605
89	1754.613	0.894	99.499
90	2009.687	0.501	100.000
91	2301.841	0.000	100.000
92	2636.467	0.000	100.000
93	3019.738	0.000	100.000
94	3458.727	0.000	100.000
95	3961.532	0.000	100.000
96	4537.433	0.000	100.000
97	5000.000	0.000	100.000

A.3. 3 particle size distribution of sanitary ceramic waste

2018.11.18 10:34:14

HORIBA Laser Scattering Particle Size Distribution Analyzer LA-960

Nom échantillon	: SCW	Diamètre médian	: 13.15150Microns
ID#	: 201811181033351	Diamètre moyen	: 30.71712Microns
Nom des données	: 201811181033351	Ecart-type	: 43.6004Microns
Transmission(R)	: 89.4 (%)	Moyenne géo. diamétre	: 13.6222Microns
Transmission(B)	: 87.0 (%)	Ecart type géo.	: 3.7866Microns
Vitesse circulation	: 5	Diamètre Mode	: 10.8051Microns
Vitesse agitation	: 5	Span	: Non-actif
Ultra-sons	: 00:39 (7)	Diamètre pour % cumulé	: (1)5.000 (%)- 1.5434Microns
Type de distribution	: Auto		: (2)10.00 (%)- 2.2277Microns
Base de distribution	: Volume		: (3)20.00 (%)- 3.9544Microns
Indice réfraction(R)	: argile1		: (4)30.00 (%)- 6.3078Microns
	[argile1(1.700 - 0.500i),water(1.333)]		: (5)40.00 (%)- 9.2419Microns
Indice réfraction(B)	: argile1		: (6)60.00 (%)- 19.4523Microns
	[argile1(1.700 - 0.500i),water(1.333)]		: (7)70.00 (%)- 30.9596Microns
Matériau	: Poudre		: (8)80.00 (%)- 48.6367Microns
Source	:		: (9)90.00 (%)- 78.4357Microns
Numéro de lot	:		

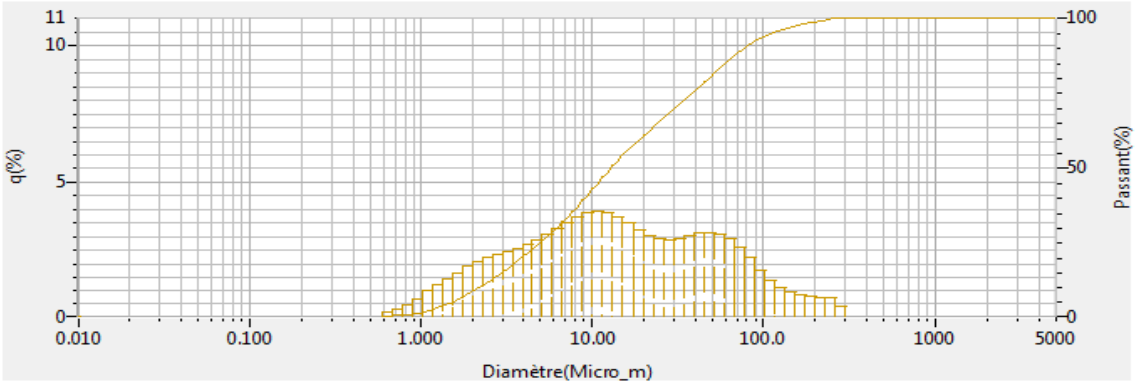

No.	Diamètre(Micro_m)	q(%)	Passant(%)
1	0.011	0.000	0.000
2	0.013	0.000	0.000
3	0.015	0.000	0.000
4	0.017	0.000	0.000
5	0.020	0.000	0.000
6	0.022	0.000	0.000
7	0.026	0.000	0.000
8	0.029	0.000	0.000
9	0.034	0.000	0.000
10	0.039	0.000	0.000
11	0.044	0.000	0.000
12	0.051	0.000	0.000
13	0.058	0.000	0.000
14	0.067	0.000	0.000
15	0.076	0.000	0.000
16	0.087	0.000	0.000
17	0.100	0.000	0.000
18	0.115	0.000	0.000
19	0.131	0.000	0.000
20	0.150	0.000	0.000
21	0.172	0.000	0.000
22	0.197	0.000	0.000
23	0.226	0.000	0.000
24	0.259	0.000	0.000
25	0.296	0.000	0.000

No.	Diamètre(Micro_m)	q(%)	Passant(%)
26	0.339	0.000	0.000
27	0.389	0.000	0.000
28	0.445	0.000	0.000
29	0.510	0.000	0.000
30	0.584	0.000	0.000
31	0.669	0.121	0.121
32	0.766	0.212	0.333
33	0.877	0.374	0.707
34	1.005	0.630	1.338
35	1.151	0.900	2.238
36	1.318	1.141	3.379
37	1.510	1.359	4.738
38	1.729	1.620	6.358
39	1.981	1.863	8.221
40	2.269	2.056	10.277
41	2.599	2.202	12.479
42	2.976	2.318	14.797
43	3.409	2.422	17.218
44	3.905	2.533	19.751
45	4.472	2.665	22.416
46	5.122	2.828	25.244
47	5.867	3.024	28.268
48	6.720	3.244	31.512
49	7.697	3.472	34.984
50	8.816	3.682	38.666

No.	Diamètre(Micro_m)	q(%)	Passant(%)
51	10.097	3.833	42.499
52	11.565	3.875	46.374
53	13.246	3.828	50.202
54	15.172	3.680	53.883
55	17.377	3.454	57.337
56	19.904	3.205	60.542
57	22.797	2.997	63.539
58	26.111	2.876	66.415
59	29.907	2.849	69.264
60	34.255	2.889	72.152
61	39.234	2.970	75.123
62	44.938	3.068	78.191
63	51.471	3.105	81.295
64	58.953	3.043	84.338
65	67.523	2.860	87.198
66	77.339	2.575	89.773
67	88.583	2.188	91.961
68	101.460	1.736	93.698
69	116.210	1.295	94.992
70	133.103	1.026	96.019
71	152.453	0.867	96.886
72	174.616	0.762	97.648
73	200.000	0.699	98.347
74	229.075	0.663	99.010
75	262.376	0.636	99.646

No.	Diamètre(Micro_m)	q(%)	Passant(%)
76	300.518	0.354	100.000
77	344.206	0.000	100.000
78	394.244	0.000	100.000
79	451.556	0.000	100.000
80	517.200	0.000	100.000
81	592.387	0.000	100.000
82	678.504	0.000	100.000
83	777.141	0.000	100.000
84	890.116	0.000	100.000
85	1019.515	0.000	100.000
86	1167.725	0.000	100.000
87	1337.481	0.000	100.000
88	1531.914	0.000	100.000
89	1754.613	0.000	100.000
90	2009.687	0.000	100.000
91	2301.841	0.000	100.000
92	2636.467	0.000	100.000
93	3019.738	0.000	100.000
94	3458.727	0.000	100.000
95	3961.532	0.000	100.000
96	4537.433	0.000	100.000
97	5000.000	0.000	100.000

THESIS RESEARCH WORKS

A. International publications

The research works in the thesis has been published in three international publications:

- Boulaiche, K., Boudeghdegh, K., Haddad, S., Roula, A., Alioui, H. Valorisation of Industrial Soda-Lime Glass Waste and Its Effect on the Rheological Behavior, Physical-Mechanical and Structural Properties of Sanitary Ceramic Vitreous Bodies. In : Annales de Chimie-Science des Matériaux, 2022, Vol. 46, pp. 147-54. doi : https://doi.org/10.18280/acsm.460306

- Boulaiche, K., Boudeghdegh, K., Roula, A., Alioui, H., Hamdi, O.M. Potential use of Algerian metallurgical slag in the manufacture of sanitary ceramic bodies and its effect on the physical-mechanical and structural properties. Iranian Journal of Chemistry and Chemical Engineering (IJCCE). 2022. doi: https://ijcce.ac.ir/article_252534.html

- Khaled, B., kamel, b., Abdelmalek, R., hichem, A., Oussama, M. Reuse of sanitary ceramic waste in the production of vitreous china bodies. Iranian Journal of Chemistry and Chemical Engineering. 2022. doi: https://ijcce.ac.ir/article_696934.html

B. National and international communication

- K. Boulaiche, K. Boudeghdegh. The effect of defflocculant type on the rheological parameters of a casting slip contains El-Hadjar blast furnace slag for sanitary ceramics. 4th international symposium on materials and sustainable development. Boumerdes, 2019.

- K. Boulaiche, K. Boudeghdegh. The effects of industrials waste (blast furnace slag, glass waste, and ceramic waste) on the rheological parameters of the pouring slip for sanitary ceramics. 2nd International Symposium on Materials Chemistry. Boumerdes, 2021.

- K. Boulaiche. Glass waste and blast furnace slag effect on the rheological behaviour of the slip casting for sanitary ceramic body. First National Virtual Conference on Chemical Process and Environmental Engineering (NVCPEE2021). Biskra, 2021.

- K. Boulaiche. Soda-lime glass waste effect on the thermal properties of sanitary ceramic body. The First national Seminar on Green Chemistry and Natural Products (GCNP'22). El-Oued, 2022.

- K. Boulaiche. Valorisation of industrial waste and its impact on energy economy in the manufacture of sanitary ceramic products. Colloque National « Ressources naturelles et développement durable : gestion, valorisation et responsabilité sociétale ». Oran, 2022.

- K. Boulaiche, H. Alioui. Valorization and effect of Algerian blast furnace slag on the thermal properties of sanitary ceramic bodies. 1 er Séminaire National des Sciences du Génie des Procédés : Applications et Innovations. USTHB Alger, 2022.

- K. Boulaiche, H. Alioui. Ceramic waste effect on the rheological behaviour and structural properties of the slip casting for anitary ceramic body. 1st International Conference on Chemical matters and Environment Preservation (IC-CMEP'22). Ouargla, 2022.

- K. Boulaiche, H. Alioui. Physical-mechanical properties of sanitary ceramic bodies contained Algerian blast furnace slag. 4th International Conference on Applied Engineering and Natural Sciences. Konya-Turkey, 2022.

ABSTRACT

The research work conducted aims at the valorisation of solid industrial waste by its incorporation in the composition of sanitary ceramic bodies. This thesis is divided into three sections:

In the first, we investigate the effect of the substitution of feldspar by blast furnace slag (BFS), on the properties of sanitary ceramic bodies. The use of Na-electrolytes at the optimum ratio Na_2CO_3/Na_2SiO_3=1.5 with a combined amount of 0.375 wt. %, is found effective to improve the rheological behaviour of the slip. The structural and morphological characterisation of these ceramic bodies were identified by XRD, SEM and FTIR spectroscopy analyses. Mullite and quartz are the main phases in the ceramic matrix with the gradual appearance of the anorthite phase. TGA/DTA analyses prove that there is no significant effect on the peaks of kaolin dehydroxylation and mullite crystallization. It was concluded that the inclusion of 10 wt. % BFS in the ceramic mixture represents the optimum composition as it increases the flexural strength from 33 to 38 MPa and reduces the water absorption from 0. 35 to 0.10%.

In the second section, we study the effect of the substitution of feldspar by soda-lime glass waste (SLGW) on the properties of sanitary ceramic bodies. The rheological behaviour of the slip is improved by SLGW addition using a small amount of electrolytes (0.075 wt. % Na_2CO_3 and 0.1 wt. % Na_2SiO_3). XRD, SEM and FTIR spectroscopy analyses show that mullite and quartz are the main phases in all ceramic bodies with a slight appearance of the anorthite phase. TGA/DTG analyses prove that there is a reduction of mass loss during the addition of SLGW. It was found that the addition of 20 wt. % SLGW in the ceramic composition increases the Bulk density (2 to 2.52 g/cm^3) and reduces water absorption (0.35 to 0.02%).

In the last, we focused on the recycling of the sanitary ceramic waste (SCW) in the formation of its unglazed bodies. The different slips containing SCW, have optimal properties when adding a combination of electrolytes at ratio Na_2CO_3 / Na_2SiO_3=0.25, with a total combined amount of 0.375 wt. %. XRD and FTIR analyses show the high intensity of quartz and mullite in bodies containing SCW. The VC5 body (5 wt. % SCW) has the best physical-mechanical results as it has a flexural strength of 44 MPa and a water absorption of 0.18 %. Moreover, the VC10 body sample has better physical-mechanical properties than the standard ceramic sample. Therefore, SCW can be recycled and incorporated in the manufacture of their unglazed bodies up to 10 wt. %.

Keywords: Sanitary ceramic body; valorisation; flexural strength; water absorption; industrial waste; BFS; SLGW: SCW.

RÉSUMÉ

Les travaux menés au cours de la réalisation de cette thèse sont basés sur la valorisation des déchets industriels solides dans la formulation de tesson de la céramique sanitaire. Pour atteindre les objectifs visés, nous avons ciblé trois parties :

La première partie a permis d'étudier l'effet de la substitution du feldspath par le laitier de haut fourneau (LHF) sur les propriétés des tessons de céramique sanitaire. L'utilisation d'électrolytes de sodium avec le rapport optimal Na_2CO_3/Na_2SiO_3=1.5 et ensuite on prend une quantité 0.375 wt. % de mélange afin d'améliorer le comportement rhéologique de la barbotine. La caractérisation structurelle et morphologique de ces corps céramiques a été identifiée par des analyses de DRX, MEB et spectroscopie FTIR. La mullite et le quartz sont les principales phases de la matrice céramique avec l'apparition progressive de la phase anorthite. Les analyses ATD/TG révèlent qu'il n'y a pas d'effet significatif sur les pics de déshydroxylation du kaolin et de cristallisation de la mullite. Il a été conclu que l'ajout de 10 wt.% de LHF dans le mélange de la céramique possède la composition optimale car il augmente la résistance à la flexion de 33 à 38 MPa et réduit l'absorption d'eau de 0.35 à 0.10 %.

La deuxième partie a été étudiée l'effet de la substitution du feldspath par des déchets de verre sodo-calcique (DVSC) sur les propriétés des tessons de céramiques sanitaires. Le comportement rhéologique de la barbotine a été amélioré par l'ajout de DVSC en utilisant une petite quantité d'électrolytes (0.075 wt. % Na_2CO_3 et 0.1 wt. % Na_2SiO_3). Les analyses par DRX, MEB et spectroscopie FTIR montrent que la mullite et le quartz sont les phases principales de tous les corps céramiques, avec une légère apparition de la phase anorthite. Les analyses ATD/TG montrent qu'il y a une réduction de perte masse pendant l'addition de DVSC. Il a été constaté que l'ajout de 20 wt. % DVSC dans la composition de tesson céramique conduit à l'augmentation de la densité apparente (2 à 2.52 g/cm^3) et réduit l'absorption d'eau (0.35 à 0.02 %).

La troisième partie, nous nous sommes concentrés sur le recyclage des déchets céramiques sanitaires (DCS) dans la formulation de tesson céramique. Les différentes barbotines contenant des déchets céramiques sanitaires ont des propriétés optimales de la barbotine en utilisant le rapport d'électrolytes Na_2CO_3 / Na_2SiO_3=0.25, ensuite on prend une quantité 0.375 wt.% du mélange. Les analyses DRX et FTIR ont montré une forte intensité de quartz et de mullite dans les corps contenant du DCS. Le tesson VC5 (5 % en poids de DCS) donne les meilleurs résultats physico-mécaniques avec une résistance à la flexion de 44 MPa et une absorption d'eau de 0.18 %. De plus, l'échantillon VC10 présente de meilleures propriétés physico-mécaniques que l'échantillon de la céramique commerciale. Par conséquent, les DCS peuvent être recyclés et incorporés dans la fabrication de leurs tessons jusqu'à 10 wt. % .

Mots-clés : Tesson de la céramique sanitaire ; valorisation ; résistance à la flexion ; absorption d'eau ; déchets industriels ; LHF ; DVSC ; DCS.

ملخص

ركّز هذا العمل على تثمين و استعادة المخلفات الصناعية الصلبة في تكوين اجسام السيراميك الصحي، حيث تم تقسيم هذا العمل إلى ثلاثة أقسام:

أتاح القسم الأول دراسة تأثير استبدال الفلسبار بخبث الفرن العالي على خصائص أجسام السيراميك الصحية. تم تحسين ريولوجيا الانزلاق بواسطة الكثروليات الصوديوم. تم تحديد الخصائص الهيكلية والمورفولوجية لهذه الأجسام الخزفية بواسطة حيود الأشعة السينية، المجهر الالكتروني الماسح ومطيافية الأشعة تحت الحمراء. المولیت والكوارتز هما المراحل الرئيسية لمصفوفة السيراميك مع الظهور التدريجي لمرحلة الأنورثيت. تثبت التحليلات الحرارية أنه لا يوجد تأثير كبير على قمم إزالة هيدروكسيل الكاولين وتبلور المولیت. تم الاستنتاج أن إضافة 10٪ بالوزن من خبث الفرن العالي في خليط السيراميك يمثل التركيبة المثلى لأنه يزيد من قوة الانحناء من 33 إلى 38 ميجا باسكال ويقلل امتصاص الماء من 0.35 إلى 0.10٪.

درس القسم الثاني تأثير استبدال الفلسبار بنفايات زجاج الصودا والجير على خواص أجسام السيراميك الصحي. تم تحسين السلوك الانسيابي للانزلاق بإضافة نفايات زجاج الصودا والجير باستخدام كمية صغيرة من إلكتروليات الصوديوم. أثبتت تحليلات حيود الأشعة السينية، المجهر الالكتروني الماسح ومطيافية الأشعة تحت الحمراء أن المولیت والكوارتز هما المرحلتان الرئيسيتان لجميع الأجسام الخزفية، مع ظهور طفيف لمرحلة الأنورثيت. تظهر التحاليل الحرارية أن هناك انخفاضًا في فقد الكتلة بإضافة نفايات زجاج الصودا والجير. وجد أن إضافة 20 ٪بالوزن من نفايات زجاج الصودا والجير تمثل تركيبة مثلى في تركيبة الأجسام الخزفية تزيد الكثافة الظاهرية (2 إلى 2.52 غ / سم 3) ويقلل من امتصاص الماء (0.35 إلى 0.02٪).

في القسم الثالث، ركزنا على إعادة تدوير مخلفات السيراميك الصحية في تشكيل أجسامها غير المزججة. كان للزلة الخزفية المحتوية على مخلفات السيراميك الصحية خصائص زلة مثالية باستخدام نسبة من الإلكتروليات (سيليكات وكربونات الصوديوم). أثبتت تحليلات حيود الأشعة السينية والمجهر الالكتروني الماسح الكثافة العالية للكوارتز والمولیت في الأجسام التي تحتوي على مخلفات السيراميك الصحية. يقدم جسم VC5 أفضل النتائج الفيزيائية الميكانيكية مع قوة انحناء تبلغ 44 ميجا باسكال وامتصاص ماء بنسبة 0.18٪. بالإضافة إلى ذلك، تُظهر عينة الجسم VC10 خصائص فيزيائية ميكانيكية أفضل من عينة السيراميك القياسية. لذلك، يمكن إعادة تدوير مخلفات السيراميك الصحية ودمجها في تصنيع أجسامها غير المزججة حتى نسبة 10٪.

الكلمات المفتاحية: أجسام الخزف الصحي; خصائص فيزيو ـميكانيكية ; قوة الانحناء; امتصاص الماء; خبث الفرن العالي; نفايات زجاج الصودا والجير; نفايات الخزف الصحي.